

# **Improved Design and Fabrication of Light Toxicity Chamber used for Light Induced Retinal Degeneration in Mice**

by

**Alan C. Haungs**

**April 4, 2011**

**A thesis submitted to the**

**Faculty of the Graduate School of**

**The University at Buffalo, State University at New York**

**in partial fulfillment of the requirements for the**

**degree of**

**Master of Science**

**Department of Electrical Engineering**

UMI Number: 1495437

All rights reserved

INFORMATION TO ALL USERS

The quality of this reproduction is dependent on the quality of the copy submitted.

In the unlikely event that the author did not send a complete manuscript and there are missing pages, these will be noted. Also, if material had to be removed, a note will indicate the deletion.



UMI 1495437

Copyright 2011 by ProQuest LLC.

All rights reserved. This edition of the work is protected against unauthorized copying under Title 17, United States Code.



ProQuest LLC.  
789 East Eisenhower Parkway  
P.O. Box 1346  
Ann Arbor, MI 48106 - 1346

## **Dedication**

To Theresa, my dear wife of 28 years who believed in me, and to the Creator, Sustainer, and Culminator of the Universe who kindly allowed me to start, continue, and finish this work.

# Acknowledgement

First of all, I want to thank Cathy Muscarella, Graduate Programs Secretary of the Department of Electrical Engineering, who took the time and effort to open my mind to the possibility of pursuing a Master of Science in Electrical Engineering. By doing so, she utterly fulfilled the spirit of her vocation, not only the impersonal mechanics of her job.

Thanks to Dr. Gonzalez-Fernandez of the VA Hospital in Buffalo, NY for challenging me to build an improved Light Toxicity Chamber, my advisor Dr. P.C. Cheng for taking an interest in this idea, and the other members of my committee, Dr. Fliesler, who used the Toxicity Chamber to see if it was effective, and Dr. Wobschall, who gave me a handy spec sheet on an appropriate photo-sensor.

Furthermore, I also thank the VA Hospital in Buffalo, New York for allowing me to participate in their research efforts to cure blindness.

Additionally, I want to thank my neighbor, Steven Kelley who suggested using 10 gauge steel for the body of the chamber when he observed me struggling with braising 1/4 aluminum plate, and my neighbor Gerald Reilly, who, despite being out of town on vacation, allowed Steven Kelley and myself access to his welding shop, in order to weld the steel shell of the chamber.

Thanks to my brother, Dennis Haungs who gave me suggestions to use a height gauge and surface plate for machining markups and lending an x-y table to me as I needed to make my cheap drill press behave like an accurate knee milling machine.

And finally, I thank our family friend, Mary Rafalski, and my wife, Theresa, who proofread this text, with a special thanks to my daughter Christine who created and painted the 3 blind mice on the Light Toxicity Chamber.



**Figure: Three Blind Mice**

# **TABLE OF CONTENTS**

<b>DEDICATION</b>	<b>ii</b>
<b>ACKNOWLEDGEMENT</b>	<b>iii</b>
<b>LIST OF FIGURES</b>	<b>vi</b>
<b>ABSTRACT</b>	<b>ix</b>
<b>CHAPTER 1 THE BACKGROUND:</b>	
<b><u>1.1 THE RATIONALE FOR LIGHT DAMAGE EXPERIMENTS ON THE EYES OF LIVING MICE</u></b>	<b><u>1</u></b>
<b><u>1.2 SIGHT DEFINED</u></b>	<b><u>3</u></b>
<b><u>1.3 LIGHT INDUCED SIGHT DEGENERATION DEFINED</u></b>	<b><u>10</u></b>
<b><u>1.4 THE HISTORY AND DESIGN FEATURES OF DR. NOELL'S LIGHT TOXICITY CHAMBER</u></b>	<b><u>15</u></b>
<b>CHAPTER 2 THE PRESENT:</b>	
<b><u>2.1 DESIGN FEATURES OF THE REDESIGNED LIGHT TOXICITY CHAMBER</u></b>	<b><u>21</u></b>
<b><u>2.2 PERFORMANCE OF THE REDESIGNED CHAMBER</u></b>	<b><u>32</u></b>
<b>CHAPTER 3 THE FUTURE:</b>	
<b><u>3.1 THE RATIONALE FOR IMPROVING LIGHT TOXICITY CHAMBERS DESIGNS</u></b>	<b><u>44</u></b>
<b><u>3.2 IMPROVEMENTS FOR THE REDESIGNED CHAMBER</u></b>	<b><u>47</u></b>
<b>APPENDIX A: THE OPERATION MANUAL FOR THE REDESIGNED LIGHT TOXICITY CHAMBER FOR MICE</b>	<b>54</b>
<b>APPENDIX B: AUTOCAD DRAWINGS OF THE LIGHT ENGINES HOLDER RACK</b>	<b>82</b>
<b>APPENDIX C: TECHNICAL DATASHEETS FOR LUXEON REBEL LIGHT EMITTING DIODES</b>	<b>105</b>
<b>APPENDIX D: TECHNICAL DATASHEETS FOR THERMALLY CONDUCTIVE ADHESIVE TAPE</b>	<b>135</b>
<b>REFERENCES:</b>	<b>137</b>

# **LIST OF FIGURES**

<b>Figure: Three Blind Mice</b>	<b>iv</b>
<b>Figure 1.4.1: Full-view of Operational 1960's Light Toxicity Chamber</b>	<b>15</b>
<b>Figure 1.4.2: Head-view of 1960's Light Toxicity Chamber</b>	<b>16</b>
<b>Figure 1.4.3: Tail view of 1960's Light Toxicity Chamber</b>	<b>17</b>
<b>Figure 1.4.4: The late Dr. Werner Noell</b>	<b>20</b>
<b>Figure 2.1.1: The Optical Integrating Sphere [14] and Its Giving Birth to Inspiration</b>	<b>22</b>
<b>Figure 2.1.2: Mouse Cage</b>	<b>23</b>
<b>Figure 2.1.3: Four Controls versus Eight Controls</b>	<b>23</b>
<b>Figure 2.1.4: Chamber Clam Only Prior to Fan Installation</b>	<b>24</b>
<b>Figure 2.1.5: Light Engines Holder Rack Only</b>	<b>25</b>
<b>Figure 2.1.6: Clam and Light Engine Rack Holder and Cage Installed Ready for Use</b>	<b>26</b>
<b>Figure 2.1.7: Adjustable Constant Current LED Drive Circuitry</b>	<b>28</b>

<b>Figure 2.1.8: Twin Quad LED Driver Circuit Cards</b>	<b>29</b>
<b>Figure 2.1.9: Experimental 3 LED Light Engine Later Abandoned For the 4 LED Light Engine</b>	<b>30</b>
<b>Figure 2.1.10: Component Placement Ready for Solder Paste to Be Melted</b>	<b>30</b>
<b>Figure 2.1.11: Properly Preheated Then Hot Air Penciled Solder Joints</b>	<b>31</b>
<b>Figure 2.2.1: Stained <u>Non-exposed</u> Albino Mouse <u>Entire Eyecup</u> with Lens Removed</b>	<b>36</b>
<b>Figure 2.2.2: Magnified Retinal Cross-sectional Cellular View of Stained <u>Non-exposed</u> Albino Mouse <u>Superior Mid-periphery Region</u></b>	<b>37</b>
<b>Figure 2.2.3: Magnified Retinal Cross-sectional Cellular View of Stained <u>Non-exposed</u> Albino Mouse <u>Superior Central Region</u></b>	<b>38</b>
<b>Figure 2.2.4: Magnified Retinal Cross-sectional Cellular View of Stained <u>Non-exposed</u> Albino Mouse <u>Optic Nerve Head Region</u></b>	<b>39</b>
<b>Figure 2.2.5: Side by Side Comparison of Stained <u>Non-exposed Versus 24 Hour Exposure Versus 48 hour Exposure</u> of Albino Mice <u>Entire Eyecup</u> with Lens Removed</b>	<b>40</b>
<b>Figure 2.2.6: Side by Side Comparison of Stained <u>Non-exposed Versus 24 Hour Exposure versus 48 Hour Exposure</u> of Albino Mice <u>Superior Mid-periphery Retinal Region</u></b>	<b>40</b>

**Figure 2.2.7: Side by Side Comparison of Stained Non-exposed Versus 24 Hour Exposure of Albino Mice Superior Central Retinal Region 41**

**Figure 2.2.8: Side by Side Comparison of Stained Non-exposed Versus 24 Hour Exposure versus 48 Hour Exposure of Albino Mice Optic Nerve Head Retinal Region 41**

**Figure 2.2.9: Side by Side Comparison of Stained 24 Hour Exposures of Superior Central Region versus Inferior Central Region of Albino Mice 42**

**Figure 2.2.10: Side by Side Comparison of Stained 48 Hour Exposures of Superior Mid-periphery Region Versus Superior Far-periphery Region of Albino Mice 43**

**Figure 2.2.11: Side by Side Comparison of Stained 48 Hour Exposures of Peri-papillary Region Versus Optic Nerve Head Region of Albino Mice 43**

**Figure 3.2.1: Experimenting with Brazing Aluminum to Build the Redesigned Chamber Clam 48**

**Figure 3.2.2: LED Output versus Current Input 52**

# **ABSTRACT**

Researchers have been trying to understand how the human eye works, what causes diseases of the eye resulting in blindness and what treatments can be found to treat human eye diseases.

Animals with eyes that are in some way similar to humans' are used experimentally to search for answers. One method of experimentation involves inducing disease into the eye of an experimental animal by using moderately intense light. For example, a certain kind of accumulative, light induced eye disease which might take 50 years to manifest itself in a human eye can be induced in a mouse eye with the use of a Light Toxicity Chamber in less than 24 hours.

In the 1960's, Dr. Noell [1] observed that moderately bright light could be used to induce and study such diseases in rats. The Light Toxicity Chamber designed by Dr. Noell is still in use today at the VA Hospital in Buffalo New York, almost 50 years later.

As a Graduate Electrical Engineering student, I was approached by Dr. Gonzalez Fernandez of the Buffalo VA Medical Center, regarding the likelihood of whether I could design and build a better Light Toxicity Chamber than Dr. Noell's.

I agreed to try; thus, this paper is the record of what I have accomplished.

In essence, I designed and built a Light Toxicity Chamber capable of blinding mice faster, with more impact and at a fraction of the energy compared to Dr. Noell's, while not polluting the laboratory with intense stray light, as his Light Toxicity Chamber does. Furthermore, my design allowed for the flexibility of a wide range of light intensities, which was not allowed in Dr. Noell's design.

The greater performance my design achieved was due to abandoning Dr. Noell's original open frame design and replacing it with an enclosed design, made possible by recent developments in LED light sources. Surface mounted LED's are more compact, easier to manage thermally, and more color/wavelength controllable than the fluorescent light bulbs and color filters Dr. Noell employed in his design.

# **THE BACKGROUND: CHAPTER 1.1**

## **THE RATIONALE FOR LIGHT DAMAGE**

### **EXPERIMENTS ON THE EYES OF LIVING MICE**

A typical light damage experiment using a light toxicity chamber often involves mice which are first defective in some genetic manner, thus less hearty. Often, the mice are placed in unnatural lighting, prior to the toxic exposure, e.g. darkness for a week, with the purpose of oversensitizing the eyeball to light. At this point, the mouse is placed in the light toxicity chamber usually during a time which overlaps when the mouse would be sleeping, thus disrupting its normal sleep and bodily repair cycle. The light intensities used are typically less bright than one would experience when sitting in shade on a sunny day, but brighter than an office. Also, the light used to damage the mouse retina is often just colored light, not UV light, as the chamber I built uses very pure bluish-green light.

If one were to place a healthy, wild, field mouse in the stressful situation and exposure of a light toxicity chamber for a day or week, damage to the retina would not be detected. However, a genetically weakened mouse, such as an albino, would display incredible retinal damage: special cells in the eye would have died with no hope of ever being replaced.

Some persons, due to age, genetics or environmental insults suffered over time, are like this albino mouse, whereas other persons are more like the healthy, wild, field mouse.

There are numerous diseases of the human eye, each with its own set of hardships. Some of these hardships are correctable or tolerable, while others are devastating. When disease involves the death of tissues that do not regenerate, resulting in permanent loss of function, the situation is particularly hopeless.

The eyeball has special cells that typically last a lifetime. These special cells maintain their robustness by daily shedding worn and possibly toxically contaminated cellular components, in addition to the usual discharge of waste chemicals. Despite this marvelous feature which ensures these special cells' longevity, most aged persons will lose some of these cells, but some unfortunate persons will lose enough of these special cells to greatly affect their sight, even during youth or middle age.

Although much is known about what stresses these special cells, and what can weaken or strengthen these special cells, it is still not known why some special cells die while others survive stress [2]. Pondering on this question, researchers have ingeniously experimented on laboratory animal eyes.

It is hoped that Light Damage Experiments done on mice will help answer the question as to why these special eye cells die in humans, and how this cellular death can be prevented.

## **THE BACKGROUND: 1.2**

### **SIGHT DEFINED**

To greater appreciate why animal experiments are done with Light Toxicity Chambers, it is helpful to have some degree of understanding of what sight is. The following explanation is narrowed in scope to focus primarily on processes that exist near the leading edge of a long chain of events that constitute sight. This narrowed, focused, and oversimplified explanation defining what sight is intended to overlap the narrowed contexts of where Light Toxicity Chambers have their effectiveness to cause Retinal Degeneration due to light induced cell death, and where normal healthy vision occurs. This is not a comprehensive definition of sight.

Sight is when light is focused on a surface arrayed with photosensitive electrical elements which exudes an electrical signal response from each of the electrical elements that absorbed light. This simplified description is equally true for the human design you can buy at the digital camera store and the natural design found in the eyes of living beings. In both cases, the electrical response of these photosensitive electrical elements is photovoltaic, meaning that light causes voltage to occur, and greater light intensity causes a higher voltage signal.

For a man-made photovoltaic element, the ability to produce a voltage from an absorbed photon arises from a photon having enough energy to break a chemical bond in some semi-conductive bulk material, thus allowing an electron and its “absence” (referred to as a “hole”)

to be free to wander in opposite directions under the influence of an electric field. The electric field is produced by two dissimilar bulk materials touching each other, as each material has its own affinity for free un-bonded electrons and holes. In this kind of photovoltaic element, the best signal it can produce is one electron for every one absorbed photon, and the voltage of the one electron device would be derived from the amount of energy required to break the chemical bond of the bulk material. In other words, if it takes 1 electron volt of energy to break the chemical bond in the bulk material, the best we can expect from such a photovoltaic element would be 1 volt, and the ability to supply one electron of current for every one photon absorbed. But, taking parasitic capacitance and leakage currents into effect, it would be hard to realize such a good device with this performance because, normally, in order to detect one photon, amplification of the signal from the photovoltaic element would have to be incorporated. This photovoltaic explanation briefly describes how digital cameras 'see' and solar cells produce electricity.

The natural photovoltaic elements in the eye, arrayed on the surface called the retina of the eye, are the living rod and cone cells. These natural photovoltaic photoreceptors work differently than man-made semiconductor photovoltaic elements and naturally possess the amplification ability. Therefore, a rod cell in a human eye can detect one photon of light without the need for further amplification. What follows is a simplified photo-chemical description behind the photovoltaic behavior of rod and cone cells which will be useful to the discussion.

Rod and cone cells are always using bio-chemical energy, busily pumping out metal ions through the cell membrane at one end of the cell, while these metal ions easily leak back in at the other end. This pumping occurs if the cell is, or is not, absorbing photons.

In darkness, each of these cells looks like a battery shorted, as the short circuit will not allow for a voltage to increase between the interior and exterior of the cell membrane. As the metal ions that leave by pumping are replaced by the metal ions that leak back in, the concentration of metal ions on either side of the cell membrane tends to stabilize. This “electrical short,” or heavy electrical current of ions, occurs when no photons are being absorbed and is exactly the opposite effect of man-made photovoltaic elements which produce no electrical current when there are no photons, but both systems share the zero voltage increase during darkness.

However, when a photon is absorbed by a rod or cone cell, the cell membrane transitions from being a conductor of ions to a dielectric. Thus, in essence, the membrane is now a capacitor. Increasing the number of photons absorbed by the rod or cone cell, increases a chemical reaction in the cell membrane to close channels, stopping ions seeking to leak in. Still, the process of pumping out ions continues even though the membrane becomes more resistive to ions entering. The result is in an increase of ion concentration difference between the interior of the membrane and the exterior of the membrane, thus an increase of voltage appears across the cell membrane. This is how the photovoltaic effect occurs in rod and cone cells.

For example, the rod cell in a human normally has about 40 millivolts across the cell membrane when no photon is absorbed. With one photon absorbed, there is about a 1 millivolt increase, with 30 photons absorbed, the rod is half saturated, and, at near full saturation, the rod can produce about 80 millivolts across the cell membrane [3].

Because the rod and cone cells contain large electrical currents during darkness as opposed to the manmade digital camera photovoltaic elements, the signal to noise ratio of the eye is superior to the digital camera [4]. Electrical noise is the electrical signal generated by heat (shaking atoms) that is superimposed on top of the intended signal. Because rods and cones in darkness have a large number of charge-carrying ions migrating by pumping, the noise signal current generated by heat is small in comparison to this pumping current. Conversely, a digital camera photovoltaic element produces zero current when no photon is absorbed, and the noise signal is large compared to the intended signal. Therefore, in low lighting, digital cameras produce pictures with “snow” superimposed on them, unless of course we cool the camera with liquid helium or nitrogen as done with super telescopes that peer into space.

In addition to being a good low light device, the eye also has a large dynamic range due to the logarithmic chemical amplifier within the rod and cone cells that controls the cell membrane’s resistivity. Having a logarithmic sensitivity means that the eye greatly amplifies dark images, but, as more and more light is available, the gain of the chemical amplifiers is reduced to prevent the photovoltaic cells from saturating. Thus, the eye has great sensitivity with a huge dynamic range.

In humans, the chemical amplifier within the rod cell has roughly 300 times more gain than the cone cells but has a very slow chemical reset or “shutter speed” [3] [4]. Thus, rod cells enable slow motion, colorless, night vision, while the cones cells enable fast moving, color, day vision, and both rods and cones work together in lighting that is in between daylight and darkness. In humans, there are 3 different kinds of cone cells, allowing for color vision, as each kind of the 3 cone types is especially sensitive to its own range of colors.

For the sake of completeness, the following is a sketch description of the chemical steps involved in the photovoltaic and signal amplifying effect in a rod cell, without explaining the cell ‘reset’ chemistry. The full description of each chemical acronym is not mentioned.

In humans, the rod cell membrane voltage is determined by the many cell membrane channels that allow metal ions to leak in. These channels are chemically controlled to remain open by cGMP molecules within the cell, but, if an enzyme hydrolyzes cGMP to become GMP, this signal chemical is reduced within the cell and the membrane channels close, increasing resistivity and voltage across the cell membrane.

PDE is the molecule enzyme that hydrolyzes cGMP. One molecule of PDE can interact with and turn off about 1000 cGMP molecules (prior to this process being terminated), which constitutes the second stage of chemical amplification in this amplification process. PDE, prior to being an active enzyme, was being inhibited by its molecular gamma subunits. Activation required

joining its gamma subunits to the liberated alpha subunits of transducin molecules, which transducin alpha subunits each was already joined as a complex to an individual GTP molecule.

The transducin alpha subunit, prior to its liberation from the transducin molecule and its union with the GTP molecule, was originally part of a regulatory protein, called transducin. As a combination of the beta and alpha subunits, the complete transducin molecule was joined to a GDP molecule. What caused the transducin molecule to lose its alpha subunit and the alpha unit to shed the GDP molecule in favor of a GTP molecule? It was when the transducin molecule interacted with a photo activated rhodopsin molecule.

Each photo activated rhodopsin molecule is capable of dissociating about 100 transducin molecules (before this process is terminated), liberating the transducing alpha subunit and causing the subunit to trade GDP for GTP [4] [5]. In a rod cell, there are many rhodopsin molecules located within the membrane of an intercellular structure called a 'disc'. The large rhodopsin molecule looks like a hollow bird cage made with twisted bars, and this whole structure juts thru the intercellular membrane that separates the interior of the intercellular disc structure from the rest of the interior of the rod cell, as the rhodopsin molecule is somewhat longer than the thickness of the disc membrane it penetrates. A rod cell has many of these rhodopsin covered disc structures, which are stacked like cards at the rod cell's most extreme end. It is here on the discs that light is absorbed by the rhodopsin molecule, which initiates the photovoltaic effect. This photovoltaic effect is sight.

Rhodopsin is a photonic crystal molecule capable of capturing a photon of light and transferring the photon's energy to a specific location in the rhodopsin molecule to perform an exact act, not a random event. Being a photonic crystal means that the shape, size and the geometry of this molecule is what gives it its photonic properties and not its bulk chemistry [6] [7].

When a photon is captured by the hollow bird-cage-like rhodopsin molecule, a molecular subunit within this cage, called retinal, transforms from an L-shaped molecule to a straightened molecule. This causes the retinal to detach from the interior of the rhodopsin cage and to move out through the cage: out and away from both the rhodopsin molecule and the intercellular disc structure and into the remaining interior of the rod cell. The rhodopsin molecule accomplishes this straightening of the retinal (a form of vitamin A) subunit by focusing the photon energy exactly on a specific double carbon bond in the retinal and causing it to rotate 180 degrees, like a nano-sized robot arm straightening itself out. The non-retinal remaining rhodopsin molecule is merely called opsin.

Once this detachment process has started, the opsin undergoes a rapid progression of steps resulting in a change of its shape. Due to its new shape, this is the molecule that dissociates many transducin molecules, which constitutes the first step in the chemical amplification process. This entire chemical process, described above, is similar in cone cells.

# **THE BACKGROUND: 1.3**

## **LIGHT INDUCED SIGHT DEGENERATION**

### **DEFINED**

Whether it's a digital camera or the human eye, there are multiple parts involved such as: focusing elements, aperture adjusting elements, signal processing electrical elements, and signal transport electrical elements. Regardless of the fact that these multiple elements are also exposed to light, it is true that almost all of the light that enters the eye or camera is absorbed by the photosensitive, photovoltaic, photoreceptor elements. This is an important point for this makes the photoreceptive elements the most susceptible elements to light damage in the eye or digital camera.

These other non-photoreceptive parts of the retina will be discussed within a context to help understand the profound nature of light induced sight damage.

The light receiving surface of the eye which holds the array of photovoltaic rod and cone cells is also layered with electrical signal processing and signal transport cells. This is because the photovoltaic signals need to be transported to the brain via an electric highway called the optic nerve. The optic nerve provides roughly only an overall average of 1 signal pathway to the brain per 150 photoreceptor cells in the eye [8], thus maintaining the optic nerve's thinness and flexibility: a necessity for the eyeball to be able to rotate in its socket . The absolute spatially

correlated ratio of photoreceptor cells to optic nerve paths to the brain drops to 2.5 photoreceptors per signal path for the area of the retina which services the dead center portion of vision, which happens to possess the greatest visual acuity of the eye [9]. This ratio gradually soars to many thousands of photoreceptors per signal pathway as one moves out to extreme periphery of sight on the retina, where acuity is the least [10].

Because there are fewer signal paths to the brain than there are photoreceptors on the retina of the eye, multiplexing and data compression is necessary.

The optic nerve is comprised of the axons of the signal transport ganglion cells which inhabit the retina, however, the photoreceptor cells do not directly contact and transfer data to the ganglion signal pathway cells. Instead, they first feed the signals to the bipolar and horizontal cells; then, the signal passes to the amacrine cells and finally to the ganglion cells. These other cells located on the retina, not the ganglion and photoreceptor cells; perform the data compression and multiplexing. This is achieved by simplifying the data to only contain imaging edge detection information and then passing this data set to the ganglion cells covering the retina. These ganglion axons eventually collect as a nerve bundle, which then routes the edge detection data to the brain which ultimately performs the “fill in” to complete the image.

It is a strange fact that all of this signal processing and routing circuitry on the retina is exposed to the light and taking up room with the photoreceptors on the retina, but even stranger is that the natural design inversely layers these devices, and it does not at least place them alongside

each other. This surprising layering is in such a manner that the light must first pass through a layer of ganglion signal transport nerves, then through a layer of amacrine cells, next a layer of bipolar cells followed by horizontal cells and finally reaches the photoreceptor cells, but from the wrong end. The light enters the non-photosensitive end of the photoreceptor cells and passes through the entire length of these elongated, thin cells before the photons are absorbed at the very tip of the cells.

Fortunately, the small blood flow in retinal capillaries and all the signal processing and signal transporting circuitry on the retina is very transparent. Thus, most of the light is absorbed by the rhodopsin molecules embedded upon the stacks of discs found inside the photoreceptive rod and cone cell tips.

It is at this point that an appreciation for light damage has a meaningful context in that the light damage action spectrum matches the absorption spectrum of rhodopsin equally as well as the action spectrum to detect light also matches this same absorption spectrum of rhodopsin [1] [2]. Both sight and light damage are initiated at the site of the rhodopsin molecule as this is where the photon is absorbed.

The purpose of the natural layering design, by physically inverting all of the components on the retina, is to maximize the probability of photon detection against the likelihood of photon caused destruction. Light absorbed creates both intended and unintended consequences. The light energy absorbed by the rhodopsin has some probability of being misrouted and causing

free oxygen to form peroxides which can damage DNA, or causing two vitamin A molecules to join to make a toxic form of double vitamin A [2]. Light, being energy, has the potential to be a destructive force, but the inverted arrangement of retinal components ensures the retina's robustness. For, as compared to roof mounted solar cells which generally have about a 20 year endurance to light absorption, the human retina after twenty years is barely worn. How can this be?

The photoreceptive, photovoltaic rod and cone cells last a lifetime, never replaced, but these cells do regenerative, daily, preventative maintenance. In humans, during morning hours, the rod cells discharge and shed the oldest photoreceptive discs formed in the cell usually formed about 10 days earlier, while forming and producing new intercellular discs daily. The cone cells perform the same preventive maintenance but at dusk. The shed discs are then engulfed, dissolved and removed by the retinal pigmented epithelium. This routine of removing worn, possibly intoxicated discs, and building new ones, in addition to the normal continuous removal of chemical waste, is what maximizes the robustness of the cell, but why is the photoreceptive cell inverted?

The retinal pigmented epithelium layer is the cellular platform that the retina is built on, and is a very vascular layer, which layer cradles the photoreceptive disc-containing tips of the rod and cone cells. In this area of very rich blood supply, the discs are shed, dissolved and carried away. Had the discs been shed in another place, say, by not having the direction of the photoreceptive cells inverted but rather facing the light's incoming direction, the rich vascular mechanisms for

disc breakdown and removal would not be present, and such extraordinary preventive maintenance would not be possible.

Light induced damage is a typical daily event offset by a regenerative process. However, if for some reason the scales tip in favor of light induced damage, then light induced sight degeneration may occur. Light induced sight degeneration is the result of cellular death, specifically, the photoreceptive rod and cone cells. These are the cells containing rhodopsin which captures the photons that can produce an action spectrum of destruction, as well as detection.

Light (in the context of this paper) kills the photon absorbing rods and cones photo-chemically, not thermally, nor thermo-acoustically, while leaving the transparent ganglion, amacrine, bipolar and horizontal retinal cells and the retinal pigmented epithelium cells unharmed. But, should an extreme die-out occur in the rod and cone cell layer, the degree of chemical cleanup left behind can also overwhelm and cause death in the retinal pigmented epithelium cells which, in turn, can undermine the survival of the ganglion, amacrine, bipolar and horizontal cells. Light intensities can also be intermediate without causing death but can leave behind permanent damage. For example, when the intensity of light causes rod or cone cells to shed an unusually high percentage of its discs, it may render these cells unable to rebuild enough discs to replenish their number back to the norm, thus reducing the light absorption properties of these cells [2].

## **THE BACKGROUND: 1.4**

### **THE HISTORY AND DESIGN FEATURES OF DR. NOELL'S LIGHT TOXICITY CHAMBER**

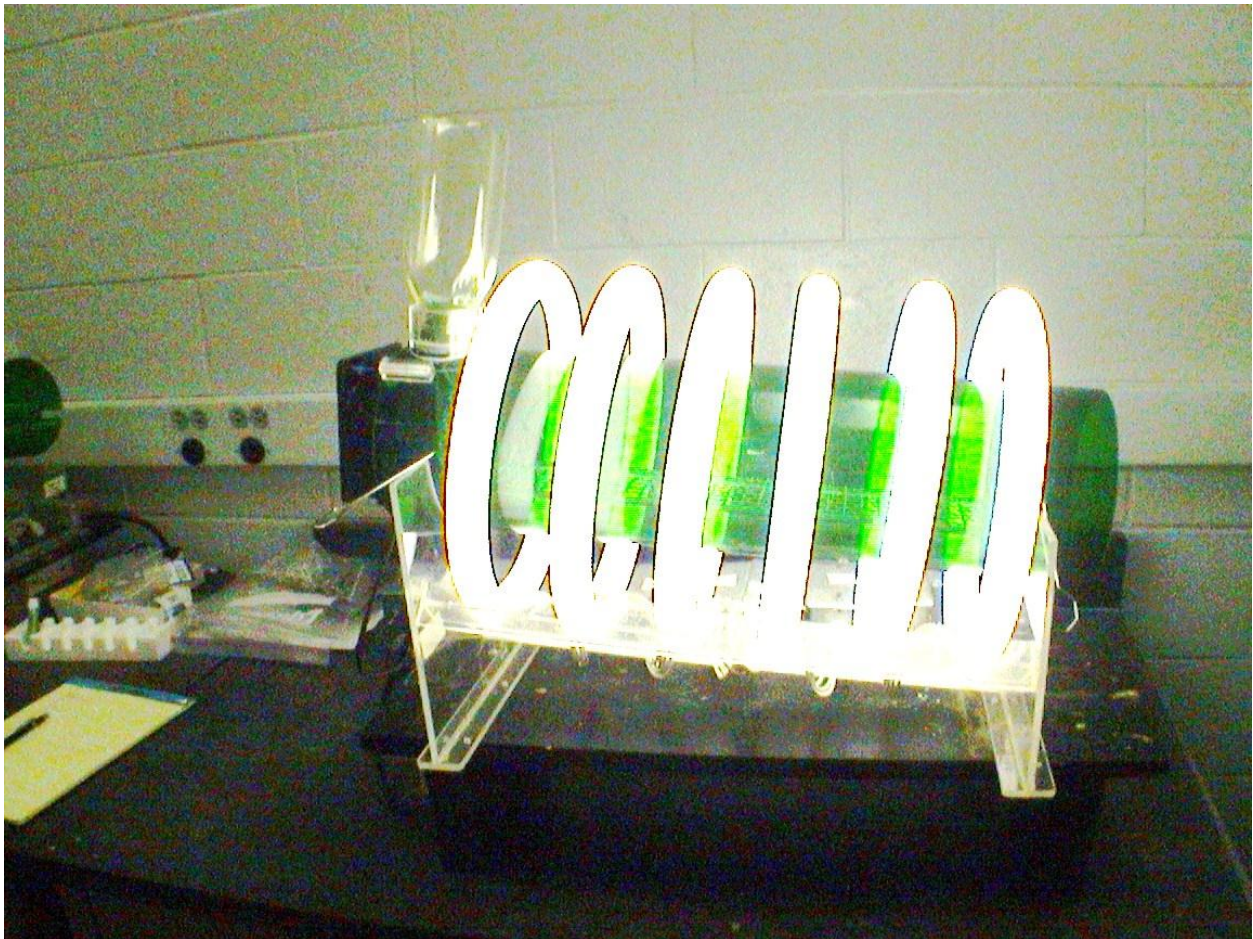
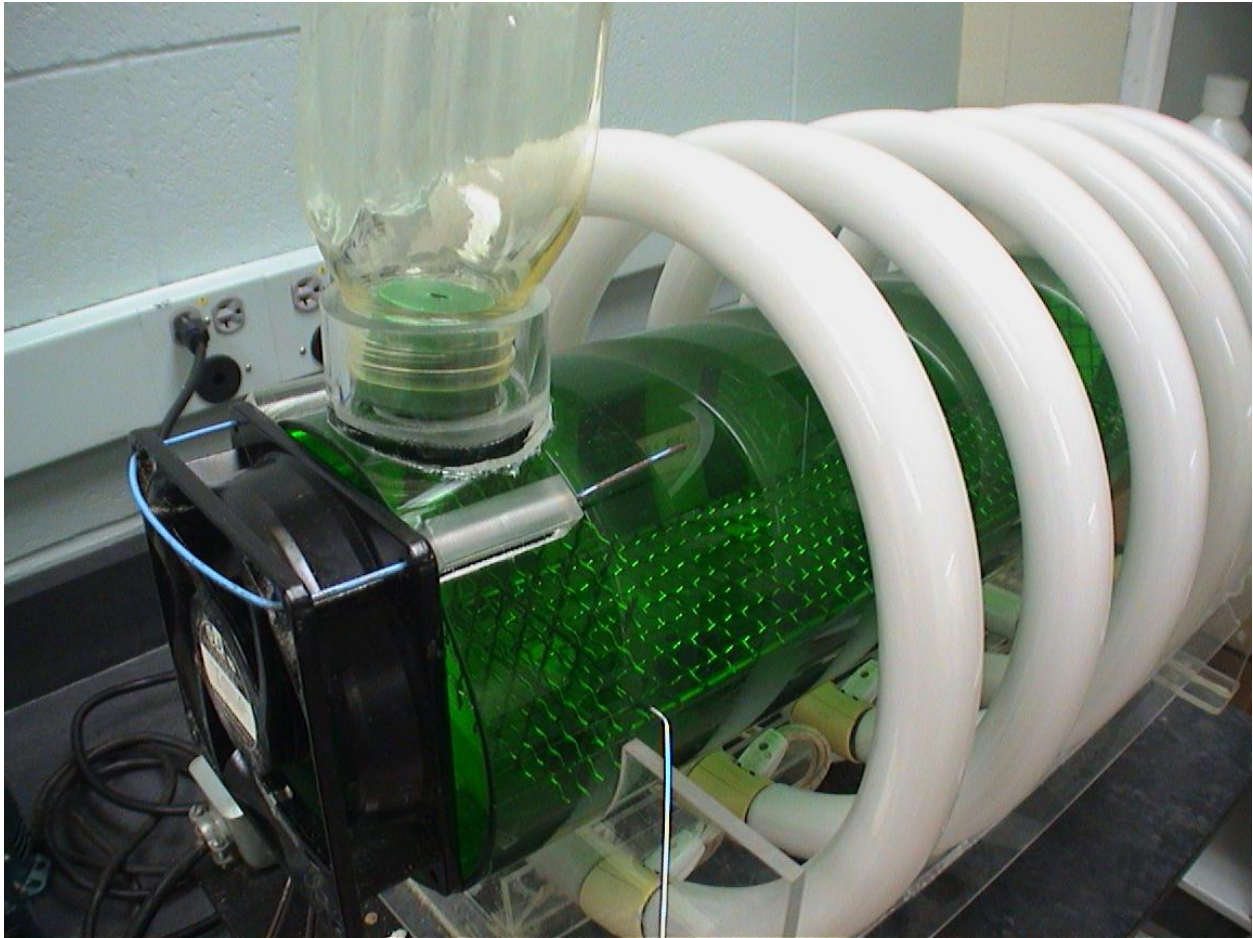
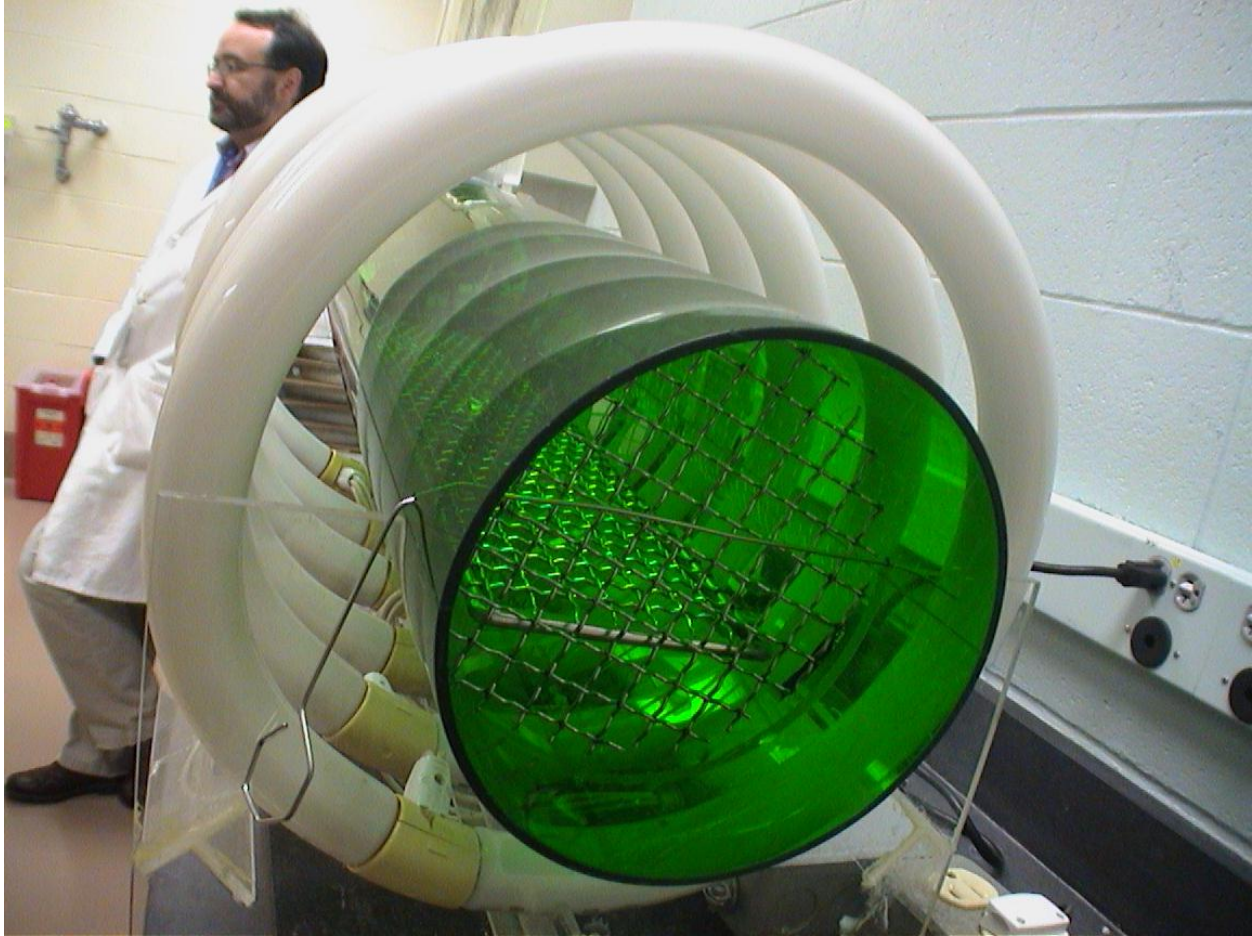


Figure 1.4.1: Full-view of Operational 1960's Light Toxicity Chamber



**Figure 1.4.2: Head-view of 1960's Light Toxicity Chamber**

Before an animal is subjected to an experiment, the imposed stress on the animal is weighed against the potential benefits of the experiment. Whether to proceed with a particular experiment is ultimately decided by a committee with the purpose of remaining within compliance of animal treatment laws and decency. Once decisions are made, they are documented as protocols, so modifications of the experiment are avoided as all future versions of the same experiment will stay within the guidelines of what has been agreed upon by the committee. Modifications of protocols are by committee action and go through an examination process again.



**Figure 1.4.3: Tail view of 1960's Light Toxicity Chamber**

The final design decisions of a light toxicity chamber are aimed to both satisfying the committee as well as causing light damage.

Although the wooden base on Dr. Noell's version of the light toxicity chamber is not up to today's standard for cleanliness and wash-ability, and is grandfathered in, the other obvious and subtle design factors are clearly up-to-date and totally committee satisfying while also well serving light damage experiments.

As required, the animal must have constant access to water; thus, a waterer is available at the head end, and the animal's requirements regarding temperature, humidity and number of air exchanges within the chamber necessitate the fan at the head end.

In rat and mouse cages, bedding is supplied and changed to separate an animal from its waste, as this is another requirement, but Dr. Noell's design fulfills this function via a metal grate for the animal to stand on, and the whole apparatus is tipped toward the tail end so liquid waste will simply run out of the tube. Food is simply placed on the grate.

The 6 fluorescent tubes operating consume 192 watts of electricity to produce a nonadjustable 1,700 LUX of light for the chamber. Mice and rats have peak rod sensitivity to cyan light; thus, Dr. Noell used a green tube to filter out the unwanted colors, leaving available a peak color of 530 nm green within a bandwidth of 90 nm [1].

Even though the green plastic tube is clear and not fogged, allowing an animal to view in between the fluorescent tubes, and regardless there is no light source at the ends of the tube, the animal's random movements and gazes tend to blur and erase these imperfections, thereby creating consistent and predictable experimental results with Dr. Noell's design.

Also, the aging of the fluorescent lamps resulting in lower light output and color shift is not great enough to need compensation as the amount of light is understood as a rough range.

Dr. Noell's rat experiments were in the hundreds: varying animal temperatures, using different color filter tubes in the light toxicity chamber (also using a smaller 3 tube version of what I've shown above) and different light sources. On occasion, his methods included constraining and anesthetizing the rats, thus allowing for a more direct and controllable amount of precise light to be introduced in the eye [1].

So, the use of a light toxicity chamber is a weighted decision as there are better engineered techniques to introduce more exact amounts of light into the eye, but this is weighed against animal stress and its justifiability.

The Researcher in essence has a "stress margin account" and must decide how and where to spend it. The greater argued and believed benefit of an experiment deposits wealth into the stress margin account, and the induced stress on the animal withdraws from the account. In many cases, precision may be sacrificed by leaving animals to roam free and non-drugged to save "stress margin" for other items.

One example of Dr. Noell's stress account spending while using the 6 tube light toxicity chamber above looked like this: for nine weeks each day, rats would receive a special diet and injection regime with night lighting set at zero LUX for 12 hours and day lighting at a very dim 20 LUX for 12 hours. Then, this 9 week cycle would be followed by a 24 hour dark period and finished with a bright 24 hour period of 1,700 LUX in the light toxicity chamber. The animal would then be sacrificed, and tissues collected for a LPO assay [12].

Dr. Noell's light toxicity experiments are credited with greatly advancing the understanding of the mechanisms of certain eye diseases and set the stage for future innovative light induced damage experiments. It was to his credit that he discovered this photochemical connection to light and death in the retina. His invention of the Light Toxicity Chamber is a great scientific contribution.

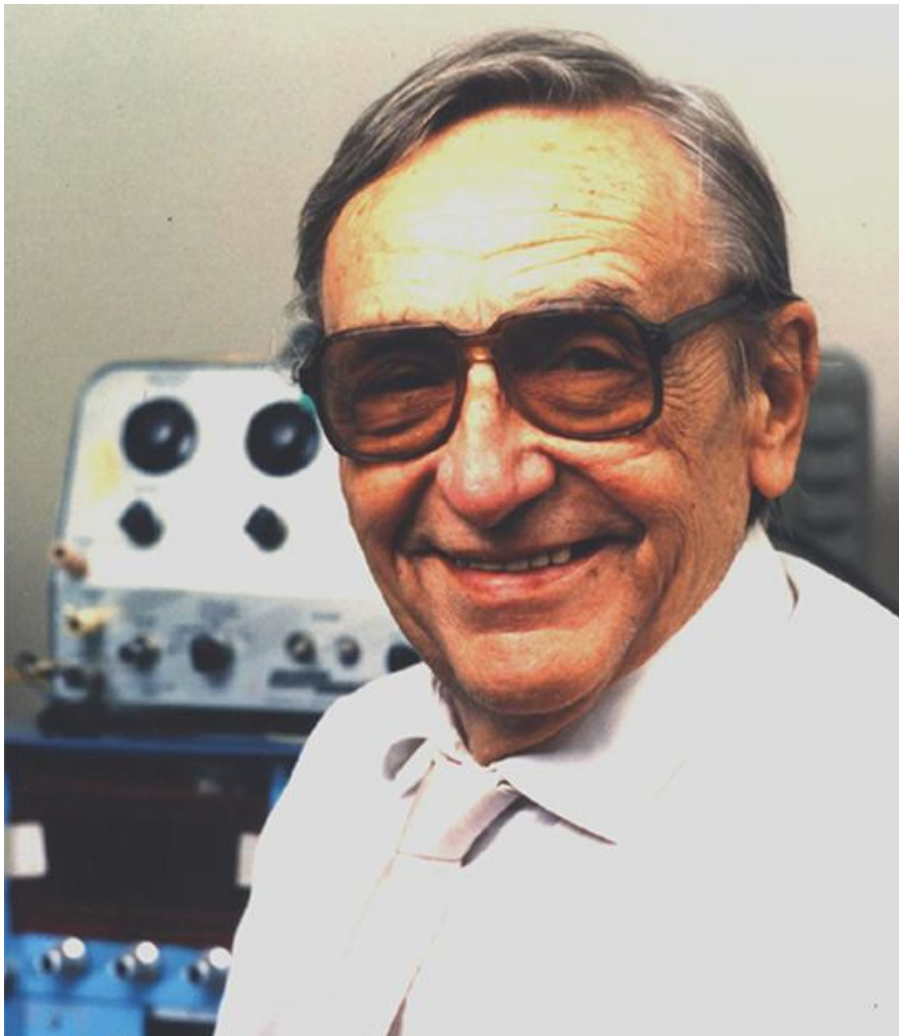


**Figure 1.4.4: The late Dr. Werner Noell [12]**

# **THE PRESENT: CHAPTER 2.1**

## **DESIGN FEATURES OF THE REDESIGNED LIGHT TOXICITY CHAMBER**

Further Design features are discussed in detail in the Operators Manual in Appendix A.

As noted earlier, Dr. Noell's light toxicity chamber is an open design. Advantages of his design are less weight and cost and the lamps cool passively. The disadvantages are it requires more light and electrical energy as each photon that passes through the habitat volume that is not absorbed doesn't get a second or third pass through. (The redesigned chamber roughly allows for 5 passes on average per photon due to reflection in the enclosure). Also, there is the problem of stray light interfering with another light toxicity chamber experiment if they were placed near each other. A performance improvement over this design would be an enclosed design, although it would add weight and cost.

The redesigned chamber design features were inspired by the optical integrating sphere, which is a device that is typically used for super-efficient coupling of light from a light source to a light sink, which is the case when accurate measurement of a light bulb is done. One small sensor can capture almost all of the radiated light from a lamp if both items are placed within an integrating sphere. An integrating sphere is nothing more than a hollow volume, whose interior is coated with a near perfect reflective surface that only allows one exit path for the light, and that unique exit path is the absorbing sensor, hence almost all of the light is coupled to the sensor. The sensor could be placed in any location and face any direction within the sphere and

would always see the same amount of light as this amount is always 100% of what the light source is radiating. The light in this sphere is perfectly homogeneous, which is the ideal case when doing light toxicity experiments.

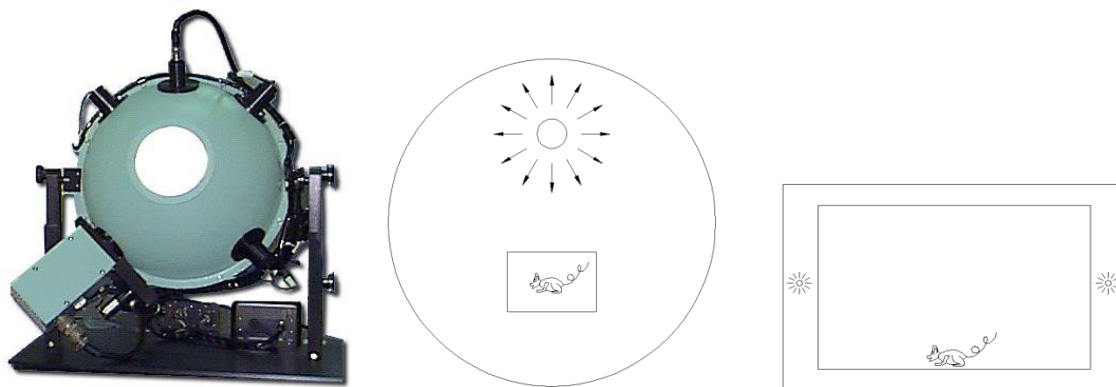


**Figure 2.1.1: The Optical Integrating Sphere [14] and Its Giving Birth to Inspiration**

Although others have also been inspired by the integrating sphere by literally placing a mouse in such a sphere to do light toxicity experiments, the first hurdle one will encounter is the tens of thousands of dollars an optical integrating sphere costs as such a sphere gets large enough to fit the air exchange, food, water and space requirements of a mouse experiment. This inspiration was only a guide for the redesigned chamber of this paper. My theory is that an imperfect optical integrating sphere could be reasonably constructed with adequate performance by changing the sphere to a box whose internal surface is white powder coat.

The second inspiration for this redesigned chamber was how to use the “stress margin” wisely. By leaving the mouse in its well suited cage complete with wood bedding that is already committee approved, and not creating a new habitat that would have to go through committee analysis, might retain more stress margin that could be spent on brighter exposures. This is why

incorporating the existing mouse cage into the light toxicity chamber was chosen. Since the cage already in use is transparent plastic, simply sand blasting this surface to frost it would cause a further diffusion of light to increase the homogeneity of light lost due to the imperfections of the optical integrating redesigned chamber's enclosure. Such flaws arise from an internally coated chamber enclosure surface with less than a 100% reflective material, which flawed integrating structure also contains maze-like vents for cooling air egress and exodus, which allows for some light leakage. To overcome the existing cage's non-symmetrical and complex shaped objects within it, would require that the lights illuminating within the chamber will have to be variable to compensate for shadowing. Therefore, I experimented first with four separate adjustable light zones, but later concluded that eight would be better.



**Figure 2.1.2: Mouse Cage**



**Figure 2.1.3: Four Controls versus Eight Controls**

The entire design is made from two main parts, the chamber clam and the light engines holder rack.

The clam is made from 10 gauge welded steel only because this was the easiest and fastest way to make a rigid box. Although aluminum was my first choice, I didn't have the time to master working with it.

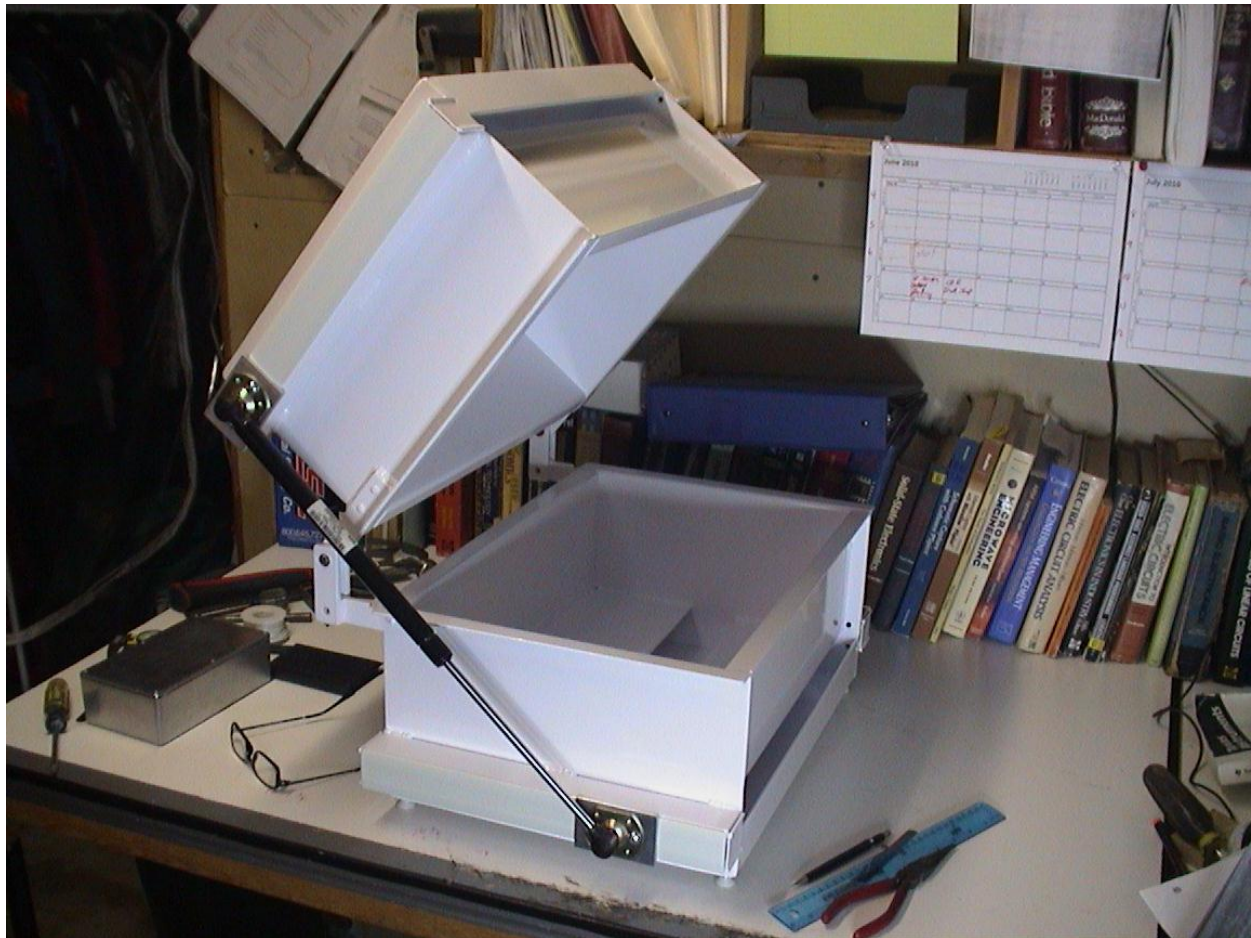


**Figure 2.1.4: Chamber Clam Only Prior to Fan Installation**

The light rack is completely separate so that another rack of another color LED light could be simply placed on the same clam if desired. The light rack is made from  $\frac{1}{4}$  inch machined extruded aluminum flats and angle stock. This material facilitates the heat removal from the LED's.

Furthermore this light rack height is positioned at the top edge of the cage to purposely put the heat sources higher than the inhabited volume of the cage. (For more information on the actual machining and construction of the light engine holder rack see Appendix B).

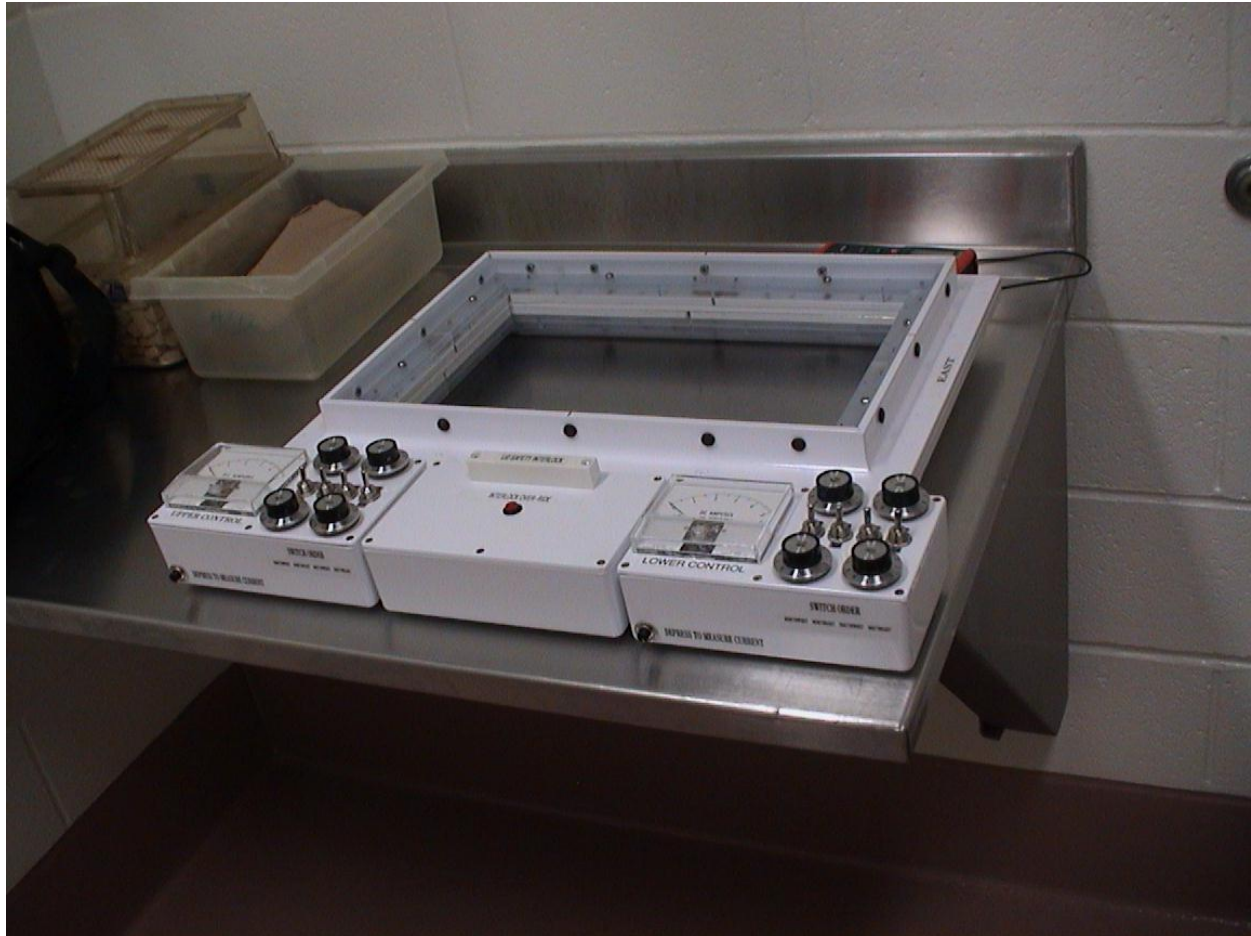


**Figure 2.1.5 Light Engines Holder Rack Only**

Originally, I hoped that convection alone would adequately move the heat out of the chamber, but the committee members insisted that I needed to place fans in the clam. So, I later added 9 fans and discovered much of the surface heating in cage is caused neither by convection nor conduction but directly by light radiation. Placing in all the fans turned out to be the right idea: otherwise the interior of the cage would start to heat up instantly directly from light radiation.



**Figure 2.1.6: Clam and Light Engine Rack Holder and Cage Installed Ready for Use at the VA**

I performed many temperature experiments as it was absolutely critical that the ambient air temperature inside the cage not go above 6 degree F of the VA's laboratory air temperature. I constructed a chart which lists the expected air temperature rise as per selection of required light intensity (see Appendix A). Select LUX points versus temperature were found experimentally and the rest were interpolated for the chart, using the curve fitting equation generating function in Excel. The method of recording experimental temperature rise was done using a dual probe thermometer which would record the greatest difference. This method is not immune to error as the air temperature rise in my home laboratory rises faster than the

temperature in the chamber. This temperature rise was due to the home heating furnace cycling on, as it was winter. With the room heating up faster than the chamber, this distorts the temperature difference by under reporting the heating in the chamber. But the air in the home laboratory also cooled faster than the interior of the chamber in-between winter heating furnace cycles. This distortion exaggerated the temperature difference in the chamber and this over-reported number would then be stored in the thermometer. This means that my chart errs on the side of caution.

If the heating and cooling temperature cycles in the VA laboratories are shallower and slower than my home laboratory, then the temperature rise numbers predicted in the Operator's Manual (Appendix A) are overly cautious. I am very confident they can use this chamber without having to worry about heat stress affecting either the wellbeing or the experimental results of a mouse. (Noell found that heat stress greatly enhanced light stress [1]).

Regarding the selection of surface mount LEDs as the light source, this decision was made to enhance performance beyond Dr. Noell's design which used fluorescent tubes and filters, although it is more expensive. With LEDs, there is more color purity, 30nm versus Dr. Noell's 90nm bandwidth, and greater color selection, 505nm cyan versus 530nm green (mouse rod sensitivity peaks approximately at 510nm). Also LEDs have greater lifetime (50,000 hours at 30% degradation versus 25,000 hours at 50% degradation), are very suitable for adjustable light output and can be populated more densely to concentrate greater light in a given volume. Surface mounted LEDs are roughly 50 times less expensive per watt than 'through the hole'

LEDs, but they are harder to solder, requiring expensive pre-heating equipment, hot air penciling, refrigerated and limited shelf life soldering paste and heat sinking for operation. (There is a wealth of information on the LED selected in Appendix c).

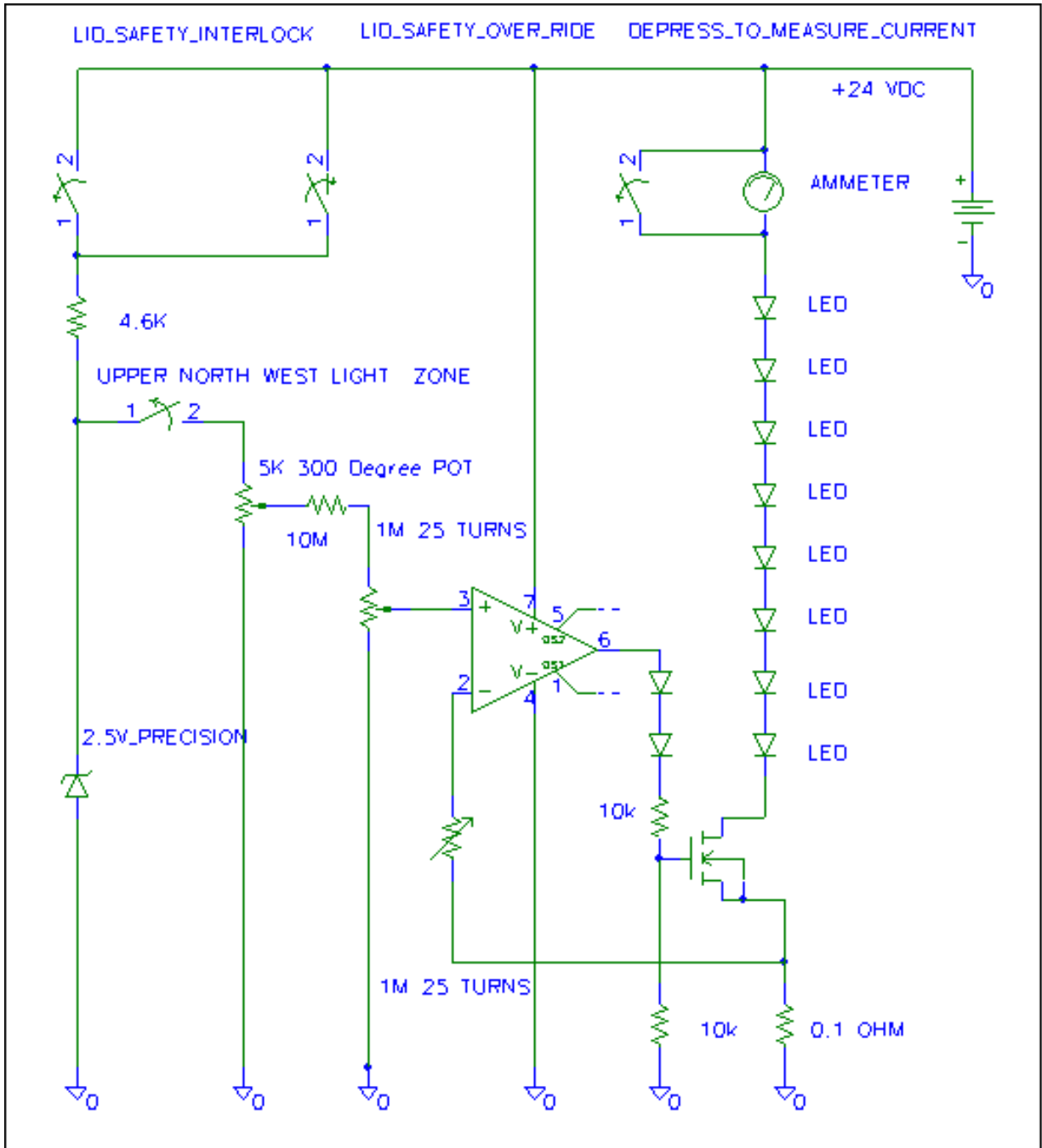


Figure 2.1.7: Adjustable Constant Current LED Drive Circuitry

The redesigned chamber has the flexibility of producing LUX values higher (10,800 LUX) and lower (500 LUX) than Dr. Noell's fixed design (1700 LUX). This requires LED drive circuitry: the adjustable constant current source schematic pictured above is the circuit I designed for this task. This circuit drives eight LED's in series which requires 2 light engines, four LED's apiece. This circuit is repeated 8 times for a grand total of 16 light engines containing 64 LEDs in all. The totality of the electronics is held on two circuit cards.



**Figure 2.1.8: Twin Quad LED Driver Circuit Cards**

The light engines are removable and replaceable, covered with frosted polycarbonate plastic and constructed on ¼ inch aluminum flat, that serves also as a heat sink. The aluminum is overlaid with two sided heat conductive heat sink adhesive tape, and then copper shim stock is

cut and placed on top of the tape. All parts are cleaned with acid (white vinegar) before assembly. The LED is dropped into position; then, with a syringe, the refrigerated solder paste is applied.

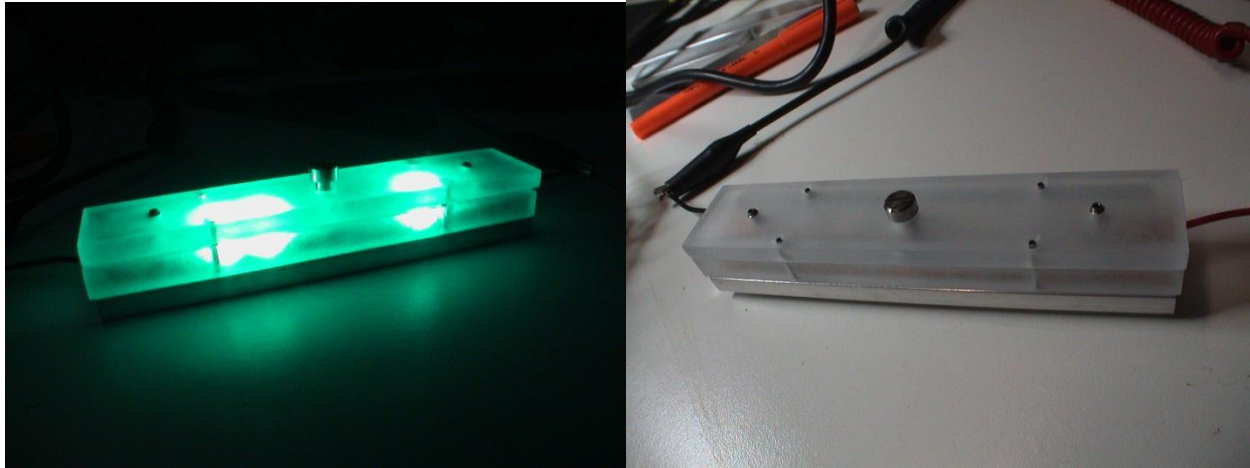


**Figure 2.1.9: Experimental 3 LED Light Engine Later Abandoned For the 4 LED Light Engine**

The timing and temperatures for the application of heat is critical: the whole unit has to reach a standing temperature within a window of time that allows the organic chemistry in the solder paste to wet, deoxidize, dry and clear before melting the metal while not overheating the LED and destroying it.



**Figure 2.1.10: Component Placement Ready for Solder Paste to Be Melted**

Once the heated chemistry in the paste has fulfilled its mission, the hot air pencil is used just long enough (about a second) to heat the gray dry solder paste into a bright and shiny solder puddle that's fully melted just long enough to bond the parts.



**Figure 2.1.11: Properly Preheated Then Hot Air Penciled Solder Joints**

This process involves expensive equipment, syringed solder paste, a hot air pencil, a quality, accurately temperature controlled hotplate and a large stop watch, a clear mind, well rested eyes, steady hands and no distractions. (For more information on the temperature windows for soldering the LEDs, see Appendix C: *Reflow Soldering Characteristics*).

By design, the two-sided adhesive tape mentioned above, reacts and tremendously bonds to the surfaces when heated. (For more information on this tape see Appendix D).

## **THE PRESENT: 2.2**

# **PERFORMANCE OF THE REDESIGNED CHAMBER**

Dr. Fliesler of the Veterans Hospital, in Buffalo New York, was the first one to use the redesigned chamber on mice. He placed two sets of mice, 3 at a time, through an exposure period in the redesigned chamber. Three at a time is a requirement of the committee as mice are social animals, and placing only one or two mice at a time in the chamber would consume too much “stress margin”. It is understood that the mice will tend to bed and shade each other. This is the acceptable compromise of accuracy versus the ease to have permission granted to perform an experiment.

The first set was exposed to 3200 LUX for 24 hours and the second set for 48 hours, then all were allowed to recover for 3 weeks before being sacrificed and the eyes dissected to see what happened. All of the mice are genetically the same and defective, as albinos, and a 7<sup>th</sup> mouse was preserved from the light toxicity chamber so as to have a comparison of exposure versus non-exposure.

Dr. Fliesler had some reservations as to whether this design would work: the cage has wood bedding below the mice the feeder and waterer above the mice, as this design is unlike Dr. Noell’s chamber in which the animals are exposed more evenly from all angles. After the mice

were placed in the chamber, it was noted at some point that they clustered under the feeder shading themselves, so Dr. Fliesler emptied the feeder for the rest of the experiment and placed food on the bedding.

After the dissection, Dr. Fliesler emailed to me the pictures of the dissected eyes stating, “Worked like a champ! In fact, we need to TURN DOWN the intensity.... too much damage! Both superior and inferior central to equatorial/midperiphery damaged.”

This answered both questions as to whether it would work and could it out perform Dr. Noell’s design.

Dr. Fliesler dissected all six mice and observed all six mice sustained the same over-damage, as compared to what is normal in experiments performed with Dr. Noell’s chamber. Typically, there is a thinning of the number of living photoreceptors, which thinning is consistently more prevalent in certain regions of the retina. There is an amount of light damage and patterned thinning that is considered sufficient for their experiment, whereas with the redesigned chamber there was extreme photoreceptor destruction, even the thinning or destruction of resistant regions and also disruption of the non-photoreceptor layers.

The over-damage in the 48 hour exposed mice was greater than in the 24 hour mice proving that there is a correlation to exposure time and light damage, as the damage in the 48 hour mice even extended to the extreme far periphery region of the retina.

(One cause of the resistance to light damage variance in regions of the retina is due to photo-stasis. Photo-stasis is the tendency to try to absorb the same amount of photons daily. As the sun usually casts light such that the lower hemisphere of the retina receives more photons than the upper hemisphere, the lower hemisphere photoreceptor cells react by producing less rhodopsin to desensitize. By absorbing photons less efficiently as the upper hemisphere, both hemispheres continue to absorb roughly the same number of photons daily. In the light toxicity chamber, the lighting tends to be the same from all angles and will tend to over-expose the most efficient photon absorption regions of the retina first. As the action spectrum of destruction matches the action spectrum of rhodopsin, the cells with the most rhodopsin are the most light damaged. Also, photo-stasis explains how the mice's eyes can be conditioned to become overly sensitive to light damage by first subjecting the mice to a regime of low light prior to placing them into the light toxicity chamber.)

This extreme damage was achieved at a 3200 LUX setting which is 30% of the redesigned chambers' capacity. I credit this extra-performance to the LED's more precise color matching of the peak sensitivity of the rod cells; thus, a LUX unit of the redesigned chamber has more punch than a LUX unit of Dr. Noell's design.

(A LUX unit assumes a peak sensitivity at 555 nm yellowish green, thus Dr. Noell's more mid-green would measure a higher LUX unit value per photon than the redesigned chambers more bluish green per photon, for the LUX unit is a human based, color, daylight response, vision

unit, not a mouse unit nor a night vision unit. This means more bluish green photons are needed than mid-green photons for any given measured LUX unit value, and the mouse rods are more sensitive to the bluish green photons, thereby granting more rod cell punch per bluish green LUX unit. A bluish green system would have to supply more photons per LUX unit than the mid-green system, and each photon supplied by the bluish green system is more efficacious than each photon in the mid-green system, thus is more mouse rod cell damaging. This same explanation of better photoreceptor cell, color matching exposure also explains the greater damage to both of the mouse's daylight color detection photoreceptors, the mid-green cone cells and the ultraviolet cone cells on the mouse retina, by the redesigned chamber.)

The pictures sent to me of the dissected eyes are stained cross sections of the entire eyecup minus the lens, and some are pictures of cellular level close-ups of a cross section of the retinal layers in a particular region of the retina.

The applied staining darkens the photoreceptor cell nuclei the most, and the lack of dark thick granular looking bands in a layer is a sign of death. After three weeks of recovery, the dead cells and their nuclei are naturally removed. This is why there is a three week recovery after exposure to see what died and what lived, in addition to allowing the swelling and deformation to recede and the cells, which eat dead cells, to vacate.

I have included comments on these pictures below to highlight key items.

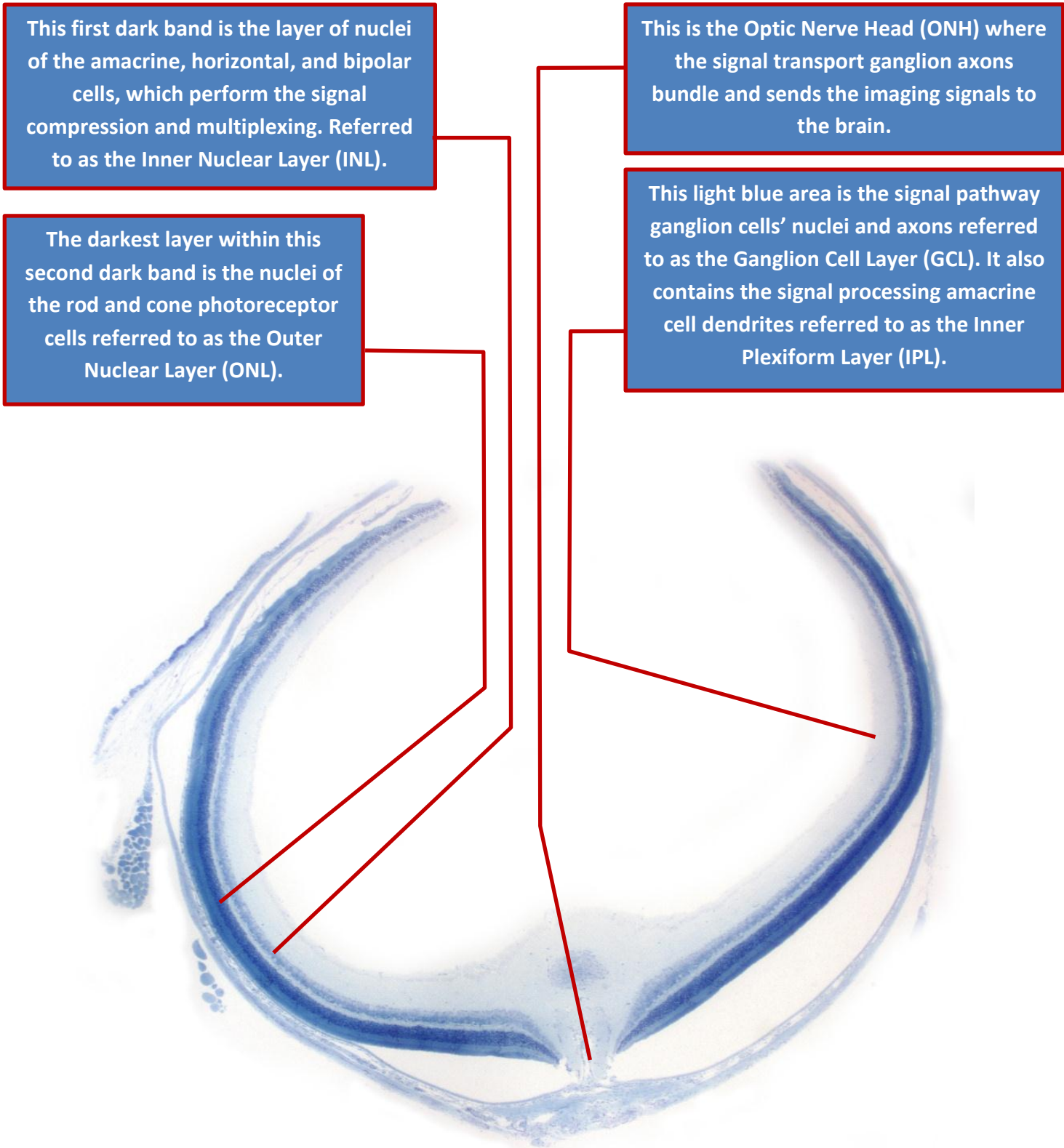


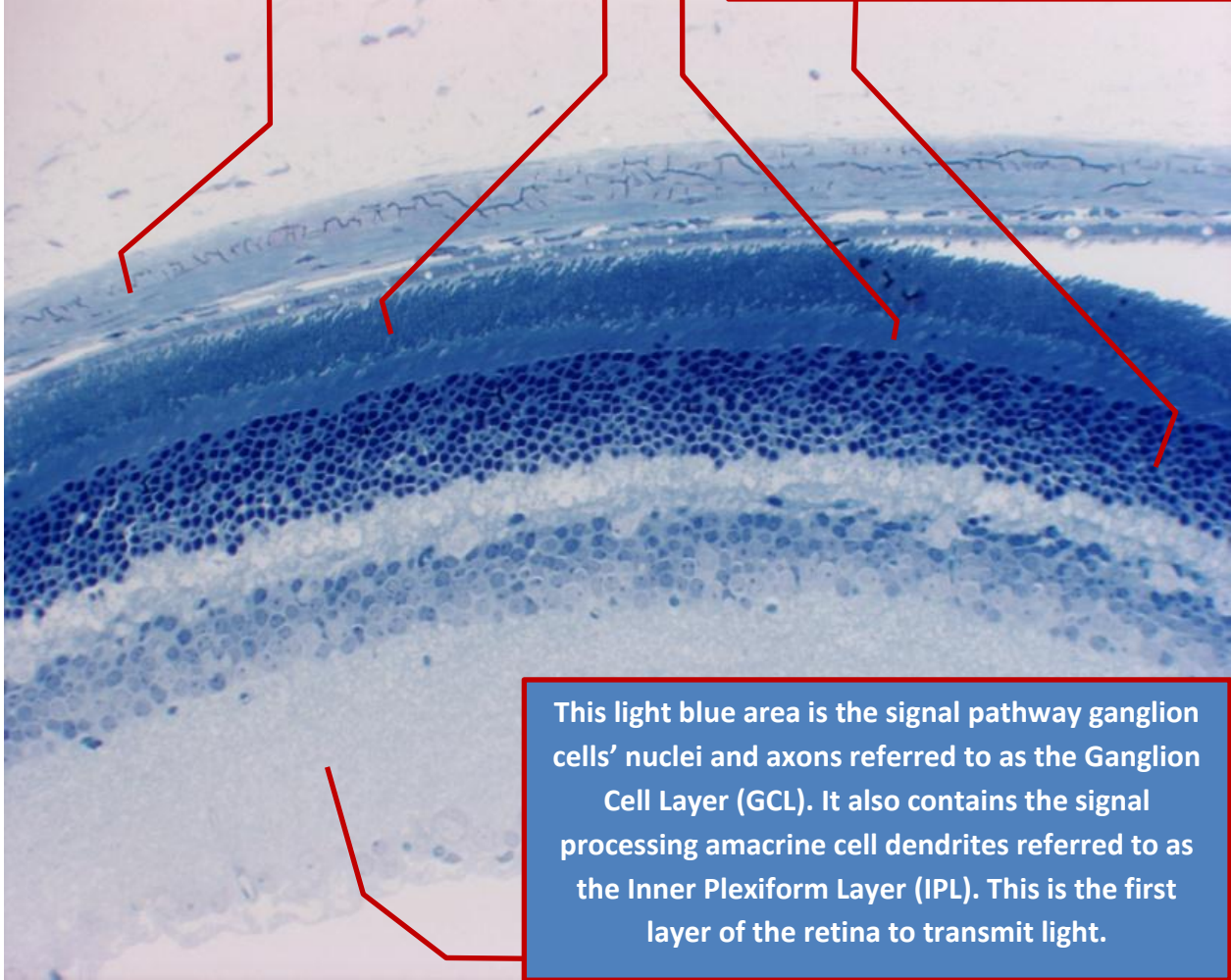
Figure 2.2.1: Stained Non-exposed Albino Mouse Entire Eyecup with Lens Removed

This hairy looking layer is called the Outer Segment (OS). It is the far end segment of the rod and cone photoreceptor cells where the inter-cellular discs containing rhodopsin abide. This is where a photon is absorbed for sight.

This layer is the Retinal Pigmented Epithelium (RPE) that provides the place and vascular riches to dissolve the spent discs discharged from the rod and cone photoreceptor cells.

This smooth layer is called the Inner Segment (IS). It contains the main body of the photoreceptor rod and cone cells containing their inter-cellular organelles.

This dotted layer is the nuclei of the rod and cone photoreceptor cells referred to as the Outer Nuclear Layer (ONL). These photoreceptive cells are very stretched out length wise and stacked side to side with their same parts aligning as layers.



This light blue area is the signal pathway ganglion cells' nuclei and axons referred to as the Ganglion Cell Layer (GCL). It also contains the signal processing amacrine cell dendrites referred to as the Inner Plexiform Layer (IPL). This is the first layer of the retina to transmit light.

Figure 2.2.2: Magnified Retinal Cross-sectional Cellular View of Stained Non-exposed Albino Mouse Superior Mid-periphery Region.

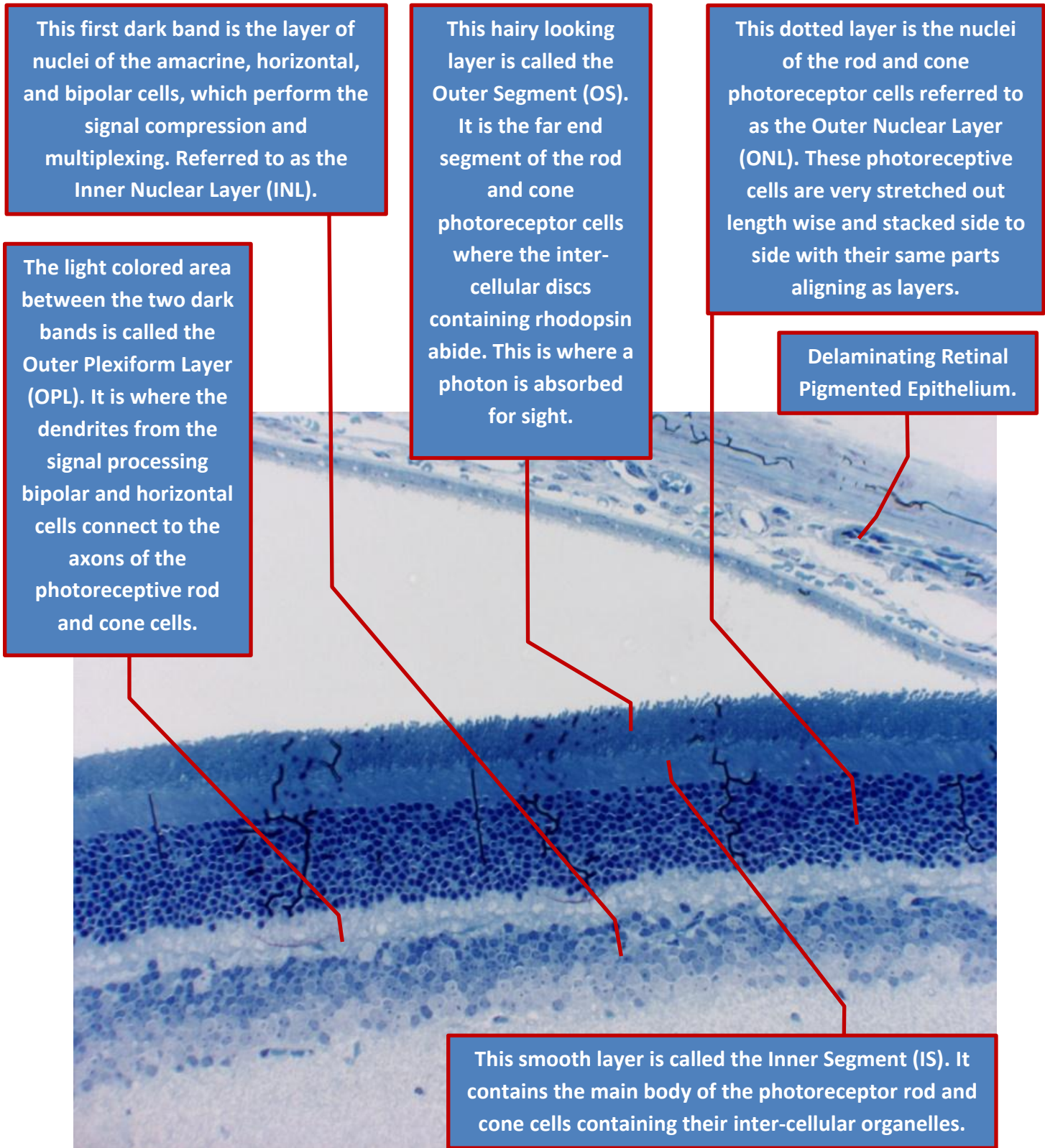


Figure 2.2.3: Magnified Retinal Cross-sectional Cellular View of Stained Non-exposed Albino Mouse Superior Central Region.

This light blue area is the signal pathway ganglion cells' nuclei and axons referred to as the Ganglion Cell Layer (GCL). It also contains the signal processing amacrine cell dendrites referred to as the Inner Plexiform Layer (IPL). This is the first layer of the retina to transmit light.

This first dark band is the layer of nuclei of the amacrine, horizontal, and bipolar cells which perform the signal compression and multiplexing. Referred to as the Inner Nuclear Layer (INL).

This is the blind spot on the retina where the ganglion signal transport cells' axons collect as a bundle and exit the back of the eye for the brain.

This dotted layer is the nuclei of the rod and cone photoreceptor cells referred to as the Outer Nuclear Layer (ONL). These photoreceptive cells are very stretched out length wise and stacked side to side with their same parts aligning as layers.

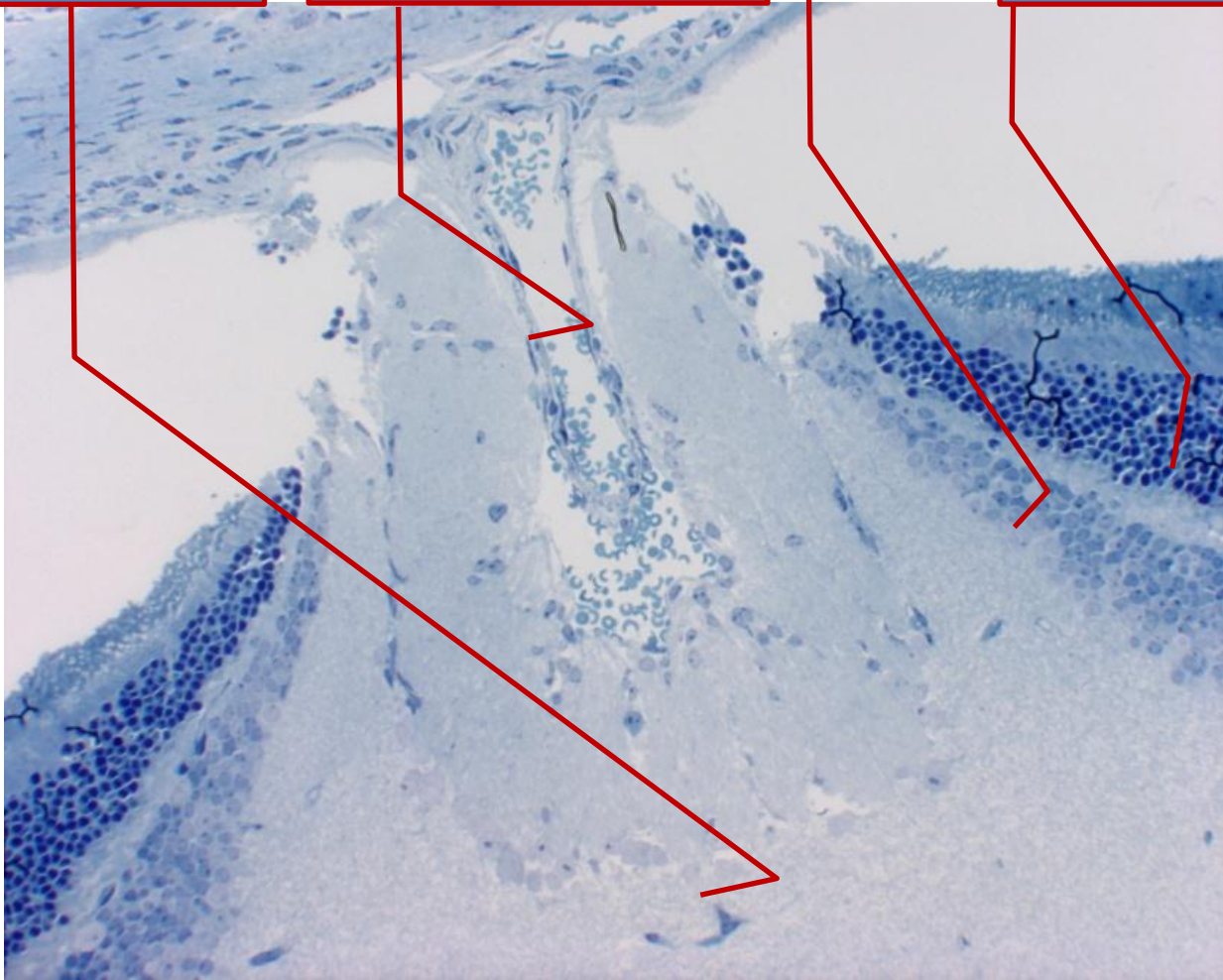


Figure 2.2.4: Magnified Retinal Cross-sectional Cellular View of Stained Non-exposed Albino Mouse Optic Nerve Head Region.

The combinations of the photoreceptor rod and cone cell's Outer Nuclear Layer, Inner Segment Layer and Outer Segment Layer forms one dark stained band. The absence of this dark thick band is the signature that these photoreceptor cells have died. In the 24-hour exposure only some of the mid-periphery and the far periphery still contains a clear multiple layering of these cells.

The 48-hour exposure only shows multiple layering of photoreceptors in the far periphery-the hardest region.

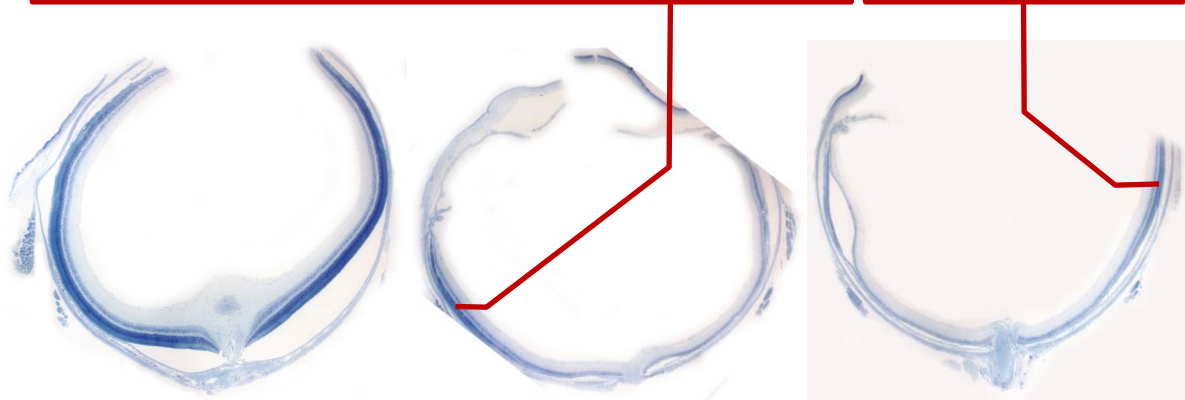


Figure 2.2.5: Side by Side Comparison of Stained Non-exposed Versus 24-Hour Exposure Versus 48-hour Exposure of Albino Mice Entire Eyecup with Lens Removed

The non-exposed retina has roughly about a 10 nuclei thickness of the photoreceptor cells' nuclei in this region of the retina. The nuclei thickness of the 24-hour sample is roughly 6 nuclei, meaning about half of the photoreceptors have died.

The 48-hour sample's nuclei thickness is less than one nuclei for this region, and it is assumed the few survivors are cones.

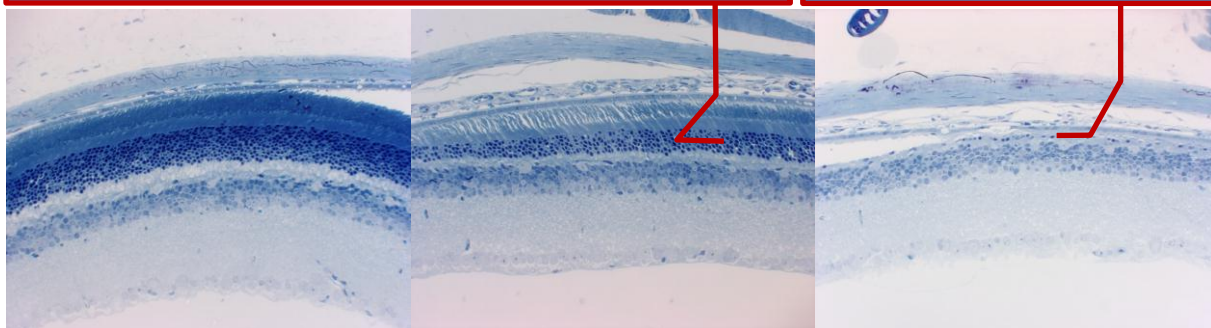


Figure 2.2.6: Side by Side Comparison of Stained Non-exposed Versus 24-Hour Exposure versus 48-Hour Exposure of Albino Mice Superior Mid-periphery Retinal Region.

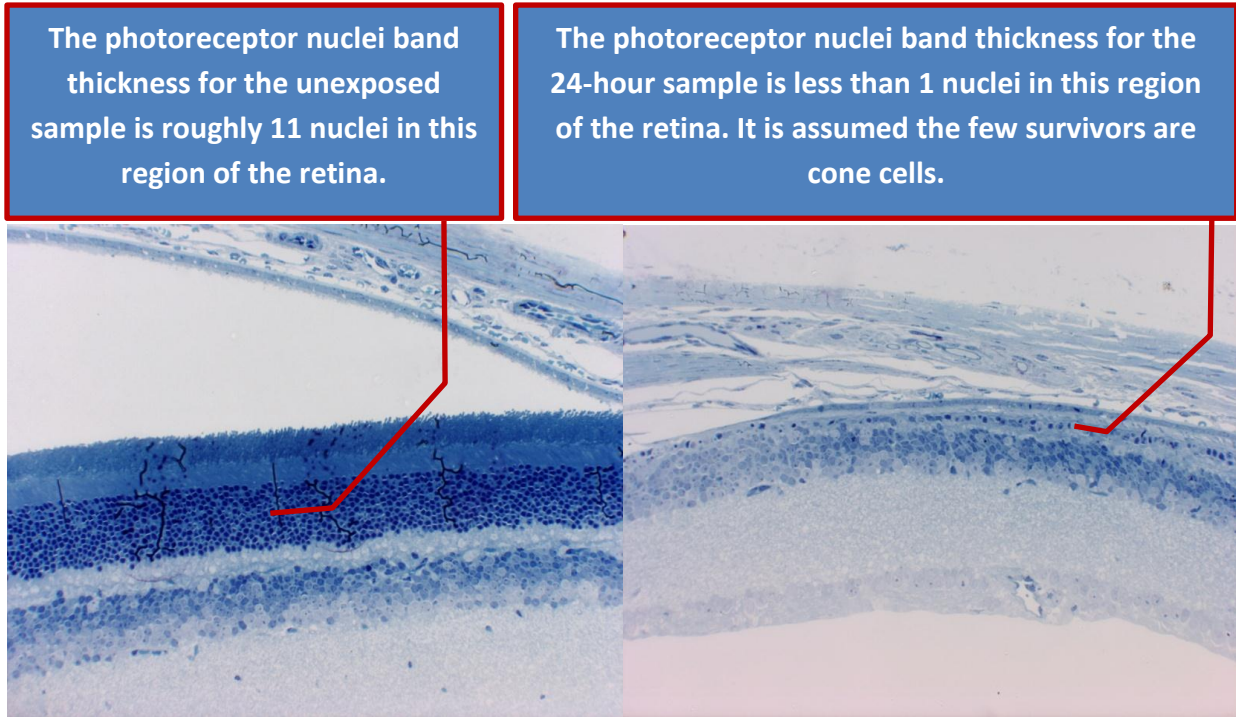


Figure 2.2.7: Side by Side Comparison of Stained Non-exposed Versus 24-Hour Exposure of Albino Mice Superior Central Retinal Region.

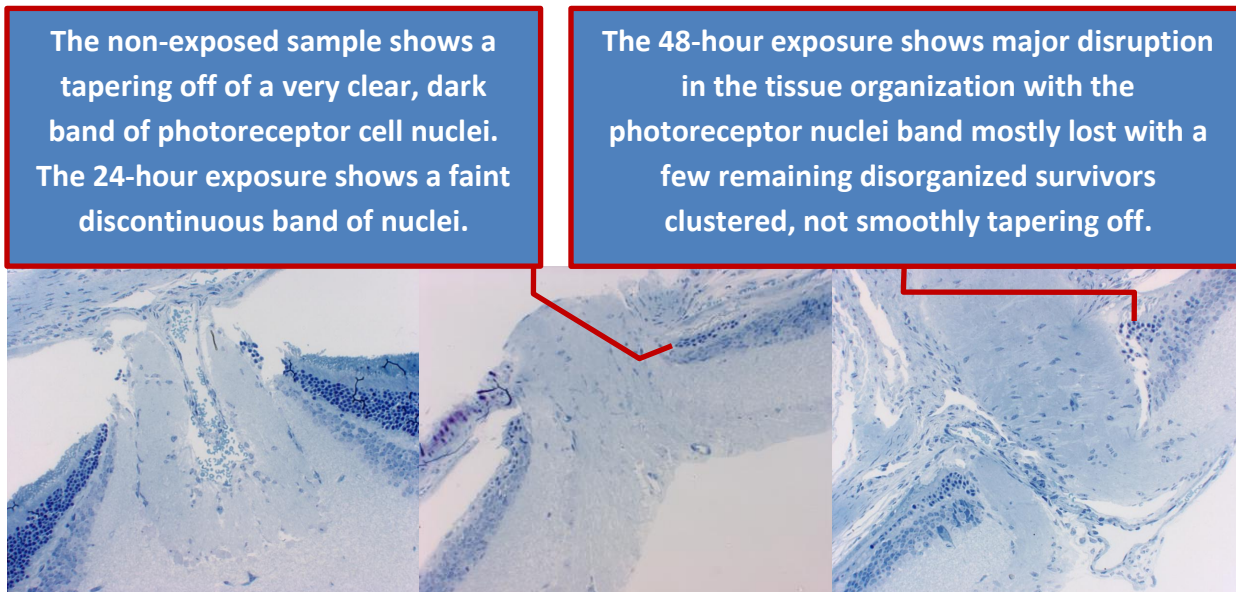


Figure 2.2.8: Side by Side Comparison of Stained Non-exposed Versus 24-Hour Exposure versus 48-Hour Exposure of Albino Mice Optic Nerve Head Retinal Region.

Typically, the closer to the Central Region of vision, the more light damage occurs, and, due to photo-stasis, the upper and lower hemispheres have differing sensitivities. On the superior hemisphere, there remains a faint, discontinuous, single row of photoreceptor nuclei.

According to photo-stasis, lighting normally comes from above; thus desensitizing the inferior hemisphere making it more resistant to light damage. I do not know why the inferior hemisphere shows more destruction of photoreceptors than the superior hemisphere, with only two photoreceptor nuclei visibly remaining. It may be that the redesigned chamber maintains the wooded bedding on the floor thus allowing more light from the top, so the lighting distribution is more natural and compensates for the inferior region's greater resistance to light damage.

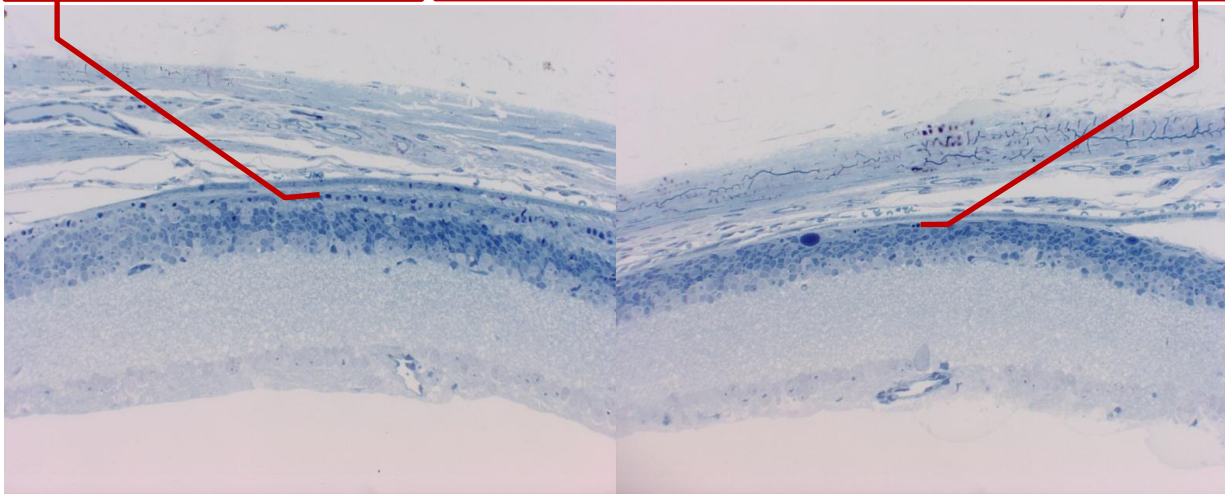


Figure 2.2.9: Side by Side Comparison of Stained 24-Hour Exposures of Superior Central Region versus Inferior Central Region of Albino Mice.

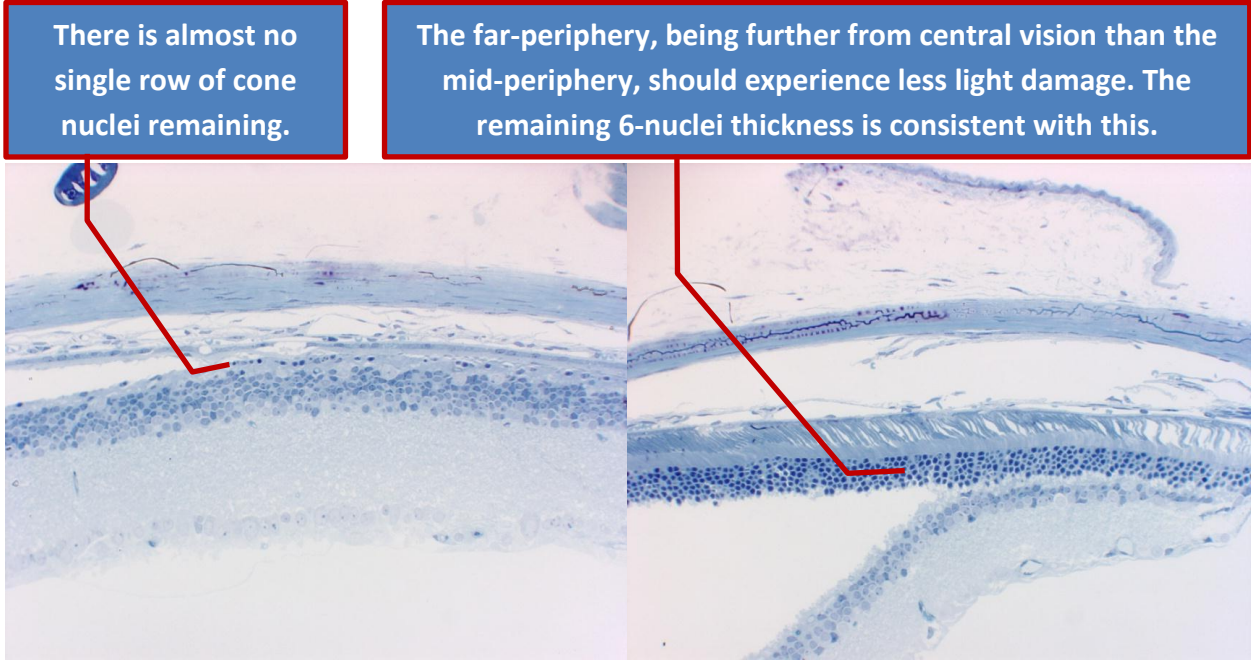


Figure 2.2.10: Side by Side Comparison of Stained 48-Hour Exposures of Superior Mid-periphery Region versus Superior Far-periphery Region of Albino Mice.

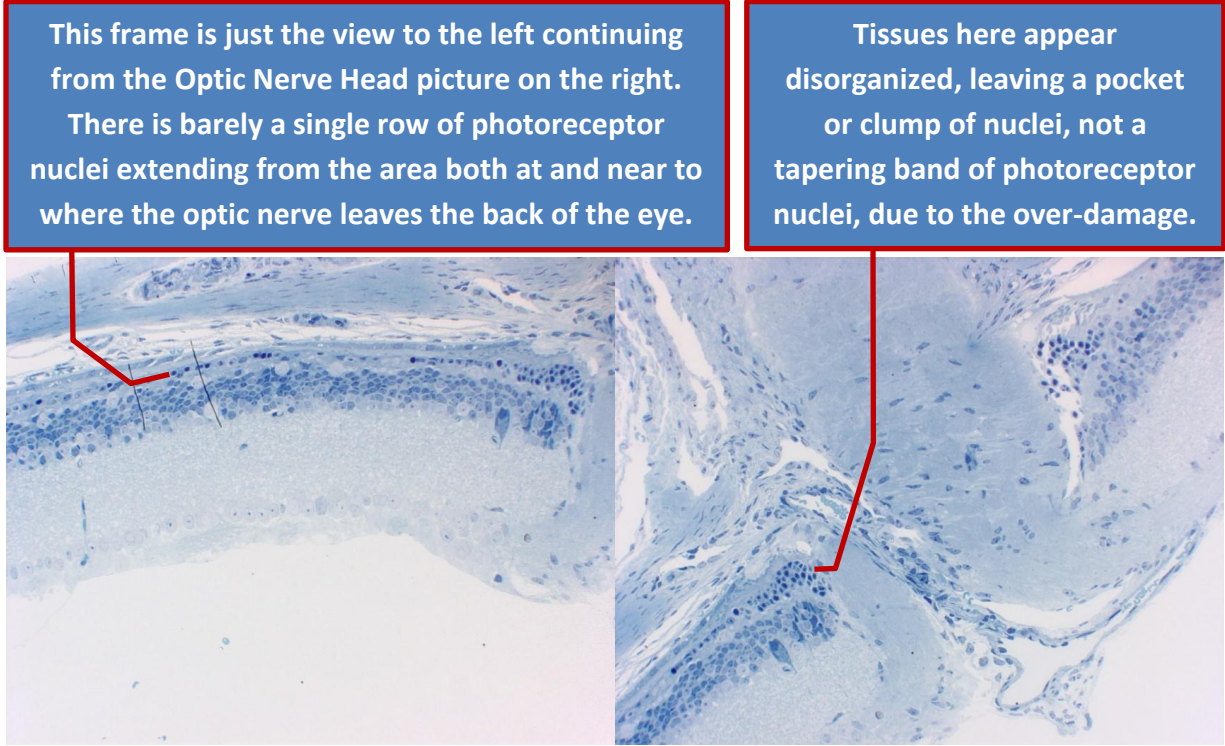


Figure 2.2.11: Side by Side Comparison of Stained 48-Hour Exposures of Peri-papillary Region Versus Optic Nerve Head Region of Albino Mice.

# **THE FUTURE: CHAPTER 3.1**

## **THE RATIONALE FOR IMPROVING LIGHT TOXICITY CHAMBERS DESIGNS**

The scope of much of the light toxicity chamber experiments has revolved around rod cell photoreceptors for two reasons: 1) Rod cells are easier to harm with moderate intense light than cone photoreceptors, thereby requiring less sophisticated equipment. 2) Rod cells happen to be the main photoreceptor found in many of the common research animals, therefore rod dominated animal research is more typical and less costly.

But, for humans who are daylight creatures, the hardy cone cell is the dominate photoreceptor, and, even more importantly, it is the only photoreceptor used when reading. The center of vision, called the fovea, is packed only with cone cells (no rod cells are present there) and has the greatest ratio of signal pathways to the brain, so, if the first 1% of retinal surface area from the center of vision is lost, a person cannot read (unless the letters are huge). The fovea utilizes 50% of all the available signal pathways to the brain in the optic nerve. This is why researchers are seeking to understand the cone cell more as fovea cone death is very devastating to humans.

Cone cells share similarities with rod cells but are not exactly the same; "...the possibility exists that there are distinctly different light damage mechanisms in rods and cones." [See reference 2, *Retinal light Damage: Mechanisms and protection* go to page 125 just before point 5.2].

Researchers who have experimented on cones can do so by selecting the color of light a cone is most sensitive to, but the problem to selectively damage cones in cone dominated animals has proven difficult as these cells are very robust. A certain researcher once found that he didn't have a bright enough light source capable of inducing light damage in a cone dominant, wild, gray squirrel's retina: "Eight hours of 15,000 lux white light in unrestrained animals, or 2h of 20,000 lux white light in an anesthetized dilated animal, produced no substantial evidence of light damage..." [See reference 2 *Retinal Damage: Mechanisms and protection* go to page 123 just before point 4.2.1].

My belief is that light toxicity chambers that can exceed direct sunlight intensities (direct sunlight ranges from 32,000 to 130,000 LUX [13]) while being monochromatic to optimize effectiveness and reduce surface radiant heating will be needed to do more research into the cone realm, and the engineering will be challenging, as radiant heating of surfaces will require much cooling and sophisticated temperature controls.

Although I have not read of research employing pulsed light, in my opinion as an Electrical Engineer, pulsed light sources could help address the radiant heat issue by optimizing light admittance to the retina, if synchronization with the natural dark adaption reflex is possible and utilized, in unrestrained non-drugged animals. LED's would be ideal for this kind of short duty cycle, high intensity pulsing, supplying peak values many times greater than direct sunlight, being monochromatic and able to saturate selective cone cells.

One guiding rationale behind the design of the redesigned chamber described in this paper was to intentionally provide light intensities that are multifold greater than Dr. Noell's light toxicity chamber as mice with various genetic conditions demonstrate different resistances to light damage. Thus, a brighter light toxicity chamber might open the door to new research on animals which Dr. Noell's chamber could not effectively provide.

Because I believe future research is being held back by inadequate light toxicity chambers, any future work on my part to design another light toxicity chamber will be focused on making the brightest chamber I could, employing some of the lessons I learned from building my first light toxicity chamber, as this first chamber is presently only using half of the available capacity of the LED's. This limitation is due to direct optical heating of the cage, when approaching the full output capacity of the redesigned chamber's LED's.

## **THE FUTURE: 3.2**

# **IMPROVEMENTS FOR THE REDESIGNED CHAMBER**

As I was designing and constructing the redesigned chamber, I came up with ideas as to how the next redesigned chamber should be designed. Also, I received constructive criticisms from the committee members. Below is the wish list with comments.

- 1) Design the next redesigned chamber to be able to accommodate either a mouse or rat cage, as both of these animals have frequent utility in light damage experiments. A rat cage looks identical to a mouse cage but has linear dimensions that are 1.625 times larger, which means that the second redesigned chamber's linear dimensions will also have to be about 1.7 times greater.
- 2) Build it lighter. The redesigned chamber's clam and light rack together weighs 116 lbs. With a linear increase of 1.625 to accommodate a rat cage, the chamber wall sheets will weight 2.64 times more. Switching to aluminum will bring the final weight to 88% of the original weight, and, if we also use half sheet thickness, this will bring the weight to 44% of the original redesigned chamber, which is 51 lbs. However, other desired design modifications for a second redesigned chamber may add a further unknown amount of weight.
- 3) Add more LED's to reduce weight and heat load. At 100 LUX the redesigned chambers LEDs provide 294 LUX per watt, but at 10,800 LUX this drops to 135 LUX per watt: power at this LUX value is only half of the full rated power these LEDs can be supplied. Instead

of half rated power, I would limit the next redesigned chamber's LEDs to be driven at a maximum of 25% of their full rated ability. Cyan GaInN LED's suffer from a significant efficacy drop at higher current values than when compared to other LED technologies. The current redesigned chamber's are surface mounted on  $\frac{1}{4}$  inch aluminum stock to facilitate heat removal. If these devices were only driven maximally at 25%, this could open the door to using a lighter gage stock aluminum, and reduce weight, but this would add cost as each LED costs \$3.00 and would require more delicate soldering.

- 4) Assemble the clam with fasteners only. Welding or brazing steel or brazing aluminum changes the sheet shape and adds inaccuracy into the final product, meaning that parts must be made to have loose fit to accommodate warping. Fasteners will add cost, but the final results will be better fitting parts. Initially, I was pursuing brazing aluminum, but heat control and part support were hard to achieve to prevent excessive warping while brazing. Fortunately, 10 gauge steel greatly resists warping while welding and made my redesigned chamber fit together reasonably well, but this also made it heavy.



**Figure 3.2.1: Experimenting with Brazing Aluminum to Build the Redesigned Chamber Clam**

- 5) Automate the cooling fans. The redesigned chamber has 3 switches for operating 9 fans. (See Appendix A for more details.) I was told the researcher prefers machines that are

simple and perform needed functions without operator's intervention. I would recommend that the next redesigned chamber's cooling fans operate by reacting to the detection of any internal clam temperature higher than the external clam temperature. This would cause the fans to automatically begin to blow at low velocity and then incrementally reach full velocity if the temperature difference exceeds one degree.

- 6) Add a digital readout displaying the exhaust air temperature leaving the clam. Although there will be turbulence mixing clam intake air with internal cage air, this mixing will not be perfect, and the air temperature inside the hottest place in the cage will be hotter than clam exhaust air. But, by knowing clam exhaust air temperature, at least there is an approximate idea of what the cage's internal temperature is.
- 7) Add a digital readout displaying LUX. This is possible, but more details will have to be decided upon. For example, it is impossible to light all surfaces in the cage at the exact same LUX value, but it is possible to light the four corners of the cage at the same LUX value, as this is what the present redesigned chamber does. This leaves a darker region in the dead center of the cage. (See Appendix A for more information on this.) It will have to be decided where the LUX value is read from, maybe the cage dead center or possibly the corners or another place. My borrowed handheld LUX meter is presently doing this function but is not a part of the permanent design of the chamber.
- 8) Increase LUX homogeneity by redesigning the cage feeder and waterer to reduce shadowing. By simply narrowing, elevating, and centering the feeder and waterer more, by either adjusting the existing cage cover design or by reinventing a new cage cover, the LUX homogeneity could be quite improved on. Currently, there is about half a foot

of empty volume above the cage in the chamber clam, allowing for a narrower and vertically arranged feeder holder and waterer.

- 9) Utilize DIN rail and Circuit Card Rack construction. If a final design is known, then using the smallest and least expensive boxes for containing controls and electronics makes sense, but, usually, custom-made machines are vulnerable to later changes. Circuit card racks with empty slots provide flexibility for the later inspiration which always occurs, and an oversized control cabinet which uses DIN rail to mount components on would do likewise. These well proven machine builders' methods have evolved over years of experience, although the temptation is always to save money and size and skip these methods. The present redesigned chamber suffers from inflexibility as the boxes holding the electronics and controls are small because it doesn't use the aforementioned builders' techniques, as the view to save on cost, weight and size prevailed this time.
- 10) Spend more for precision OPAMP chips to make a steadier Constant Current Driver for the LED's. The offset in the cheap OPAMP chips employed in the redesigned chamber's constant current LED drivers requires a resistor on the negative input. But, this method of nullifying the offset also made these current sources inversely dependent on the supply voltage. Thus, increasing the draw of current from one light zone will cause a slight decline in rail-to-rail supply voltage, resulting in the other current sources reacting by driving more current to the LEDs in the other light zones of the redesigned chamber. Although these slight changes have no real effect on the operation of the chamber from an operator's point of view, such a flaw in design cannot be tolerated if this chamber were ever modified to employ software to adjust the ratios of each light zone to achieve

lighting homogeneity. I modeled the light zones with a matrix of linear simultaneous equations which determined the ratio of currents to be fed to the eight light zones to cause the cage lighting to be the same in the 4 cage corners. However, because of the offset nullifying circuit, it produced repeatedly consistent results with around 5% error or less. To reduce this error, I had to experimentally adjust the light zones to determine the ratios that would give me results that had consistently 3% error or less, as the simultaneous equations assume simple linearity which linearity is degraded by the offset nullifying circuit. This means that the flawed constant current circuit would not work well with a system of linear equations and software based on those equations, should, at a future point in time, this redesigned chamber arrive at this amount of automation, where it could readjust and set lighting zone ratios on the fly to account for various cage arrangements of food or without food or other objects being moved around the cage. The next redesigned chambers current drivers will be designed with rail-to-rail, zero-offset OPAMPs to reduce the amount of components and will make for more ideal mathematical modeling. Consequently, light zone intensity ratios could be accurately automated through software if desired, or, minimally, this would make for a better power supply voltage rejection for the LED current drivers.

11) Use only one control knob to adjust the light intensity. My initial circuit drawings consisted of one over-all light intensity adjustment followed by four individual adjustments to balance each zone. Initially, I hoped all of these adjustments would fit into one box. But, due to using this small box, limiting surface for controls, I dropped this idea and went with only four balancing adjustments. After experimentation and

more thought, I added two more boxes and decided to go with 8 adjustable light zones which required eight adjustments. The reason I dropped the one adjustment in favor of the 8 is that I didn't know if the ratios of the light zones would remain the same, as each light zone is being driven at a different current and is, therefore, on a different part of the Current/Lumen curve. If this curve were a perfectly straight line these ratios would remain as a constant despite the over-all intensity settings. But this is not the case: as mentioned before in item 3 of this wish list, the efficiency of these devices can swing two fold when driven from minimum to maximum power.

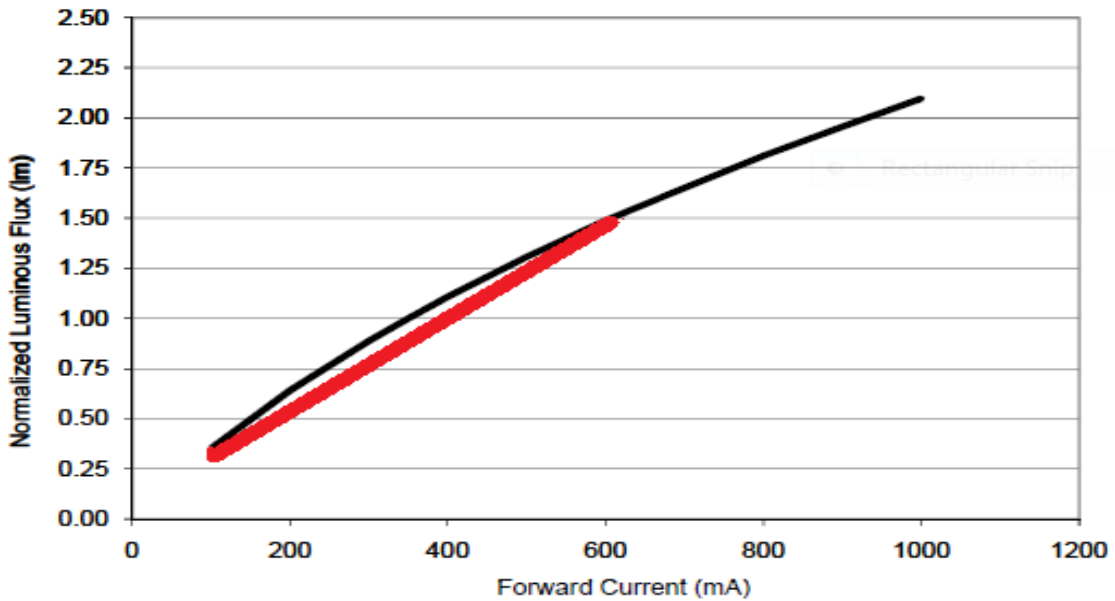


**Figure 3.2.2: LED Output versus Current Input (see Appendix C).**

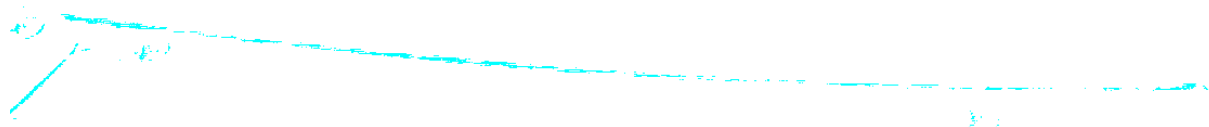
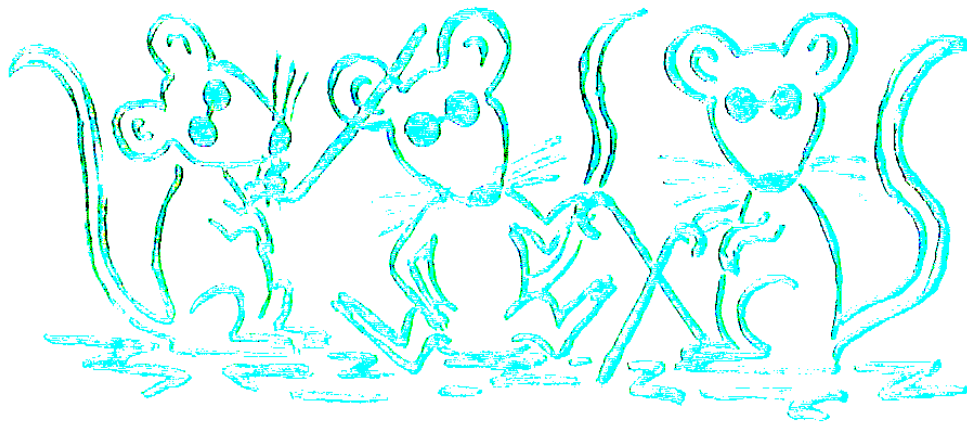
After much experimentation, it was found that the errors introduced by keeping the ratios fixed while proceeding through the full range of intensities was very small. Therefore, one over-all current control is possible, but, in some way, there also needs to be access to adjusting all eight zones to accommodate ratios that may change as different arrangements in cage layout might occur. The operators would have to decide

how they would like to see the controls arranged to do this, but I imagine that, within a large control panel (behind its closed lid), the eight individual light zone balancing adjustments could be placed, and the one individual over-all adjustment could be placed externally on the control panel, along with all the desired digital readouts.

# APPENDIX A

## THE OPERATION MANUAL FOR THE REDESIGNED LIGHT TOXICITY CHAMBER FOR MICE

# Operation Manual For The Light Toxicity Chamber For Mice



# Operation Manual For The Light Toxicity Chamber For Mice

Manual Version: 2.28.2011

Machine Type:

64 Cyan LEDs @ 505 nm

Bandwidth 30 nm

Five Hundred LUX to 10,800 LUX

1.78 to 79.7 Watts LED Power

8 Separate Adjustable Light Zones

All Nine Cooling Fans @ 25.92 Watts Total Power

by Alan Haungs

# Table of Contents

Page 4:	Cooling Fans
Page 4:	Operating a Light Zone
Page 5:	Adjusting all 8 Light Zone Intensities to Achieve a Desired Value of LUX in the 4 Corners of the Cage
Page 9:	Helpful Hints
Page 11:	Attention! Beware When Moving the Light Toxicity Chamber!
Page 12:	Chart: Electrical Currents Required to Generate the Desired LUX Value
Page 19	Pictures Showing Cage Installation

### Cooling Fans

Nine cooling fans are located in the bottom of the clam shell, arranged in such a manner as to force air upward. Air is drawn in from the bottom of the lower half of the clam shell, then blown past the cage and LED rack, where it then proceeds to the top of the clam shell and is forced out. These fans are controlled by 3 switches on the right side of the lower clam shell and are mounted on the Unistrut rail. They are labeled as; "2 FANS", "3 FANS" and "4 FANS" (see signage). By using on/off combinations of these three switches, one can operate either zero, two, three, four, five, six, seven or all nine fans at once.

The fans are powered by a 12 volt DC power supply which plugs into the lower right Unistrut rail in its far back end, labeled as "12 VDC" (see signage). The chart provided with this Operator's Manual that shows desired LUX levels versus the required Current levels, assume that the operator has all 9 fans operating. With fewer than 9 fans operating at once, the above ambient air temperature rise will be higher in the Light Toxicity Chamber than listed on the LUX/Current Chart.

The 1's and 0's listed next to these fan switches give an indication as to which fans will be operated by that switch. For example, the "2 FANS" (see signage) switch is labeled "10000001". This means that this switch controls the two outermost fans located in the row of fans found in the bottom center of the lower clam half.

### Operating a Light Zone

The LED light sources are powered by two 24 Volt DC power supplies, which plug into the receptacles located behind the leftmost control knob panel, labeled as "Upper Control". These receptacles are labeled as "24 VOLTS DC" (see signage).

The LEDs will not operate unless the upper half of the chamber is fully lowered and closed. There are two ways to over-ride this feature. The first is to depress the red button on the center control panel labeled "INTERLOCK OVER-RIDE" (see signage). This will also allow the LEDs to operate (assuming the appropriate switches are on and the appropriate knobs are turned to an intensity greater than zero).

The second way to operate the LEDs while the clam is open is to find the small box labeled "LID SAFETY INTERLOCK", located on the center control panel, next to the red "INTERLOCK OVER-RIDE" switch. The "LID SAFETY INTERLOCK" is a magnetically controlled switch, therefore by placing a magnet near this "LID SAFETY INTERLOCK", it will be interpreted by the safety control circuitry the same as if the clam lid is closed, which will allow the LEDs to operate. Understanding this might be helpful for troubleshooting

## APPENDIX\_A

---

purposes should one desire the LEDs to light with the clam opened while freeing the hand which otherwise would have been needed to depress the "INTERLOCK OVER-RIDE" switch.

Normally the LEDs are operated with the clam fully closed for the containment of the maximum light within the Toxicity Chamber. Also, this protects operator's eyes from light shock and fatigue and prevents unwanted light pollution in the Lab.

There are 8 light zones controlled by 8 knobs and 8 switches. For example, if one wants to illuminate the **upper North West zone**, one would merely have to flip on the switch associated with the upper North West zone, located on the left control panel labeled "UPPER CONTROL", and turn the knob labeled "NW" clockwise. The switch layout is shown under the phrase "SWITCH ORDER" (see signage). Doing this will cause the upper NW zone to light up, if the clam is closed, or the "INTERLOCK OVER-RIDE" is depressed if the chamber is opened. This will also cause the ammeter located on this same control panel to deflect, indicating that electrical current is being delivered to the North West zone.

The reading on the ammeter will reflect approximately 1/7 of the actual current being delivered, thus a reading of 70 milliamps would in fact be an indication of 10 milliamps of delivered current. Unless one depresses the button on the "UPPER CONTROL" panel labeled "DEPRESS TO MEASURE CURRENT", (see signage), which will cause the ammeter to measure the actual electrical current accurately

The "UPPER CONTROL" panel controls the LED light zones that shine light in an upward manner. These LEDs are located on the LED holding rack above the LEDs controlled by the "LOWER CONTROL" Panel.

The "LOWER CONTROL" panel controls the LED light zones that shine light in a downward manner. These LEDs are located on the LED holding rack below the LEDs controlled by the "UPPER CONTROL" panel.

## **Adjusting All Eight Light Zone Intensities to Achieve a Desired Value of LUX in the Four Corners of the Cage**

The Chart labeled, *Electrical Currents Required to Generate the Desired LUX Value*, is in the end pages of this manual, which lists the currents needed to achieve the DESIRED LUX in the four corners of the mouse cage. Included in each row of this chart is the amount of RESULTANT LUX found in the darkest area under the waterer; as well as the RESULTANT LUX value in the dead center of the cage; the amount of RESULTANT WATTS being consumed by the LEDs in order to achieve the given LUX values; and the amount of ABOVE AMBIENT AIR ROOM TEMPERATURE RISE.,

### Start of Process

- 1) Chose a Desired LUX Value.
- 2) Note that you will be reading chart Current Values left to right in the applicable Desired LUX row, and you will be physically adjusting Current Values left to right, then top to bottom on the control panels, in the same manner one reads a book. Doing so makes the adjustments very natural and faster, and will ensure accurate results.

#### Template of Action: UPPER NORTH WEST ZONE

- 3) Start with All switches in the OFF POSITION, the clam door is closed, and all power supplies are plugged in.
- 4) To set the Current value for the **Upper North West zone**, flip on **Upper North West zone** switch only.
- 5) Use your thumb to depress panel button labeled DEPRESS TO MEASURE CURRENT on the UPPER CONTROL panel.
- 6) Adjust the knob labeled **NW** on the UPPER CONTROL panel to achieve the Required Current on the ammeter on the UPPER CONTROL panel.
- 7) Release the DEPRESS TO MEASURE CURRENT switch.
- 8) Turn off the **Upper North West zone** switch. All switches are off at this point.

#### 1st Iteration: UPPER NORTH EAST ZONE

- 9) Start with All switches in the OFF POSITION, the clam door is closed, and all power supplies are plugged in.
- 10) To set the Current value for the **Upper North East zone**, flip on **Upper North East zone** switch only.
- 11) Use your thumb to depress panel button labeled DEPRESS TO MEASURE CURRENT on the UPPER CONTROL panel.
- 12) Adjust the knob labeled **NE** on the UPPER CONTROL panel to achieve the Required Current on the ammeter on the UPPER CONTROL panel.
- 13) Release the DEPRESS TO MEASURE CURRENT switch.
- 14) Turn off the **Upper North East zone** switch. All switches are off at this point.

## APPENDIX\_A

---

### 2nd Iteration: UPPER SOUTH WEST ZONE

- 15) Start with All switches in the OFF POSITION, the clam door is closed, and all power supplies are plugged in.
- 16) To set the Current value for the **Upper South West zone**, flip on **Upper South West zone** switch only.
- 17) Use your thumb to depress panel button labeled DEPRESS TO MEASURE CURRENT on the UPPER CONTROL panel.
- 18) Adjust the knob labeled **SW** on the UPPER CONTROL panel to achieve the Required Current on the ammeter on the UPPER CONTROL panel.
- 19) Release the DEPRESS TO MEASURE CURRENT switch.
- 20) Turn off the **Upper South West zone** switch. All switches are off at this point.

### 3rd Iteration: UPPER SOUTH EAST ZONE

- 21) Start with All switches in the OFF POSITION, the clam door is closed, and all power supplies are plugged in.
- 22) To set the Current value for the **Upper South East zone**, flip on **Upper South East zone** switch only.
- 23) Use your thumb to depress panel button labeled DEPRESS TO MEASURE CURRENT on THE UPPER CONTROL panel.
- 24) Adjust the knob labeled **SE** on the UPPER CONTROL panel to achieve the Required Current on the ammeter on the UPPER CONTROL panel.
- 25) Release the DEPRESS TO MEASURE CURRENT switch.
- 26) Turn off the **Upper South East zone** switch. All switches are off at this point.

### 4th Iteration: LOWER NORTH WEST ZONE

- 27) Start with All switches in the OFF POSITION, the clam door is closed, and all power supplies are plugged in.
- 28) To set the Current value for the **Lower North West zone**, flip on **Lower North West zone** switch only.
- 29) Use your thumb to depress panel button labeled DEPRESS TO MEASURE CURRENT on the LOWER CONTROL panel.
- 30) Adjust the knob labeled **NW** on the Lower Control panel to achieve the Required Current on the ammeter on the LOWER CONTROL panel.

## APPENDIX\_A

---

31) Release the DEPRESS TO MEASURE CURRENT switch.

32) Turn off the **Lower North West zone** switch. All switches are off at this point.

### 5th Iteration: **LOWER NORTH EAST ZONE**

33) Start with All switches in the OFF POSITION, the clam door is closed, and all power supplies are plugged in.

34) To set the Current value for the **Lower North East zone**, flip on **Lower North East zone** switch only.

35) Use your thumb to depress panel button labeled DEPRESS TO MEASURE CURRENT on the LOWER CONTROL panel.

36) Adjust the knob labeled **NE** on the LOWER CONTROL panel to achieve the Required Current on the ammeter on the LOWER CONTROL panel.

37) Release the DEPRESS TO MEASURE CURRENT switch.

38) Turn off the **Lower North East zone** switch. All switches are off at this point.

### 6th Iteration: **LOWER SOUTH WEST ZONE**

39) Start with All switches in the OFF POSITION, the clam door is closed, and all power supplies are plugged in.

40) To set the Current value for the **Lower South West zone**, flip on **Lower South West zone** switch only.

41) Use your thumb to depress panel button labeled DEPRESS TO MEASURE CURRENT on the LOWER CONTROL panel.

42) Adjust the knob labeled **SW** on the LOWER CONTROL panel to achieve the Required Current on the ammeter on the LOWER CONTROL panel.

43) Release the DEPRESS TO MEASURE CURRENT switch.

44) Turn off the **Lower South West zone** switch. All switches are off at this point.

### Final Iteration: **LOWER SOUTH EAST ZONE**

45) Start with All switches in the OFF POSITION, the clam door is closed, and all power supplies are plugged in.

46) To set the Current value for the **Lower South East zone**, flip on **Lower South East zone** switch only.

## APPENDIX\_A

---

47) Use your thumb to depress panel button labeled DEPRESS TO MEASURE CURRENT on the LOWER CONTROL panel.

48) Adjust the knob labeled **SE** on the LOWER CONTROL panel to achieve the Required Current on the ammeter on the LOWER CONTROL panel.

49) Release the DEPRESS TO MEASURE CURRENT switch.

50) Turn off the **Lower South East zone** switch. All switches are off at this point.

### Last Step

51) NOW TURN ON ALL 8 SWITCHES. Your Light Toxicity Chamber is now illuminated in each corner at the value of Desired LUX. Having all nine 9 fans operating will ensure the above ambient air temperature rise will be of a value listed on the chart.

## END OF PROCESS

## HELPFUL HINTS

1) To make the procedure above faster, one can leave their thumb on the DEPRESS TO MEASURE CURRENT switch, not lifting it off repetitively, but being sure to release it before turning on all the switches simultaneously. Failure to do so will cause the ammeter to measure the total current in all 4 zones controlled by a knob control panel, whose current may exceed the maximum current value on the ammeter. Temporarily over-driving the ammeter will not hurt it, but leaving the DEPRESS TO MEASURE CURRENT switch on indefinitely, while constantly over-driving the ammeter could eventually damage the meter.

2) AFTER COMPLETING CURRENT ADJUSTMENTS, BE CAREFUL NOT TO BUMP THE KNOBS AND ACCIDENTILY MISADJUST THEM WHEN OPENING AND CLOSING THE CLAM LID, AS THIS IS EASY TO DO. If it is suspected that a knob may have been bumped, the quickest way to determine if a knob is misadjusted is to observe the ammeters, while holding the DEPRESS TO MEASURE CURRENT switch, and uniquely turning on the NW switch, then off, then uniquely the NE switch on, then off, and continuing through all the switches, in the same order as listed in the chart, from left to right.

3) When turning off all the light zones in between subsequent experiments requiring the same amount of LUX, do not turn all the knobs to zero current, thus requiring readjusting the knobs again. Instead, turn off all the switches, or partially or completely open the clam lid, or pull out the 24 volt DC power jacks, or unplug the DC power supplies from the wall.

## APPENDIX\_A

---

4.) Regarding the “ABOVE AMBIENT AIR TEMPERATURES RISES”, A dual probe digital thermometer was used to measure and record the maximum difference of the ambient room air temperature from the internal cage while the chamber operated and obtained a steady state temperature rise.

In this experiment, the “ABOVE AMBIENT AIR TEMPERATURES RISES” that were recorded and interpolated in the chart labeled “*ELECTRICAL CURRENTS REQUIRED TO GENERATE THE DESIRED LUX VALUE*”, were taken from a home laboratory during winter months where there was a constant change in ambient air temperature due to the home heating cycle. Heating cycles in the home lab occur as often as every half hour, while the toxicity chamber takes at least three hours to achieve a steady state temperature. Ambient air temperature can rise and fall faster than the toxicity chamber's ABOVE AMBIENT AIR TEMPERATURE can rise and fall. These different rates of temperature change tend to exaggerate the result of the recorded maximum ABOVE AMBIENT AIR TEMPERATURE RISE.

The results were also affected by any slight movement of air, whether it was the opening of a door, entering the room stirring the cooler air from the floor, or the furnace blower turning on. By observation it was noted that by entering the room, causing air movement and mixture, there was an immediate, short lived, transient of about 1° F which was then superimposed on top of the already existing exaggerated temperature difference and then recorded as the maximum ABOVE AMBIENT AIR TEMPERATURE RISE. These transients further exaggerated the results.

Because of this constantly varying specific environment, the chart reflects the worse case ABOVE AMBIENT AIR TEMPERATURE RISE observed in a specific home/lab during a specific time, and thus the ABOVE AMBIENT AIR TEMPERATURE RISES in the chart can only be used as a general guide. Worse case ABOVE AMBIENT AIR TEMPERATURE RISES, that are measured at the VA hospital may differ from the chart depending on the speed, depth and duration of temperature fluctuations from the heating/cooling cycles of the specific experimental environment at the hospital.

If a more accurate numerical temperature gauge is desired, I would recommend using a Charting Thermometer, or one that is capable of storing the internal cage temperature history electronically while the chamber is in use during the light experiments on the mice. The priority of average or maximum cage temperature should be decided, as a constant steady state cage temperature is not likely achievable. Also determining whether the ABOVE AMBIENT AIR TEMPERATURE RISE is dangerous may be through observing the behavior of the mice. Note if they are showing signs of heat stress by sprawling open.

The “ABOVE AMBIENT AIR TEMPERATURES RISES” values are color coded based on the assumption that the VA Hospital’s labs are maintained accurately at 72°F and that heat stress will definitely occur at temperatures 80°F or higher. Raises in temperature of up to 3°F are acceptable and are highlighted in green. Raises in temperature from 3°F to 6°F are not ideal, but may be acceptable and are highlighted in yellow. Raises in temperature exceeding 6°F are cause for concern and are highlighted in red.

## **ATTENTION! BEWARE WHEN MOVING THE LIGHT TOXICITY CHAMBER!**

*For examination or transport purposes, the LED rack simply lifts out of the lower clam half and is kept there by gravity alone. It is recommended to lift the LED rack out of the clam if the chamber is going to be moved from one surface to another, especially if moving to different elevations. Doing so will make the clam lighter, and reduce the risk of the clam and the LED rack separating during lifting and causing a dropping incident. Although one strong person can lift and move this entire chamber, being 116 pounds all together, it would be best to use two strong persons, when moving the clam, even with the LED rack already removed, to prevent bodily strain as the clam is large and awkward to handle. (Clam weight 91 lbs, LED rack 25 lbs).*

*Tipping the clam during movement WILL cause the clam to open as the clam lid is counter balanced by a gas charged cylinder to make the clam lid lift easier. This cylinder has allot of force and beware of it. Furthermore pulling on the gas cylinder sideways, using it as a handle for moving purposes, can bend its shaft, which would cause the gas spring to malfunction and need replacement.*

**And finally, now safely enjoy using your new Light Toxicity Chamber for many years!**

ELECTRICAL CURRENTS REQUIRED TO GENERATE THE DESIRED LUX VALUE (Assuming Full Waterer and Empty Feeder Bin) Version 2.18.2011 Page 1																
DESIRED LUX	RESULTANT LUX		RESULTANT WATTS	RESULTANT DEGREES F	REQUIRED MILLIAMPS FOR UPPER CONTROL PANEL						REQUIRED MILLIAMPS FOR LOWER CONTROL PANEL					
	Value in the Dead Center of Cage	Value of Darkest Region Under Waterer			North West Zone	North East Zone	South West Zone	South East Zone	North West Zone	North East Zone	South West Zone	South East Zone				
100	77	57	0.34	0.1	2.2	2.2	2.2	2.2	2.2	2.2	2.2	1.8	2.2	0.8	0.9	
200	153	113	0.69	0.2	4.4	4.4	4.4	4.4	4.4	4.4	4.4	3.7	4.4	1.6	1.8	
300	230	170	1.05	0.3	6.6	6.6	6.6	6.6	6.6	6.6	6.6	5.5	6.6	2.4	2.8	
400	306	227	1.41	0.4	8.9	8.9	8.9	8.9	8.9	8.9	8.9	7.5	8.9	3.2	3.7	
500	383	283	1.78	0.5	11	11	11	11	11	11	11	9.4	11	4.0	4.7	
600	460	340	2.16	0.6	14	14	14	14	14	14	14	11	14	4.9	5.7	
700	536	396	2.55	0.7	16	16	16	16	16	16	16	13	16	5.8	6.7	
800	613	453	2.94	0.8	19	19	19	19	19	19	19	16	19	6.7	7.8	
900	689	510	3.35	0.9	21	21	21	21	21	21	21	18	21	7.6	8.8	
1000	766	566	3.75	1.0	24	24	24	24	24	24	24	20	24	8.5	9.9	
1100	843	623	4.17	1.1	26	26	26	26	26	26	26	22	26	9.4	11	
1200	919	680	4.59	1.2	29	29	29	29	29	29	29	24	29	10.4	12	
1300	996	736	5.03	1.3	32	32	32	32	32	32	32	27	32	11	13	
1400	1072	793	5.46	1.4	34	34	34	34	34	34	34	29	34	12	14	
1500	1149	850	5.91	1.5	37	37	37	37	37	37	37	31	37	13	16	
1600	1226	906	6.36	1.6	40	40	40	40	40	40	40	34	40	14	17	
1700	1302	963	6.82	1.7	43	43	43	43	43	43	43	36	43	15	18	
1800	1379	1019	7.29	1.8	46	46	46	46	46	46	46	39	46	17	19	

**ELECTRICAL CURRENTS REQUIRED TO GENERATE THE DESIRED LUX VALUE  
(Assuming Full Waterer and Empty Feeder Bin) Version 2.18.2011 Page 2**

DESIRED LUX	RESULTANT LUX		RESULTANT WATTS	RESULTANT DEGREES F	REQUIRED MILLIAMPS FOR UPPER CONTROL PANEL				REQUIRED MILLIAMPS FOR LOWER CONTROL PANEL			
	Value in the Dead Center of Cage	Value of Darkest Region Under Waterer			North West Zone	North East Zone	South West Zone	South East Zone	North West Zone	North East Zone	South West Zone	South East Zone
1900	1455	1076	7.77	1.9	49	49	49	49	41	49	18	21
2000	1532	1133	8.25	2.0	52	52	52	52	44	52	19	22
2100	1609	1189	8.74	2.1	55	55	55	55	46	55	20	23
2200	1685	1246	9.24	2.2	58	58	58	58	49	58	21	24
2300	1762	1303	9.74	2.3	61	61	61	61	52	61	22	26
2400	1838	1359	10.3	2.4	65	65	65	65	54	65	23	27
2500	1915	1416	10.8	2.5	68	68	68	68	57	68	24	28
2600	1992	1473	11.3	2.5	71	71	71	71	60	71	26	30
2700	2068	1529	11.8	2.6	74	74	74	74	63	74	27	31
2800	2145	1586	12.4	2.7	78	78	78	78	65	78	28	33
2900	2221	1643	12.9	2.8	81	81	81	81	68	81	29	34
3000	2298	1699	13.5	2.9	85	85	85	85	71	85	31	36
3100	2375	1756	14.0	3.0	88	88	88	88	74	88	32	37
3200	2451	1812	14.6	3.1	92	92	92	92	77	92	33	39
3300	2528	1869	15.2	3.1	96	96	96	96	80	96	34	40
3400	2604	1926	15.8	3.2	99	99	99	99	83	99	36	42
3500	2681	1982	16.4	3.3	103	103	103	103	87	103	37	43
3600	2758	2039	17.0	3.4	107	107	107	107	90	107	38	45

**ELECTRICAL CURRENTS REQUIRED TO GENERATE THE DESIRED LUX VALUE  
(Assuming Full Waterer and Empty Feeder Bin) Version 2.18.2011 Page 3**

DESIRED LUX	RESULTANT LUX		RESULTANT WATTS	RESULTANT DEGREES F	REQUIRED MILLIAMPS FOR UPPER CONTROL PANEL				REQUIRED MILLIAMPS FOR LOWER CONTROL PANEL			
	Value in the Dead Center of Cage	Value of Darkest Region Under Waterer			North West Zone	North East Zone	South West Zone	South East Zone	North West Zone	North East Zone	South West Zone	South East Zone
3700	2834	2096	17.6	3.5	111	111	111	111	93	111	40	46
3800	2911	2152	18.2	3.5	115	115	115	115	96	115	41	48
3900	2987	2209	18.8	3.6	119	119	119	119	100	119	43	50
4000	3064	2266	19.5	3.7	122	122	122	122	103	122	44	51
4100	3141	2322	20.1	3.8	126	126	126	126	106	126	46	53
4200	3217	2379	20.7	3.8	131	131	131	131	110	131	47	55
4300	3294	2435	21.4	3.9	135	135	135	135	113	135	48	57
4400	3370	2492	22.1	4.0	139	139	139	139	117	139	50	58
4500	3447	2549	22.7	4.1	143	143	143	143	120	143	51	60
4600	3524	2605	23.4	4.1	147	147	147	147	124	147	53	62
4700	3600	2662	24.1	4.2	152	152	152	152	127	152	55	64
4800	3677	2719	24.8	4.3	156	156	156	156	131	156	56	65
4900	3753	2775	25.5	4.3	160	160	160	160	135	160	58	67
5000	3830	2832	26.2	4.4	165	165	165	165	138	165	59	69
5100	3907	2889	26.9	4.5	169	169	169	169	142	169	61	71
5200	3983	2945	27.6	4.5	174	174	174	174	146	174	63	73
5300	4060	3002	28.3	4.6	178	178	178	178	150	178	64	75
5400	4136	3058	29.1	4.7	183	183	183	183	154	183	66	77

ELECTRICAL CURRENTS REQUIRED TO GENERATE THE DESIRED LUX VALUE (Assuming Full Waterer and Empty Feeder Bin) Version 2.18.2011 Page 4																
DESIRED LUX	RESULTANT LUX		RESULTANT WATTS LED Electrical Power Usage	RESULTANT DEGREES F Above Ambient Air Temp. Rise in Cage	REQUIRED MILLIAMPS FOR UPPER CONTROL PANEL						REQUIRED MILLIAMPS FOR LOWER CONTROL PANEL					
	Value in the Dead Center of Cage	Value of Darkest Region Under Waterer			North West Zone	North East Zone	South West Zone	South East Zone	North West Zone	North East Zone	South West Zone	South East Zone				
5500	4213	3115	29.8	4.7	188	188	188	188	188	188	158	188	68	79		
5600	4290	3172	30.6	4.8	192	192	192	192	192	192	162	192	69	81		
5700	4366	3228	31.3	4.9	197	197	197	197	197	197	166	197	71	83		
5800	4443	3285	32.1	4.9	202	202	202	202	202	202	170	202	73	85		
5900	4519	3342	32.9	5.0	207	207	207	207	207	207	174	207	74	87		
6000	4596	3398	33.6	5.1	212	212	212	212	212	212	178	212	76	89		
6100	4673	3455	34.4	5.1	217	217	217	217	217	217	182	217	78	91		
6200	4749	3512	35.2	5.2	222	222	222	222	222	222	186	222	80	93		
6300	4826	3568	36.0	5.2	227	227	227	227	227	227	190	227	82	95		
6400	4903	3625	36.8	5.3	232	232	232	232	232	232	195	232	83	97		
6500	4979	3682	37.6	5.3	237	237	237	237	237	237	199	237	85	99		
6600	5056	3738	38.5	5.4	242	242	242	242	242	242	203	242	87	102		
6700	5132	3795	39.3	5.5	247	247	247	247	247	247	208	247	89	104		
6800	5209	3851	40.1	5.5	253	253	253	253	253	253	212	253	91	106		
6900	5286	3908	41.0	5.6	258	258	258	258	258	258	217	258	93	108		
7000	5362	3965	41.8	5.6	263	263	263	263	263	263	221	263	95	111		
7100	5439	4021	42.7	5.7	269	269	269	269	269	269	226	269	97	113		

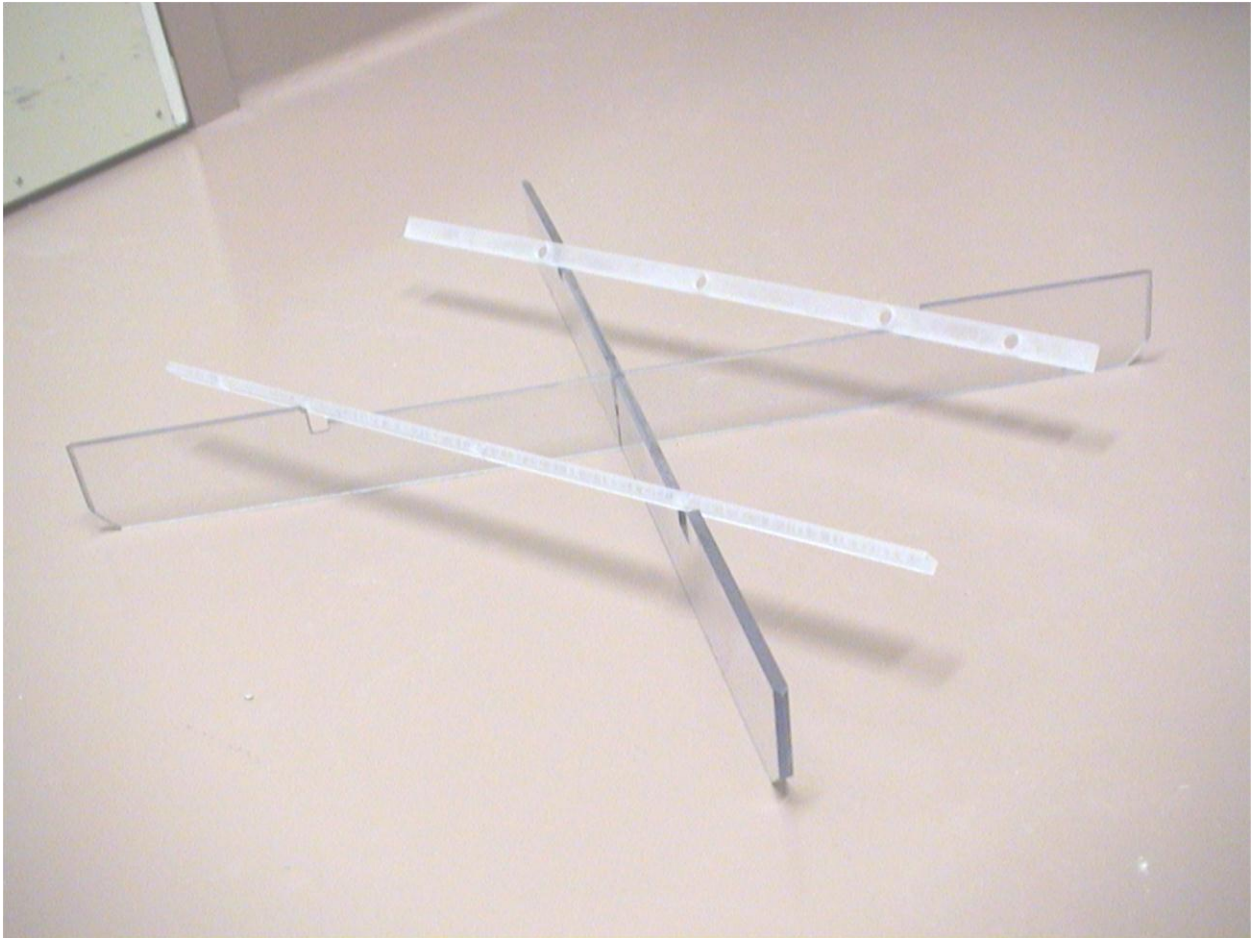
ELECTRICAL CURRENTS REQUIRED TO GENERATE THE DESIRED LUX VALUE (Assuming Full Waterer and Empty Feeder Bin) Version 2.18.2011 Page 5													
DESIRED LUX	RESULTANT LUX		RESULTANT WATTS	RESULTANT DEGREES F	REQUIRED MILLIAMPS FOR UPPER CONTROL PANEL				REQUIRED MILLIAMPS FOR LOWER CONTROL PANEL				
	Value in the Dead Center of Cage	Value of Darkest Region Under Waterer			LED Electrical Power Usage	Above Ambient Air Temp. Rise in Cage	North West Zone	North East Zone	South West Zone	South East Zone	North West Zone	North East Zone	South West Zone
7200	5515	4078	43.6	5.7	274	274	274	274	230	274	99	115	
7300	5592	4135	44.4	5.8	280	280	280	280	235	280	101	117	
7400	5669	4191	45.3	5.8	285	285	285	285	240	285	103	120	
7500	5745	4248	46.2	5.9	291	291	291	291	244	291	105	122	
7600	5822	4305	47.1	5.9	296	296	296	296	249	296	107	125	
7700	5898	4361	48.0	6.0	302	302	302	302	254	302	109	127	
7800	5975	4418	48.9	6.0	308	308	308	308	259	308	111	129	
7900	6052	4474	49.8	6.1	314	314	314	314	263	314	113	132	
8000	6128	4531	50.8	6.1	320	320	320	320	268	320	115	134	
8100	6205	4588	51.7	6.1	325	325	325	325	273	325	117	137	
8200	6281	4644	52.6	6.2	331	331	331	331	278	331	119	139	
8300	6358	4701	53.6	6.2	337	337	337	337	283	337	121	142	
8400	6435	4758	54.5	6.3	343	343	343	343	288	343	124	144	
8500	6511	4814	55.5	6.3	349	349	349	349	293	349	126	147	
8600	6588	4871	56.5	6.3	356	356	356	356	299	356	128	149	
8700	6664	4928	57.5	6.4	362	362	362	362	304	362	130	152	
8800	6741	4984	58.4	6.4	368	368	368	368	309	368	132	155	

ELECTRICAL CURRENTS REQUIRED TO GENERATE THE DESIRED LUX VALUE (Assuming Full Waterer and Empty Feeder Bin) Version 2.18.2011 Page 6																
DESIRED LUX	RESULTANT LUX		RESULTANT WATTS	RESULTANT DEGREES F	REQUIRED MILLIAMPS FOR UPPER CONTROL PANEL						REQUIRED MILLIAMPS FOR LOWER CONTROL PANEL					
	Value in the Dead Center of Cage	Value of Darkest Region Under Waterer			North West Zone	North East Zone	South West Zone	South East Zone	North West Zone	North East Zone	South West Zone	South East Zone				
8900	6818	5041	59.4	6.5	374	374	374	374	374	374	374	314	374	314	374	157
9000	6894	5097	60.4	6.5	380	380	380	380	380	380	380	320	380	320	380	160
9100	6971	5154	61.5	6.5	387	387	387	387	387	387	387	325	387	325	387	162
9200	7047	5211	62.5	6.6	393	393	393	393	393	393	393	330	393	330	393	165
9300	7124	5267	63.5	6.6	400	400	400	400	400	400	400	336	400	336	400	168
9400	7201	5324	64.5	6.6	406	406	406	406	406	406	406	341	406	341	406	171
9500	7277	5381	65.6	6.7	413	413	413	413	413	413	413	347	413	347	413	173
9600	7354	5437	66.6	6.7	419	419	419	419	419	419	419	352	419	352	419	176
9700	7430	5494	67.7	6.7	426	426	426	426	426	426	426	358	426	358	426	179
9800	7507	5551	68.7	6.8	433	433	433	433	433	433	433	363	433	363	433	182
9900	7584	5607	69.8	6.8	439	439	439	439	439	439	439	369	439	369	439	184
10000	7660	5664	70.9	6.8	446	446	446	446	446	446	446	375	446	375	446	187
10100	7737	5721	71.9	6.8	453	453	453	453	453	453	453	380	453	380	453	190
10200	7813	5777	73.0	6.9	460	460	460	460	460	460	460	386	460	386	460	193
10300	7890	5834	74.1	6.9	467	467	467	467	467	467	467	392	467	392	467	196
10400	7967	5890	75.2	6.9	474	474	474	474	474	474	474	398	474	398	474	199
10500	8043	5947	76.3	7.0	481	481	481	481	481	481	481	404	481	404	481	202

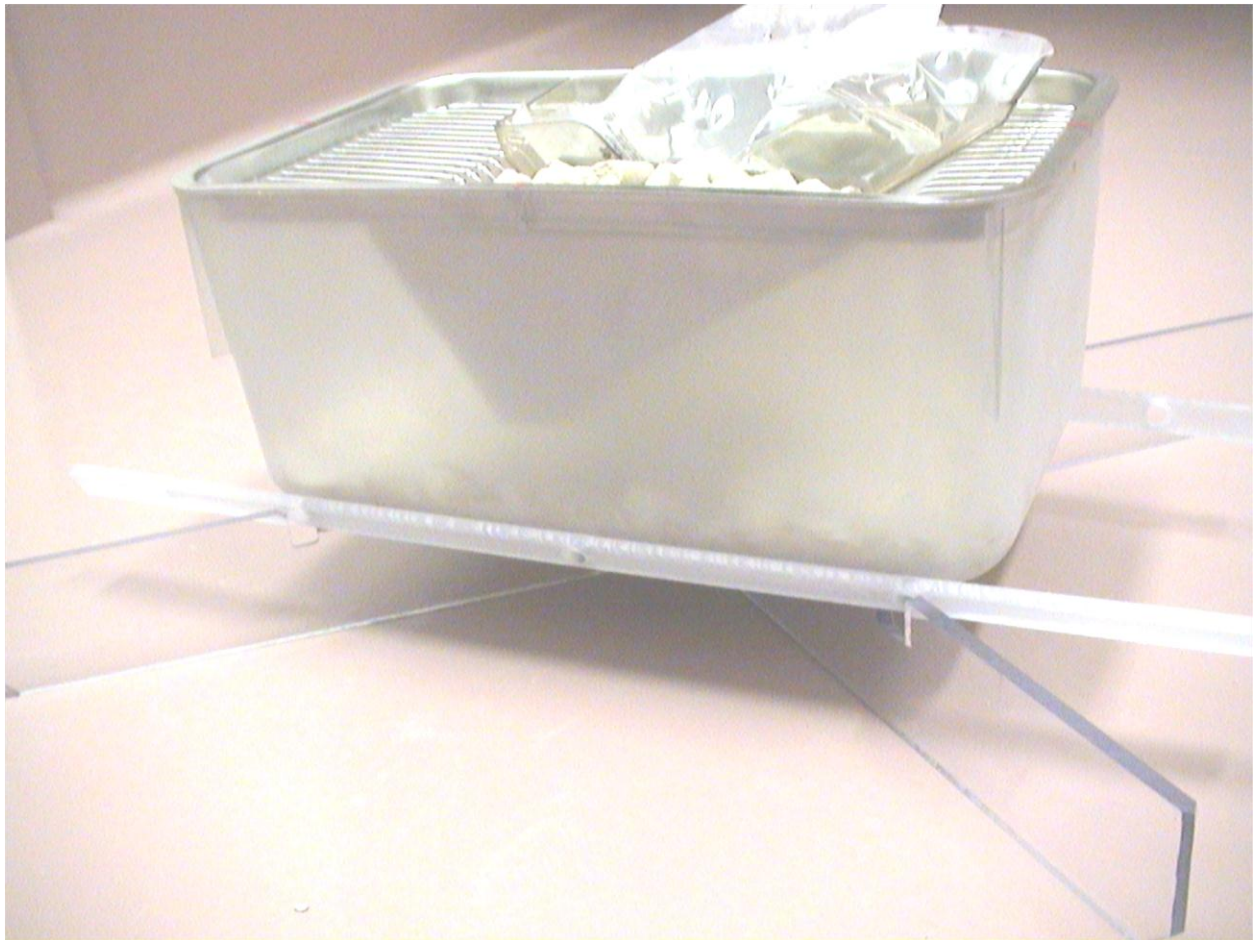
**ELECTRICAL CURRENTS REQUIRED TO GENERATE THE DESIRED LUX VALUE  
(Assuming Full Waterer and Empty Feeder Bin) Version 2.18.2011 Page 7**

DESIRED LUX	RESULTANT LUX		RESULTANT WATTS	RESULTANT DEGREES F	REQUIRED MILLIAMPS FOR UPPER CONTROL PANEL						REQUIRED MILLIAMPS FOR LOWER CONTROL PANEL					
	Value in the Dead Center of Cage	Value of Darkest Region Under Waterer			LED Electrical Power Usage	Above Ambient Air Temp. Rise in Cage	North West Zone	North East Zone	South West Zone	South East Zone	North West Zone	North East Zone	South West Zone	South East Zone		
10600	8120	6004	77.5	7.0	488	488	488	488	488	488	488	488	410	488	176	205
10700	8196	6060	78.6	7.0	495	495	495	495	495	495	495	495	416	495	178	208
10800	8273	6117	79.7	7.0	502	502	502	502	502	502	502	502	422	502	181	211
10900	8350	6174	80.9	7.0	509	509	509	509	509	509	509	509	428	509	183	214
11000	8426	6230	82.0	7.1	516	516	516	516	516	516	516	516	434	516	186	217

## Pictures Showing Cage Installation



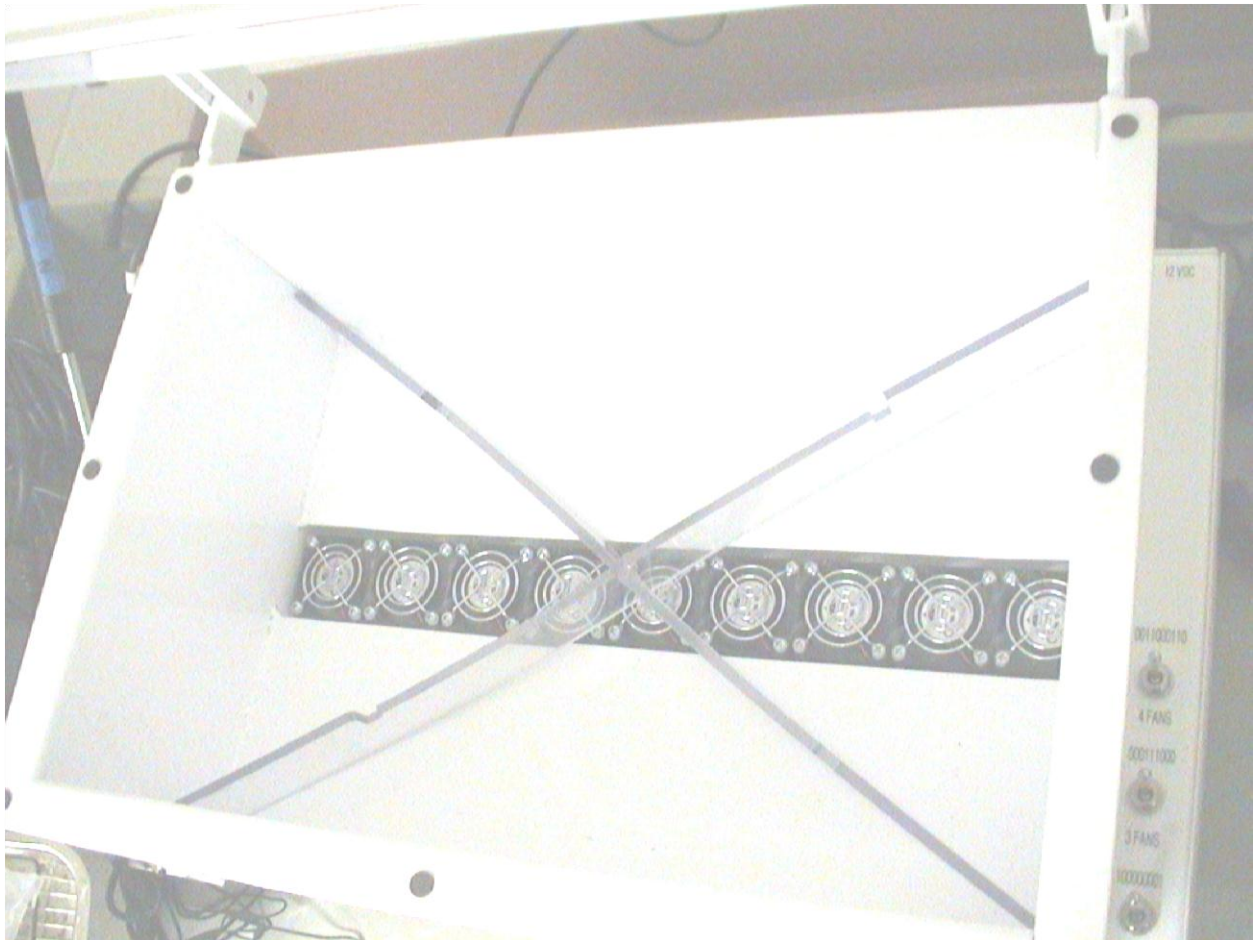
## Pictures Showing Cage Installation



## Pictures Showing Cage Installation



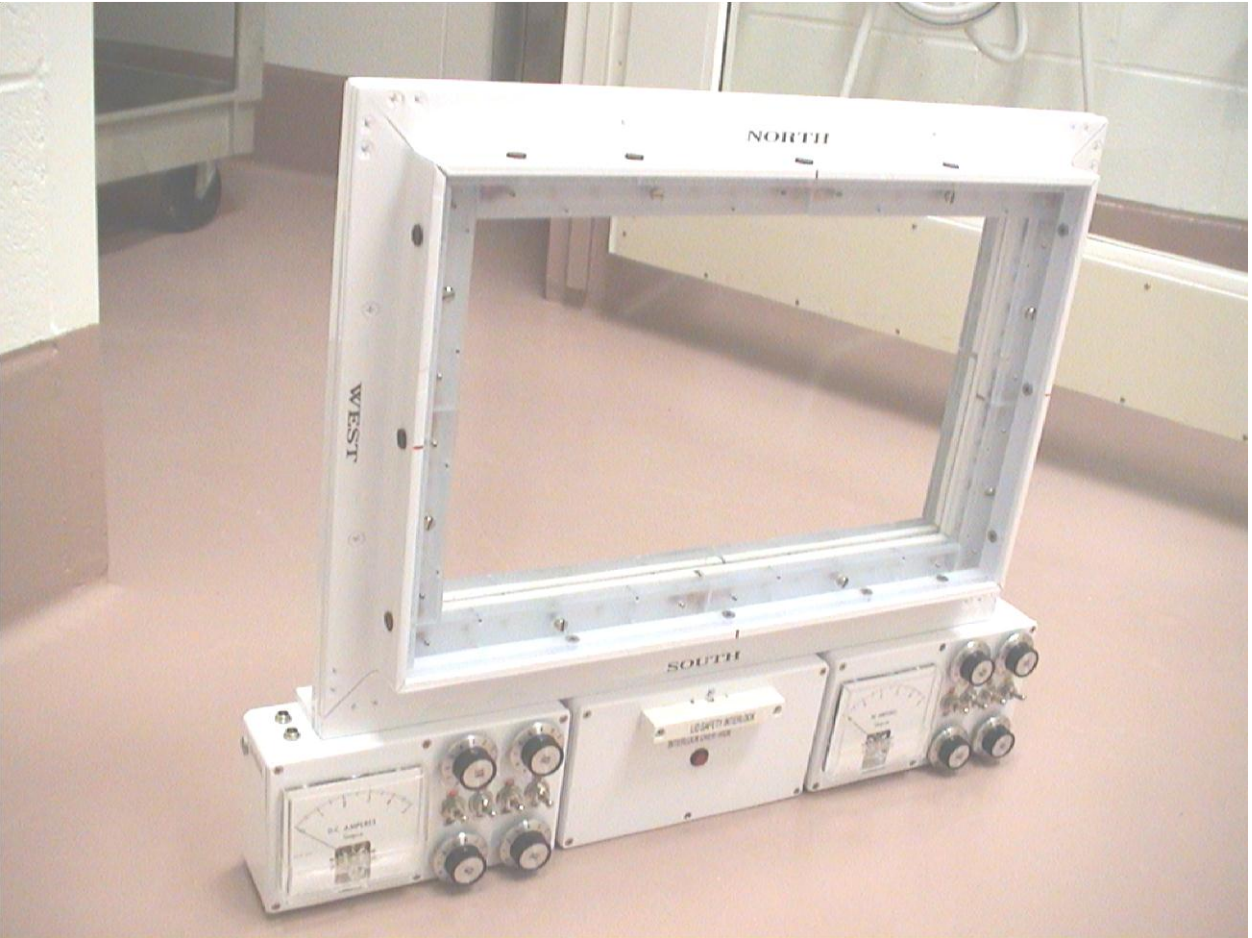
## Pictures Showing Cage Installation



## Pictures Showing Cage Installation



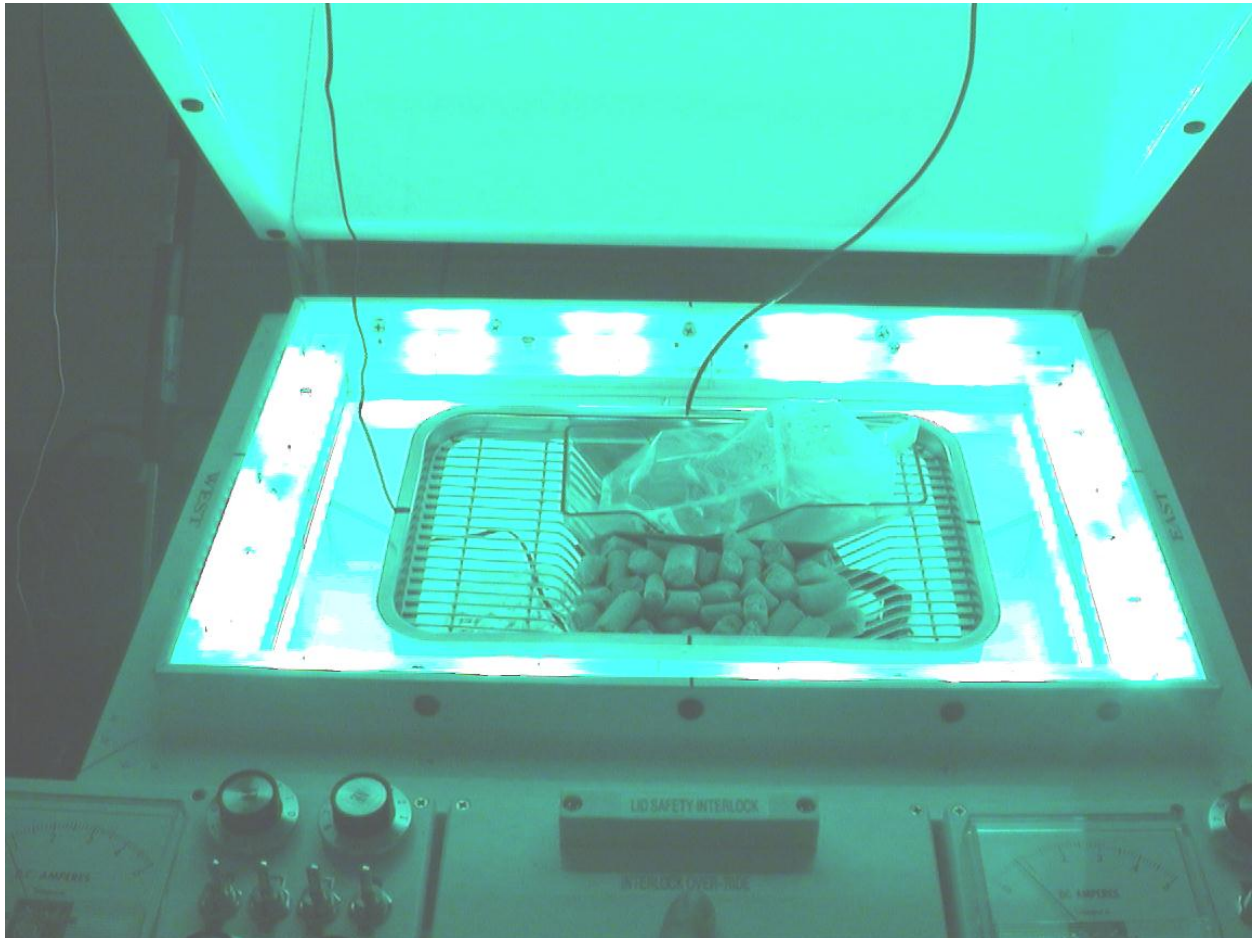
Pictures Showing Cage Installation



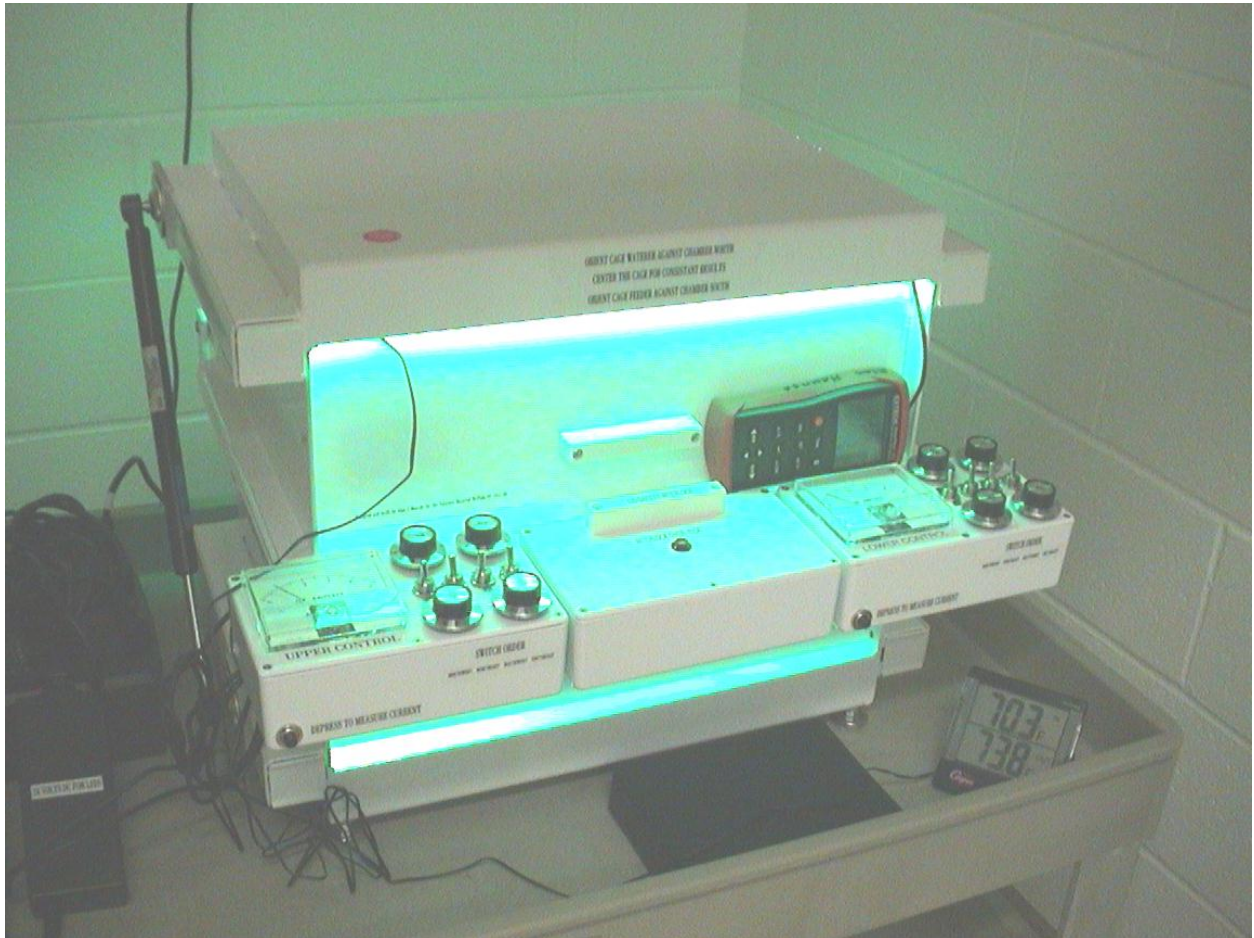
## Pictures Showing Cage Installation



## Pictures Showing Cage Installation



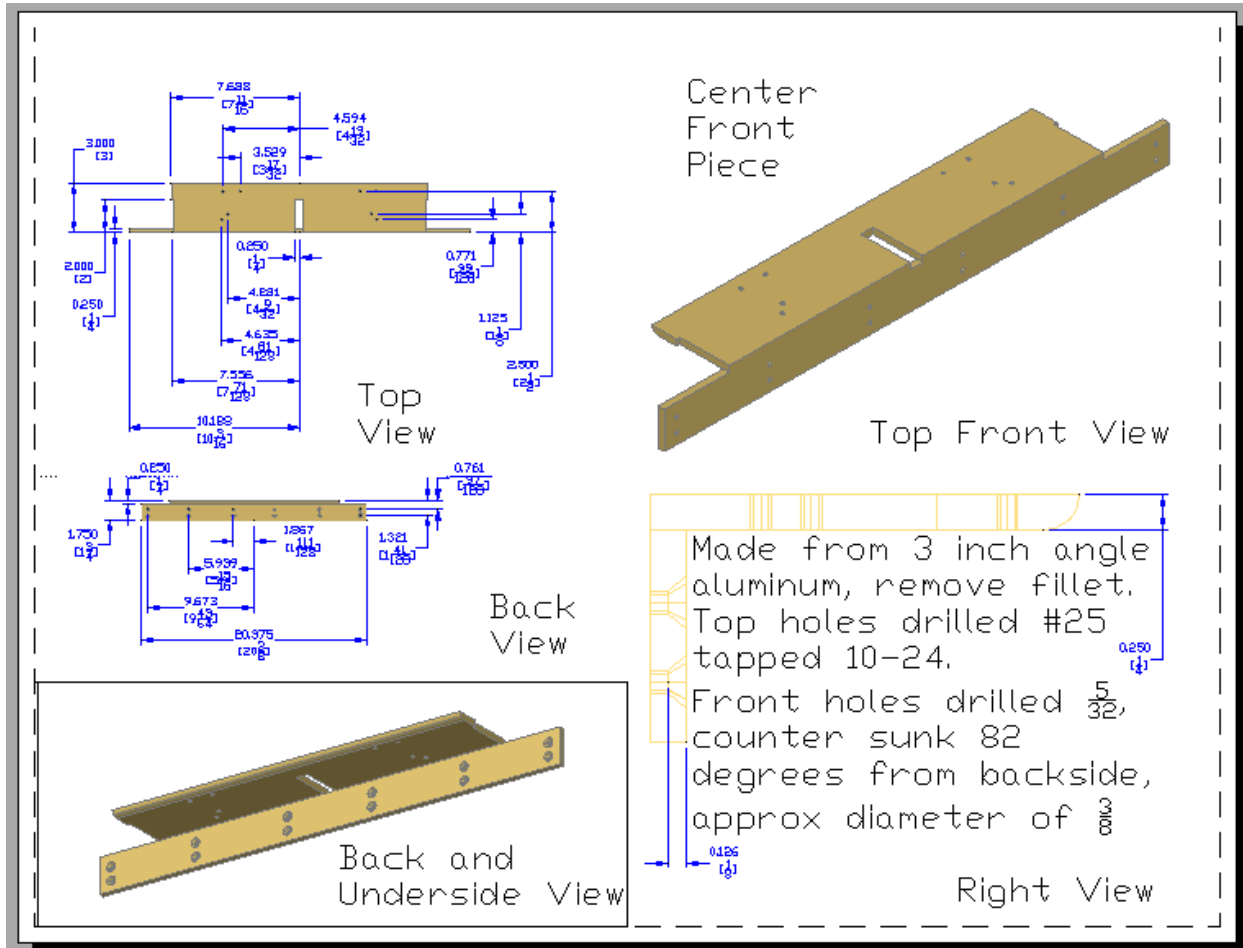
## Pictures Showing Cage Installation



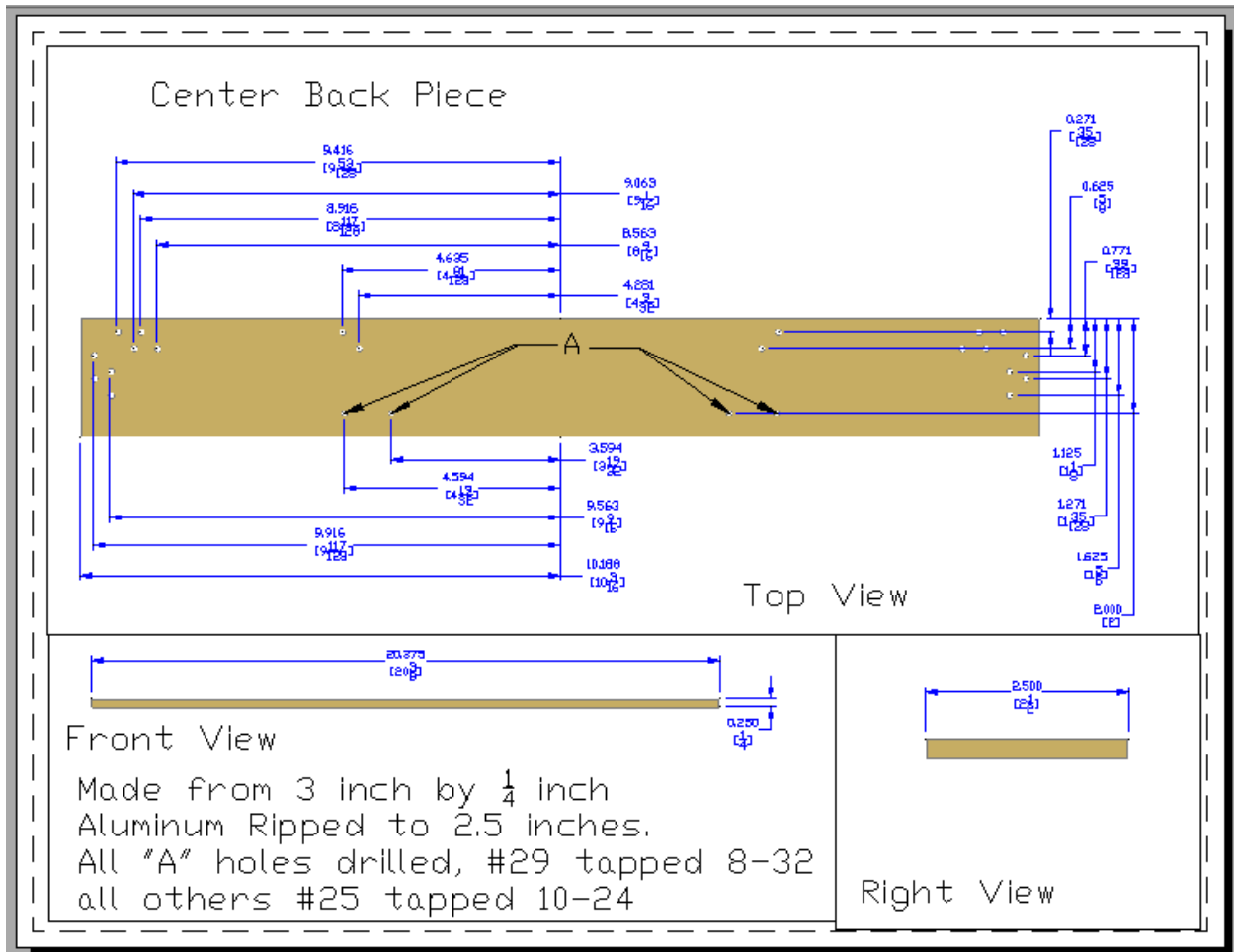
# APPENDIX B

## AUTOCAD DRAWINGS OF THE LIGHT ENGINES HOLDER RACK

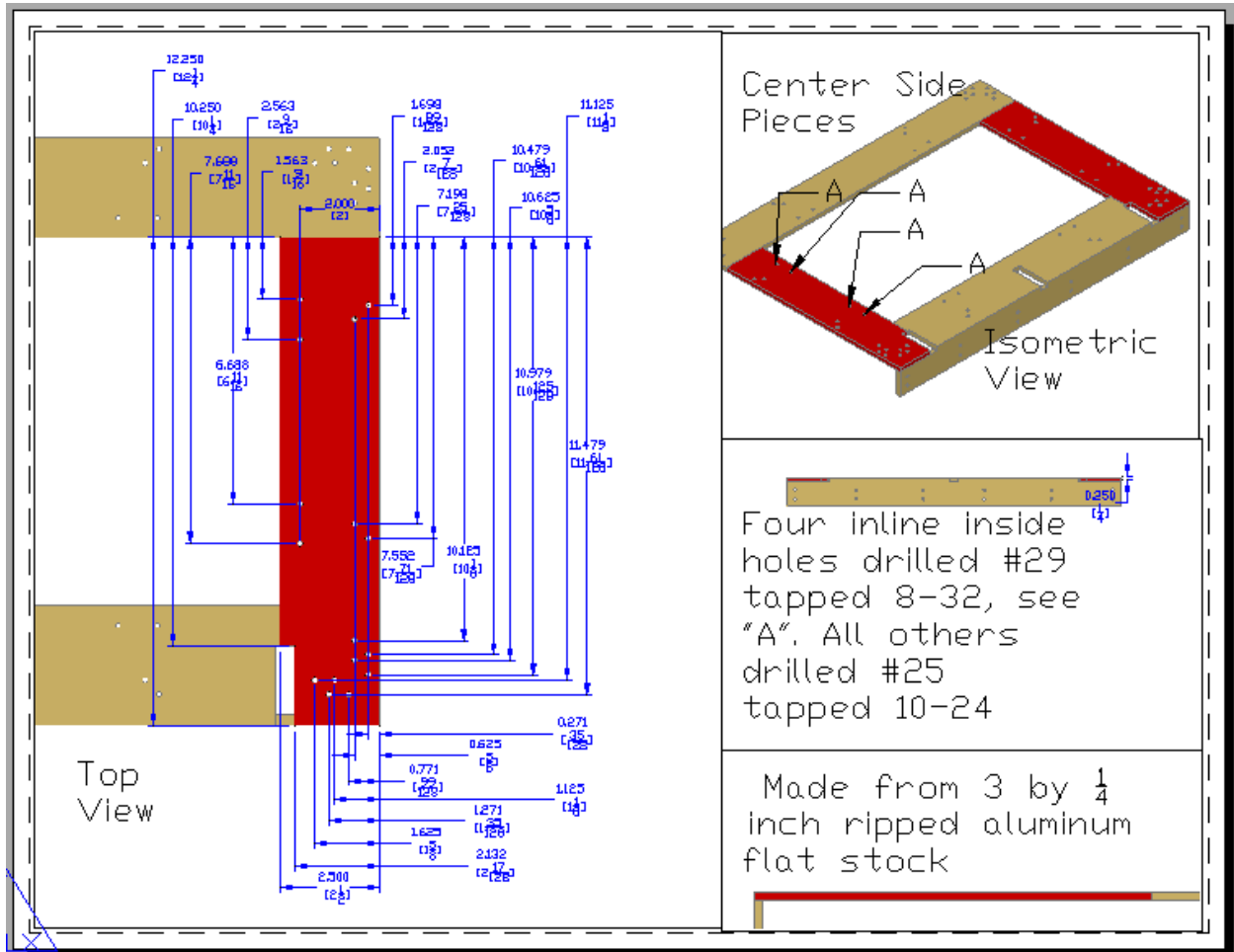
# APPENDIX\_B



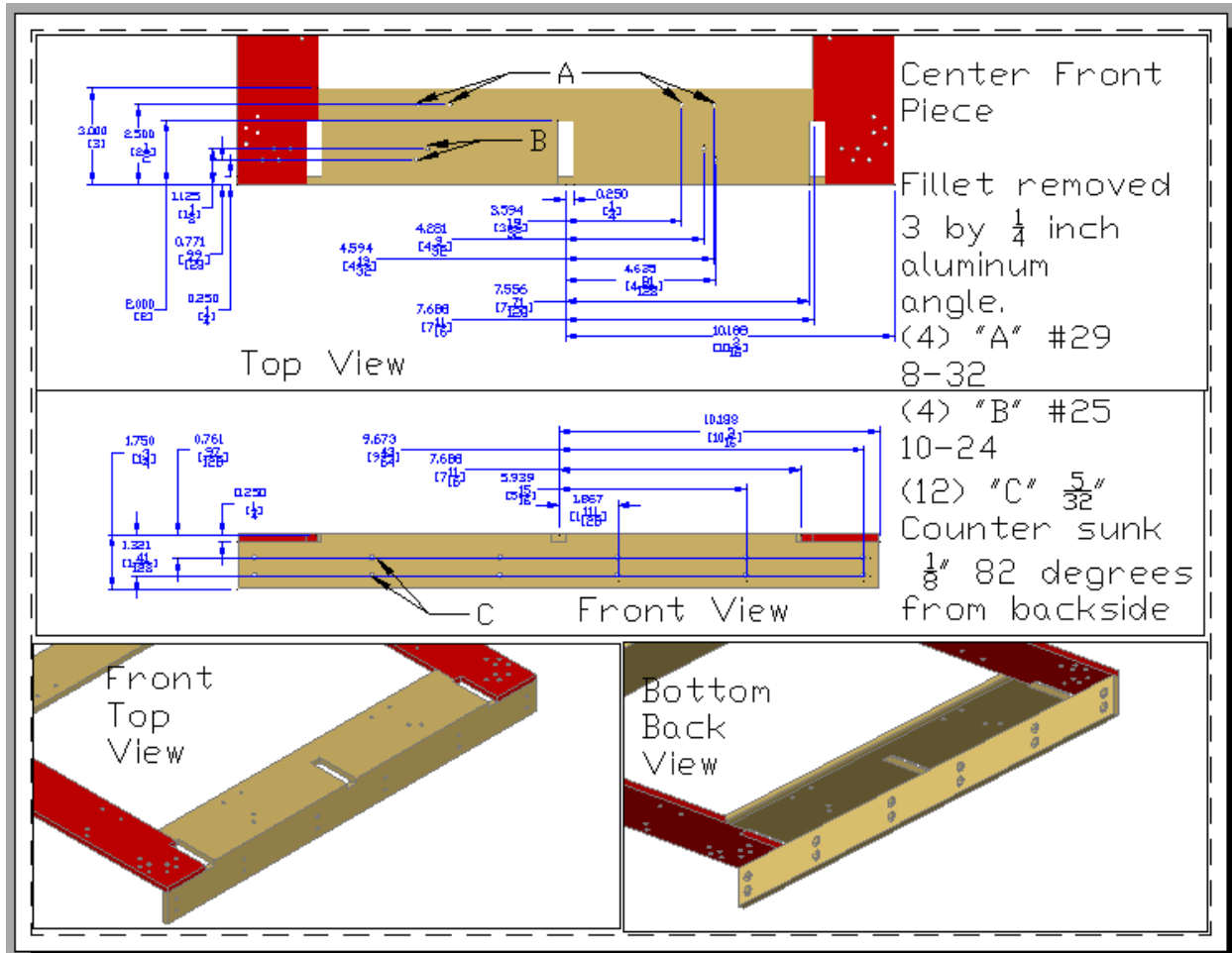
# APPENDIX\_B



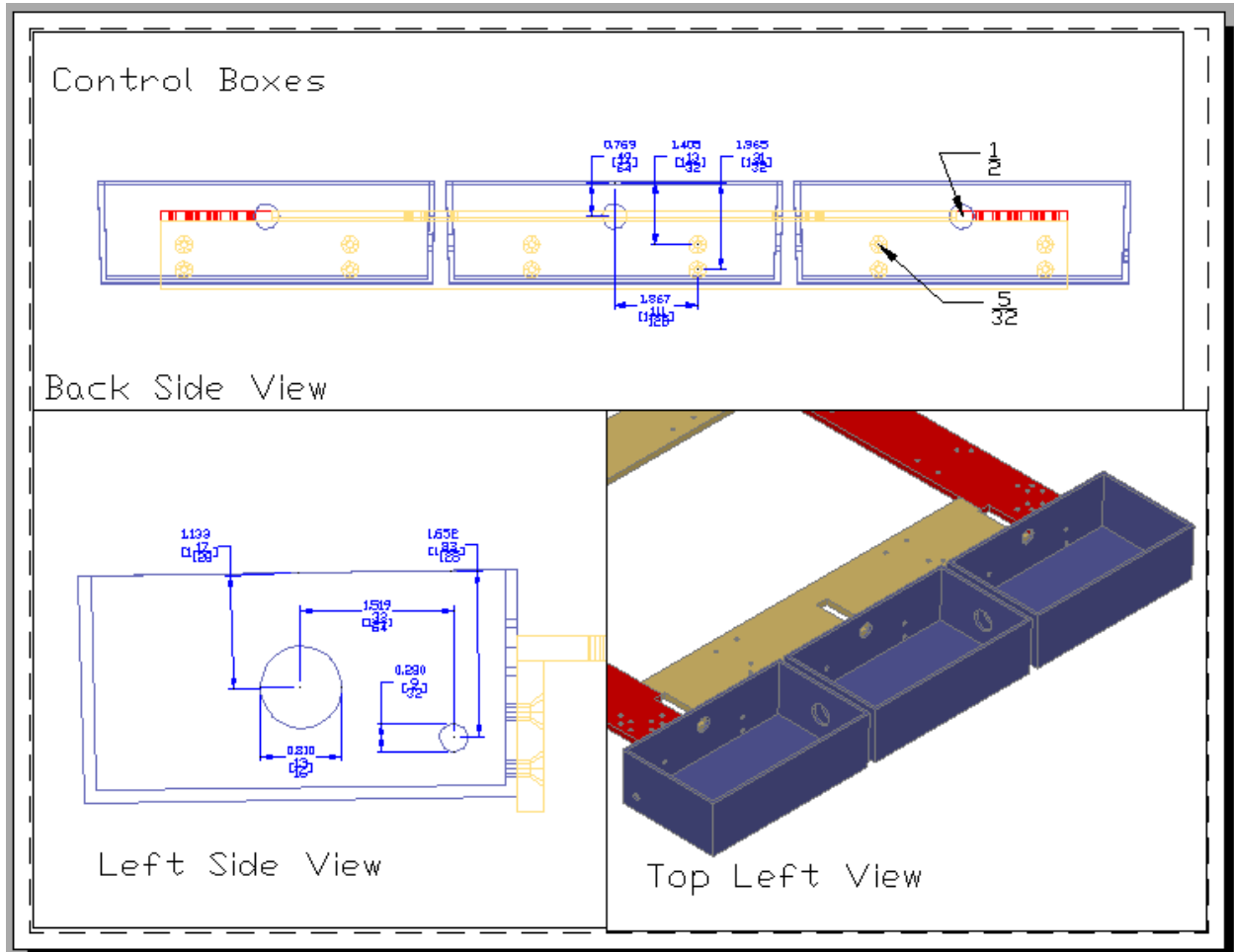
# APPENDIX\_B



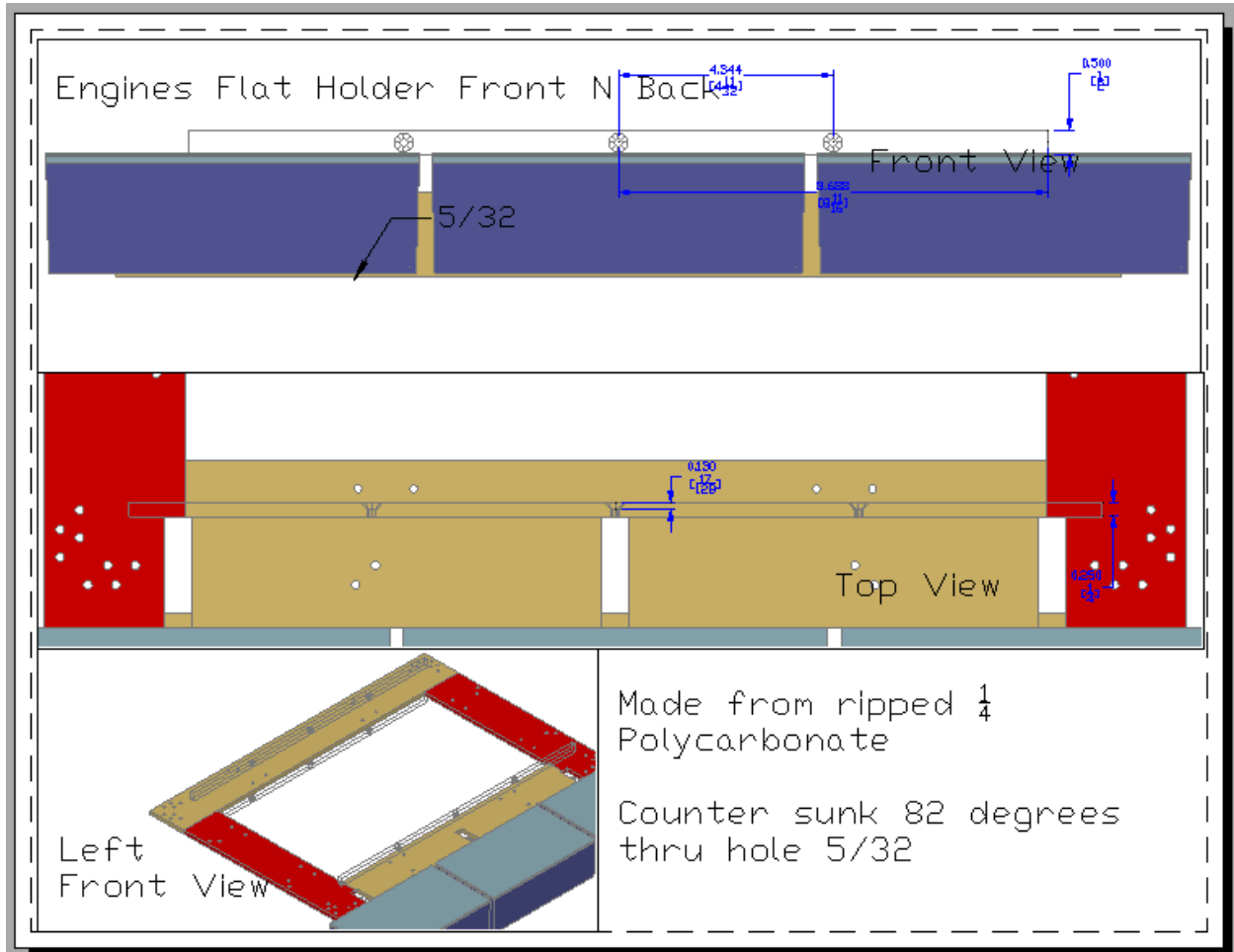
# APPENDIX\_B



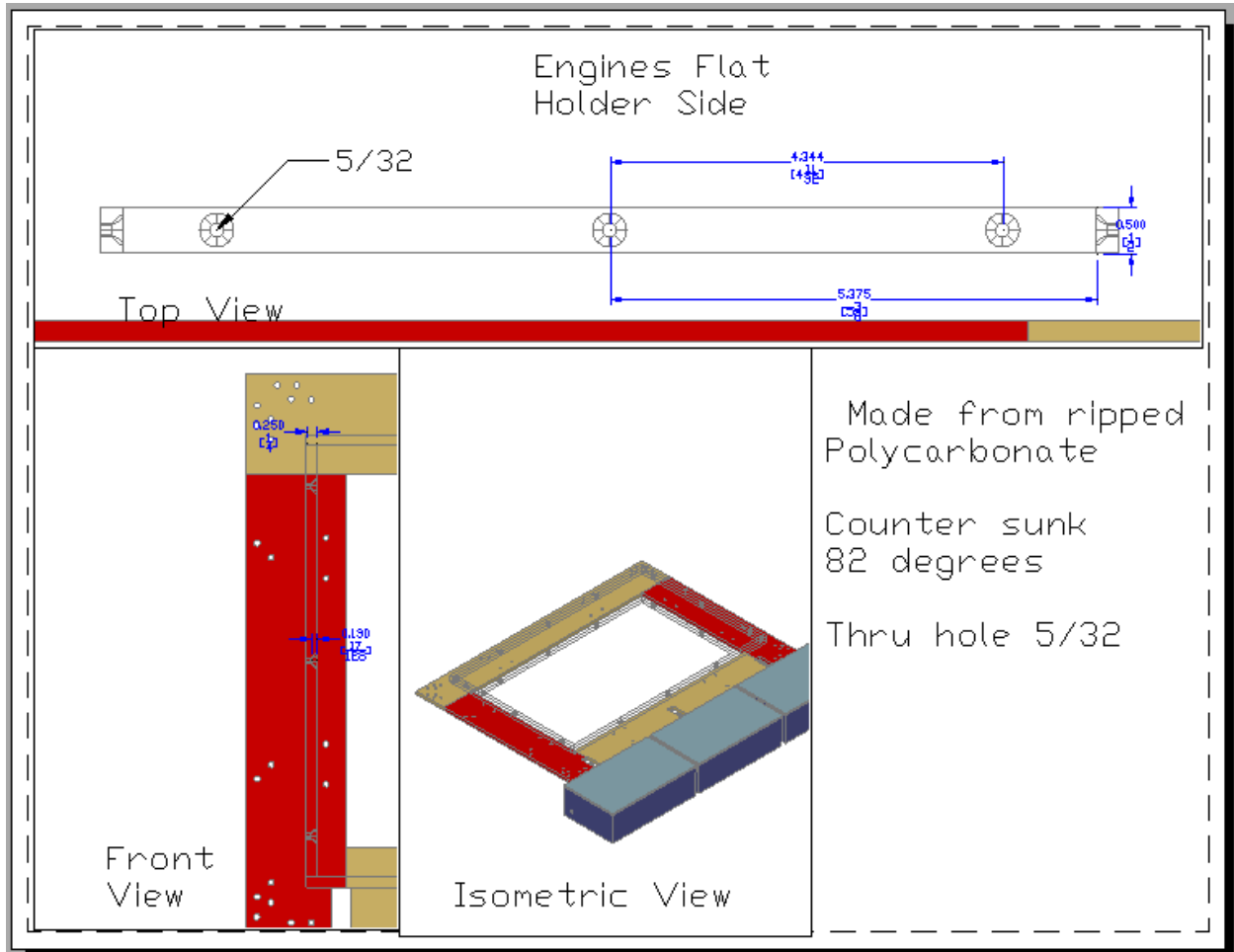
# APPENDIX\_B



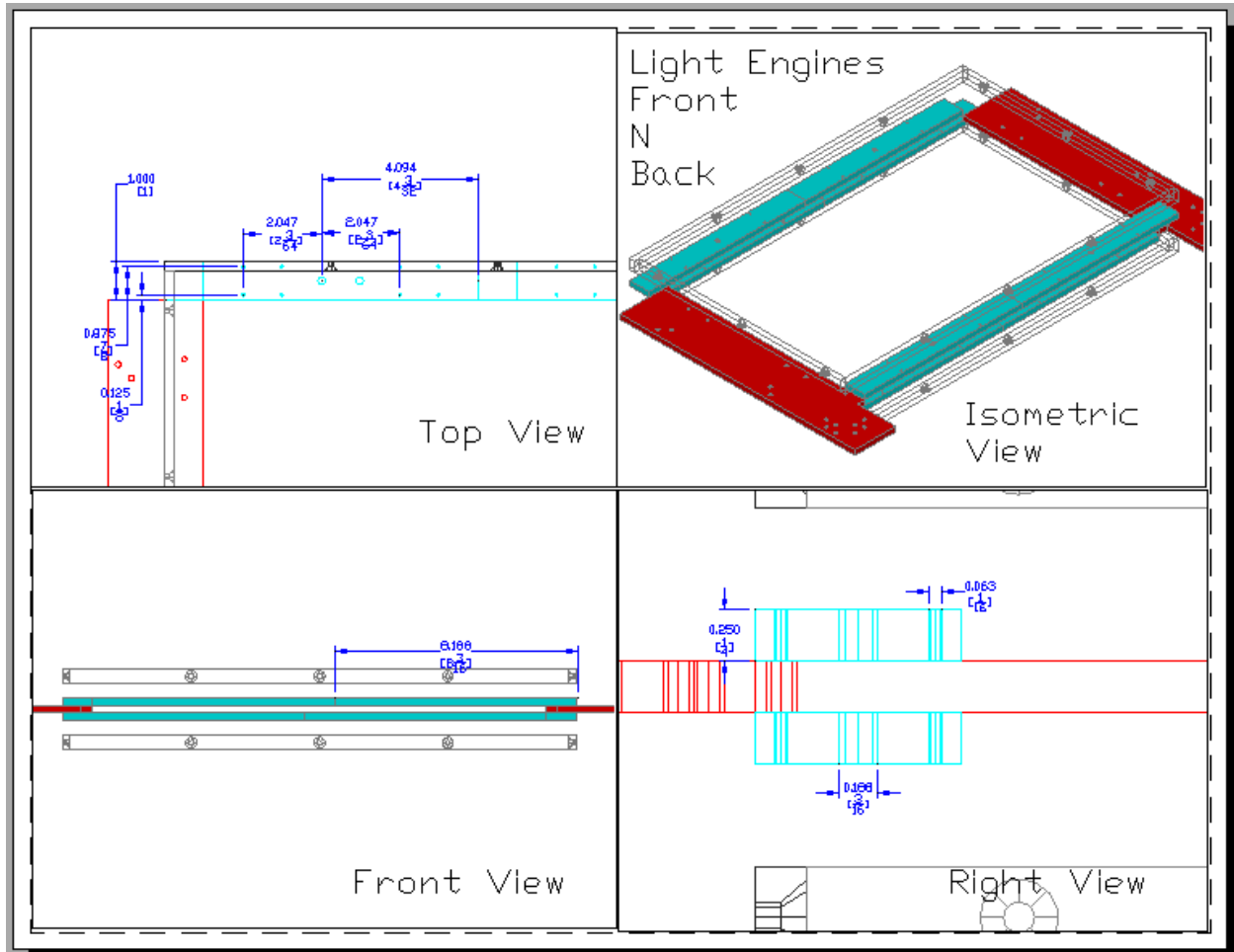
# APPENDIX\_B



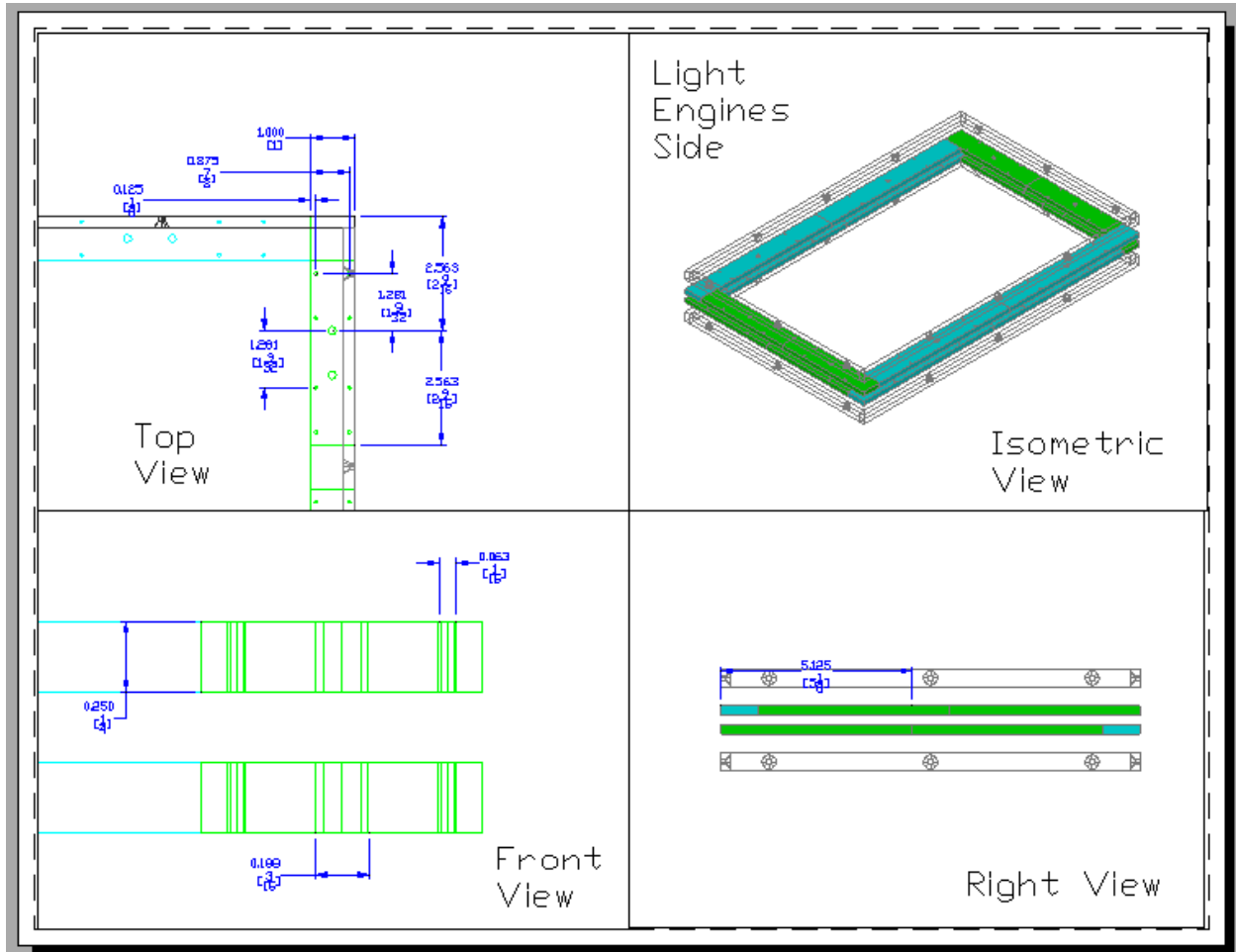
# APPENDIX\_B



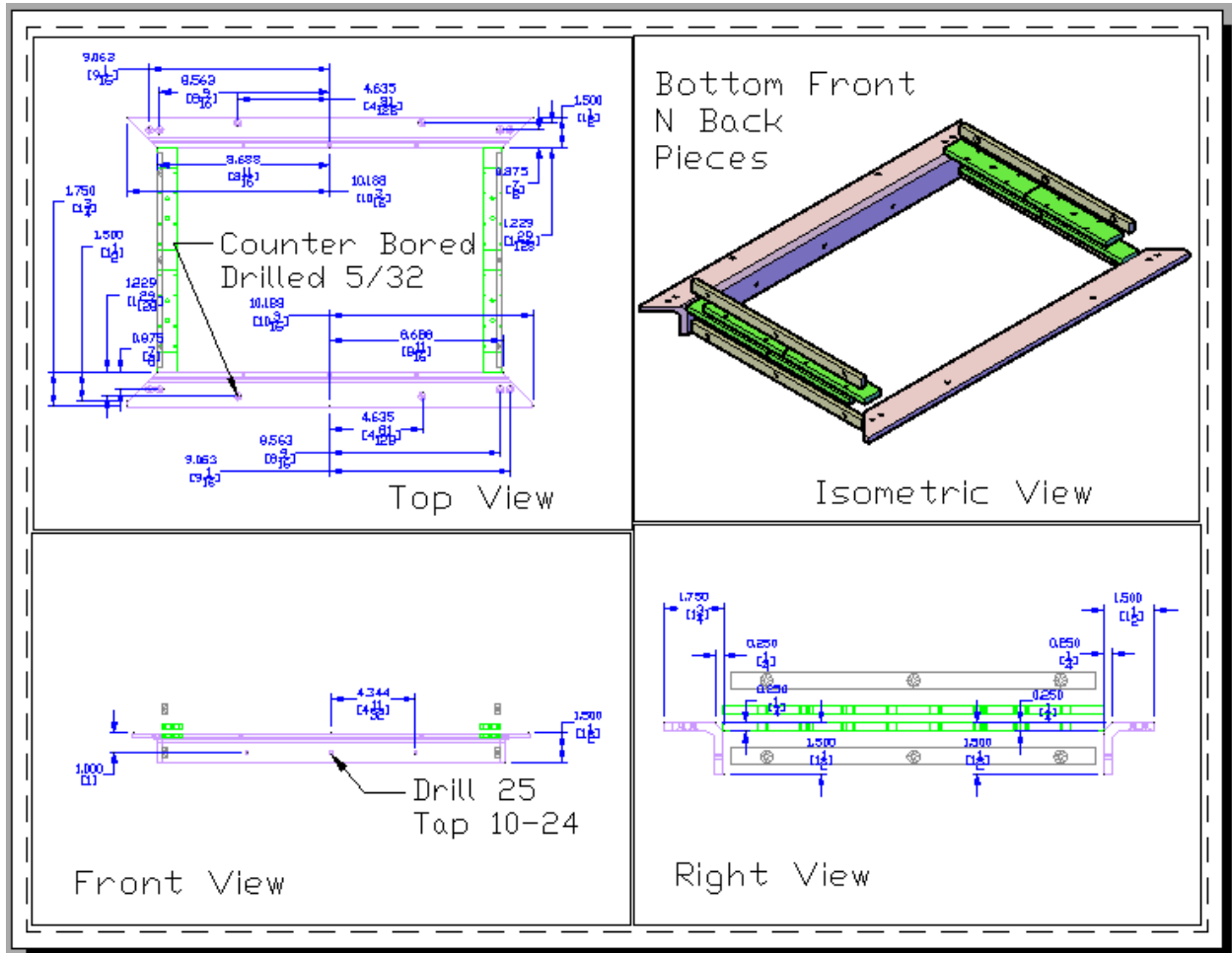
# APPENDIX\_B



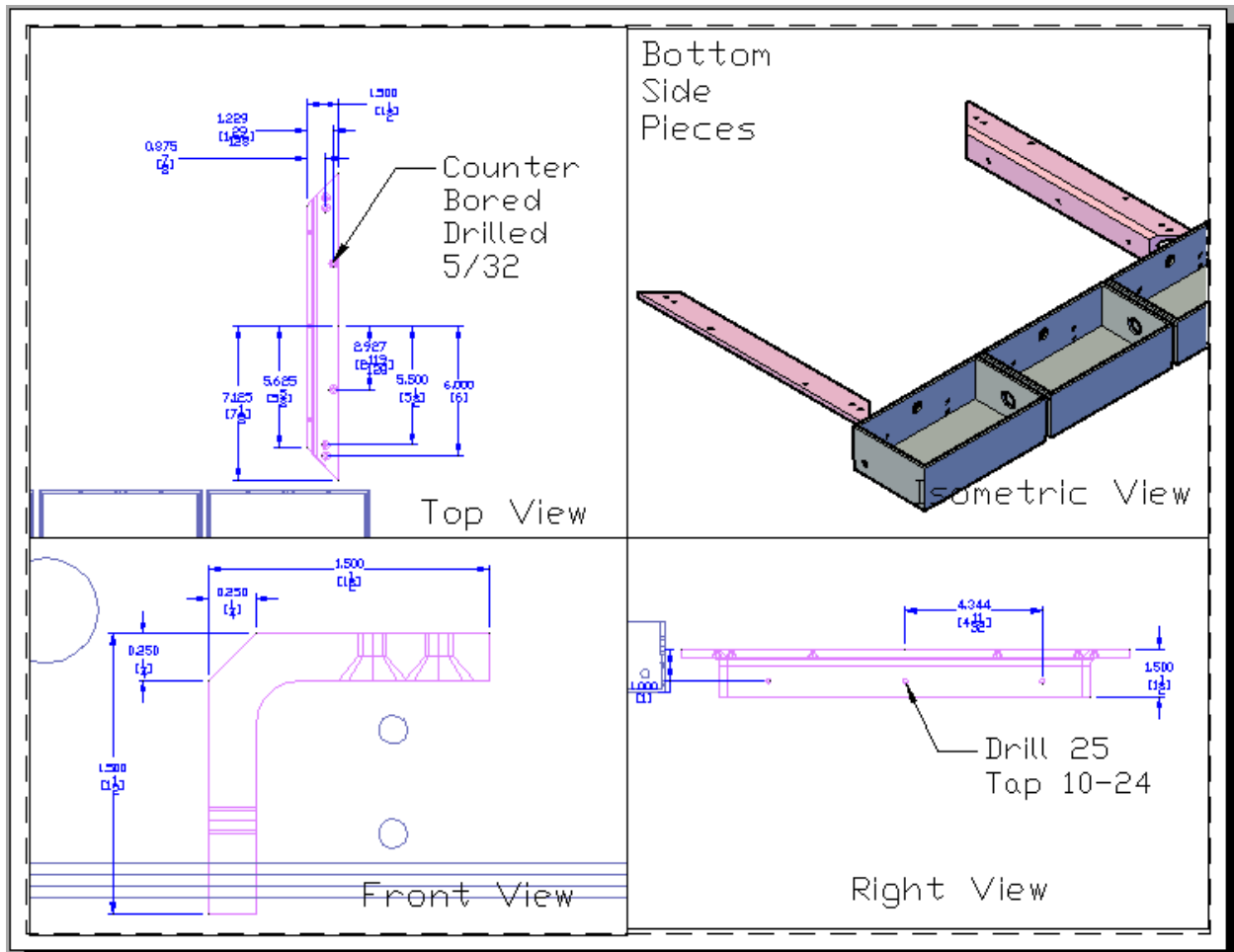
# APPENDIX\_B



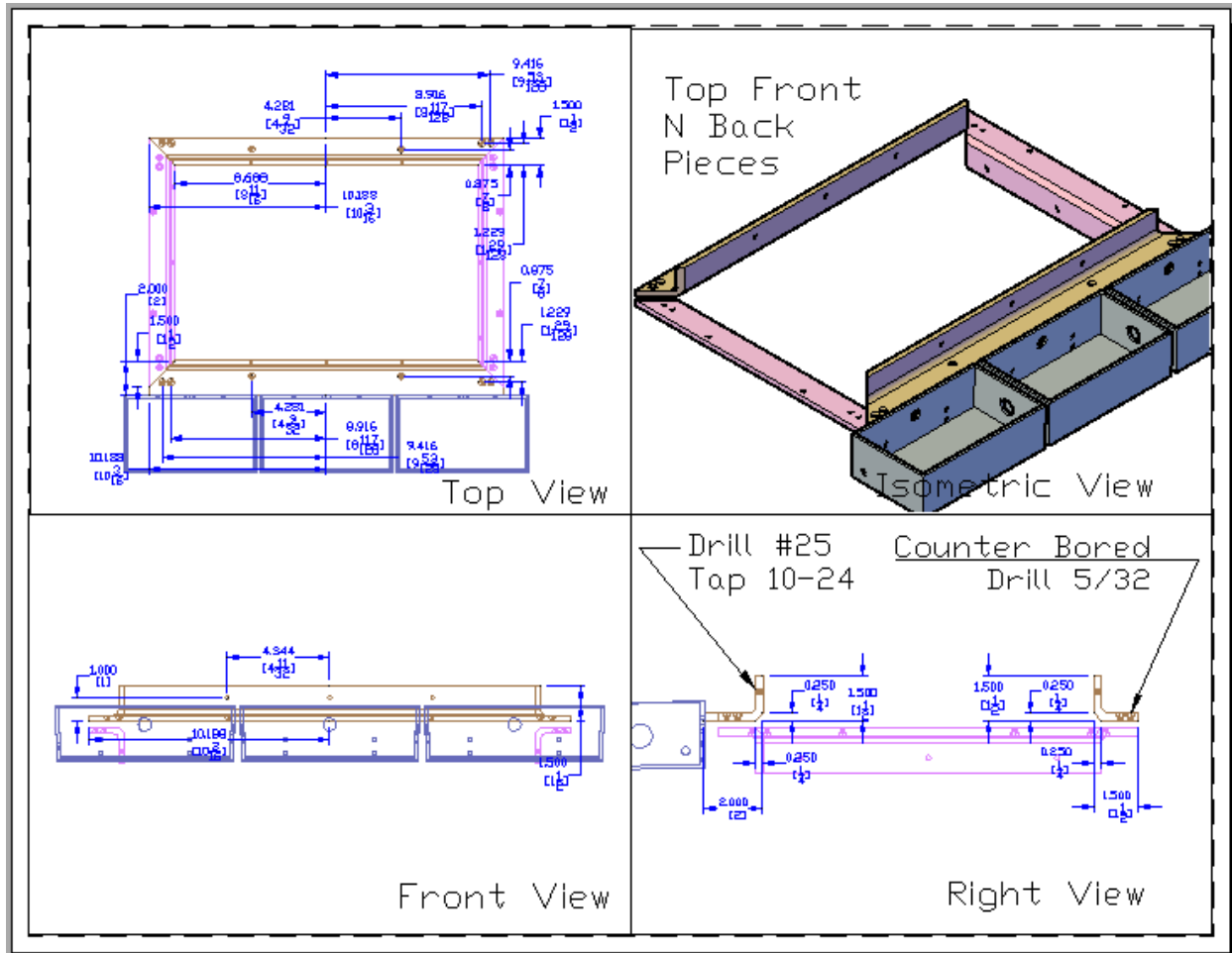
# APPENDIX\_B



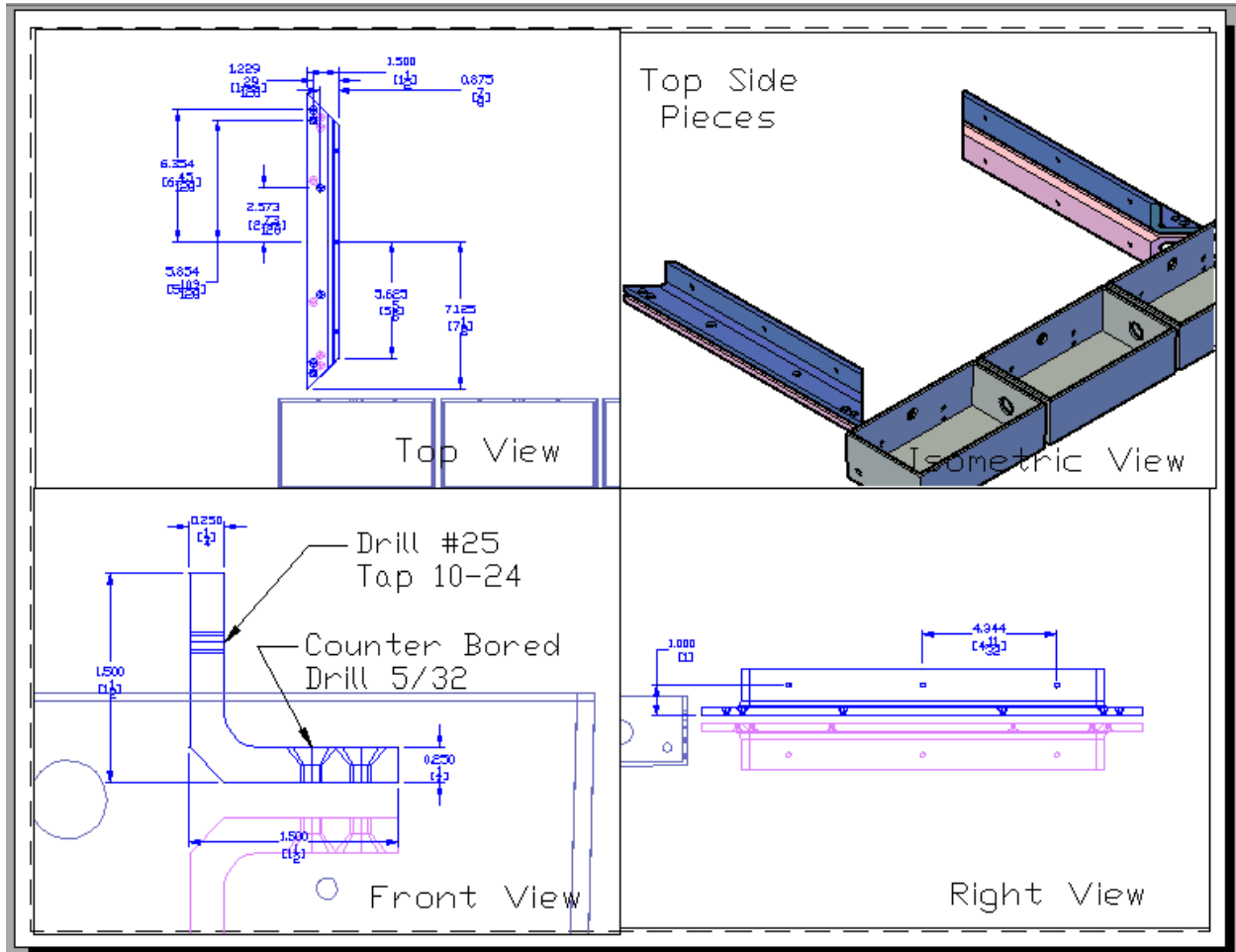
# APPENDIX\_B



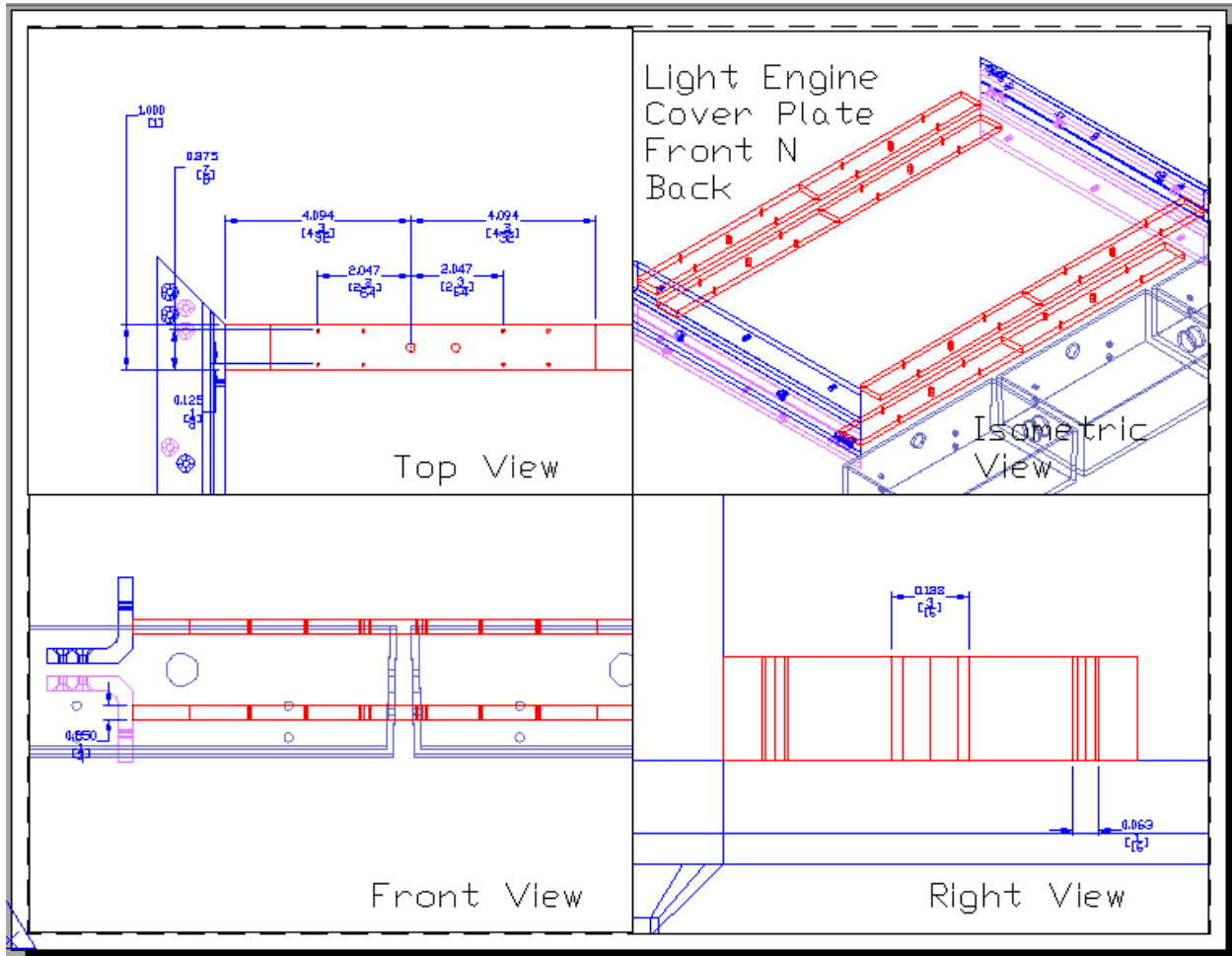
# APPENDIX\_B



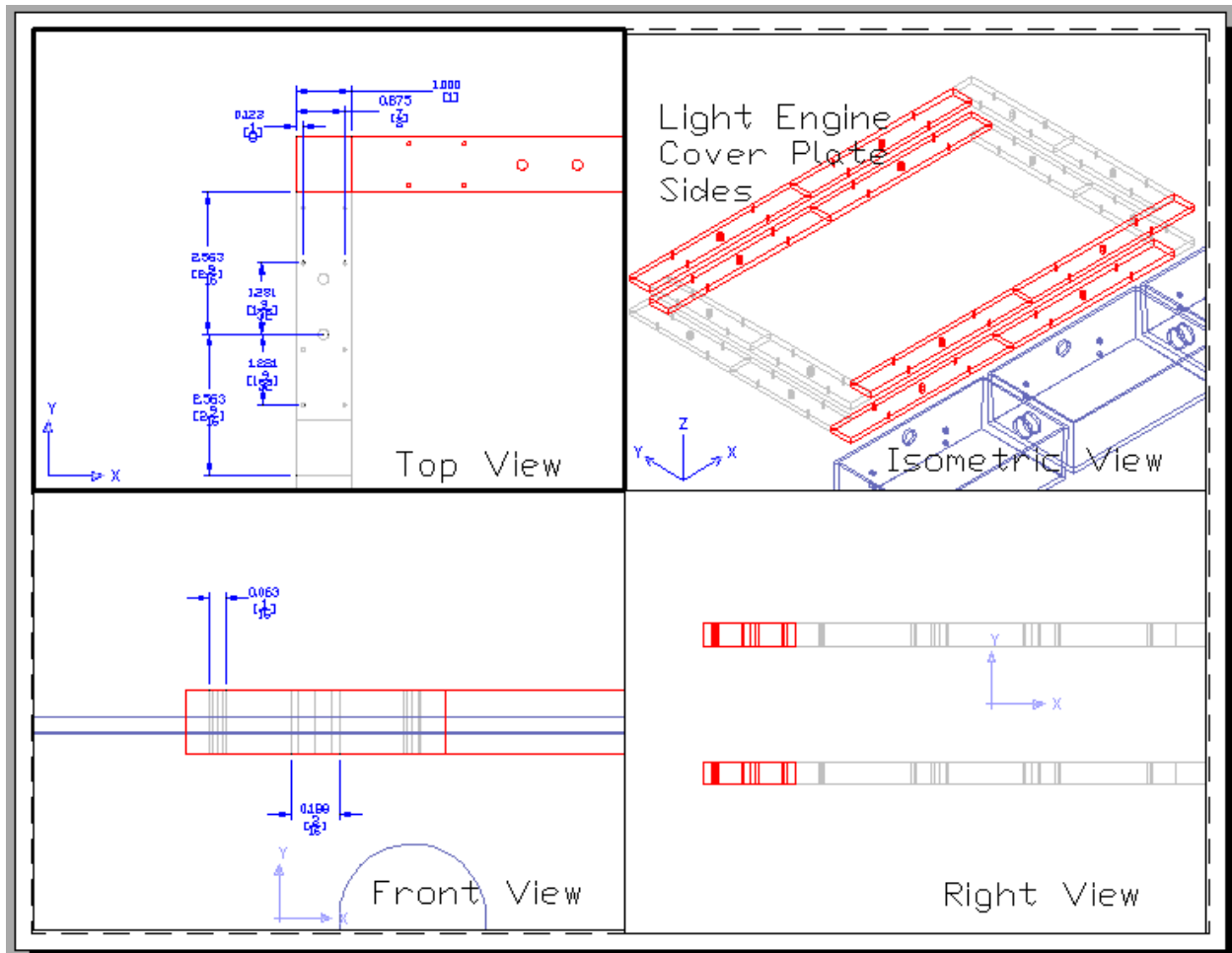
# APPENDIX\_B



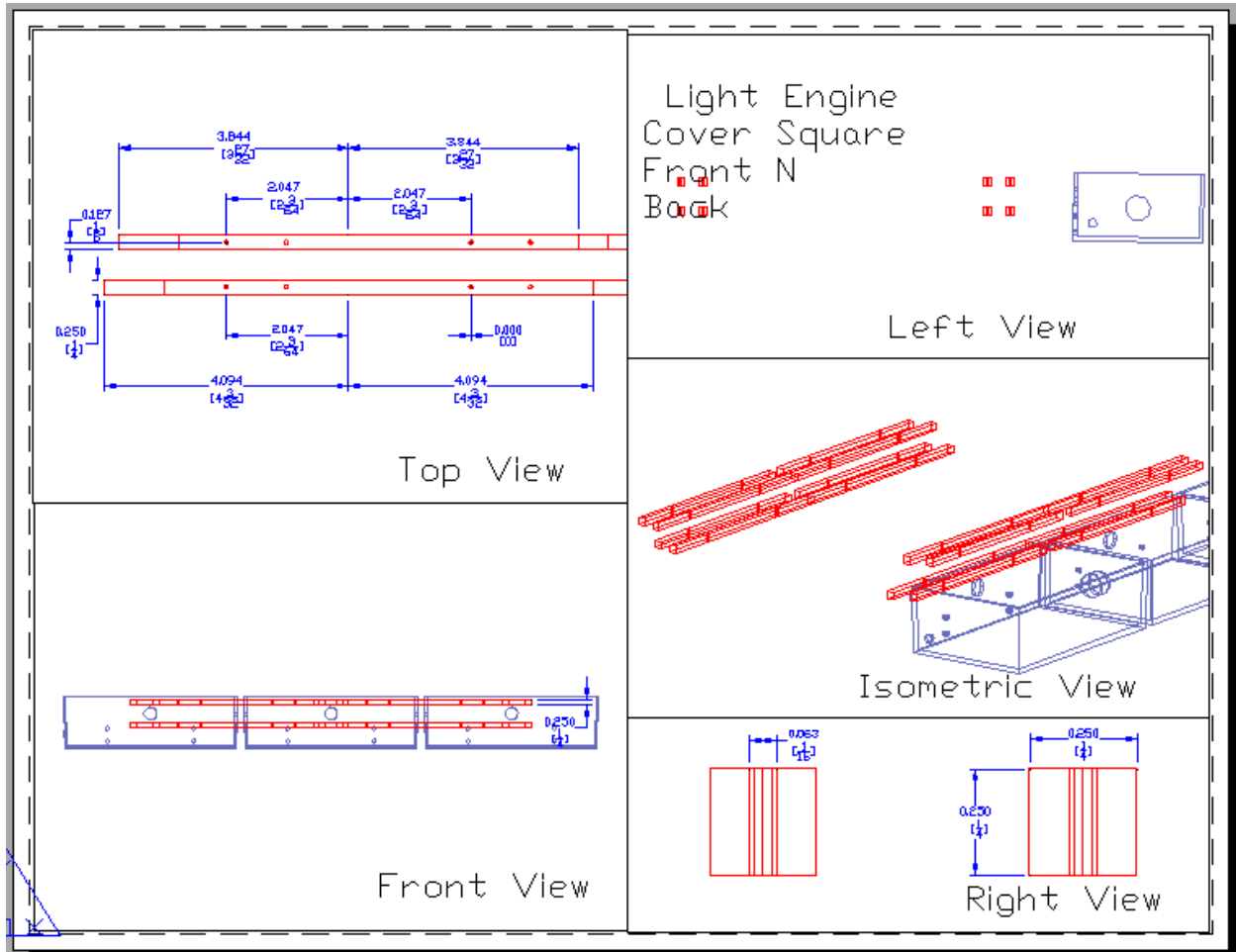
# APPENDIX\_B



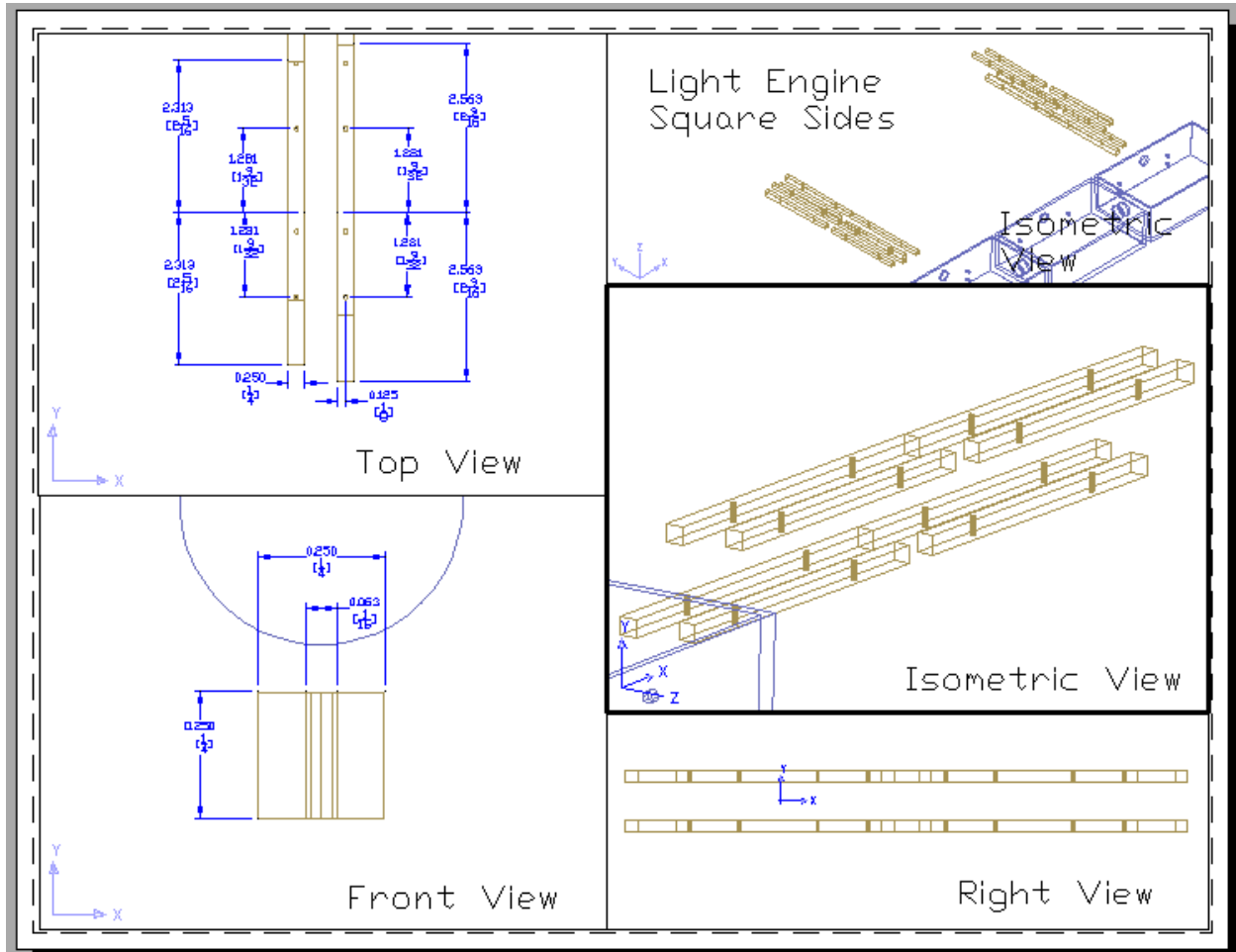
# APPENDIX\_B



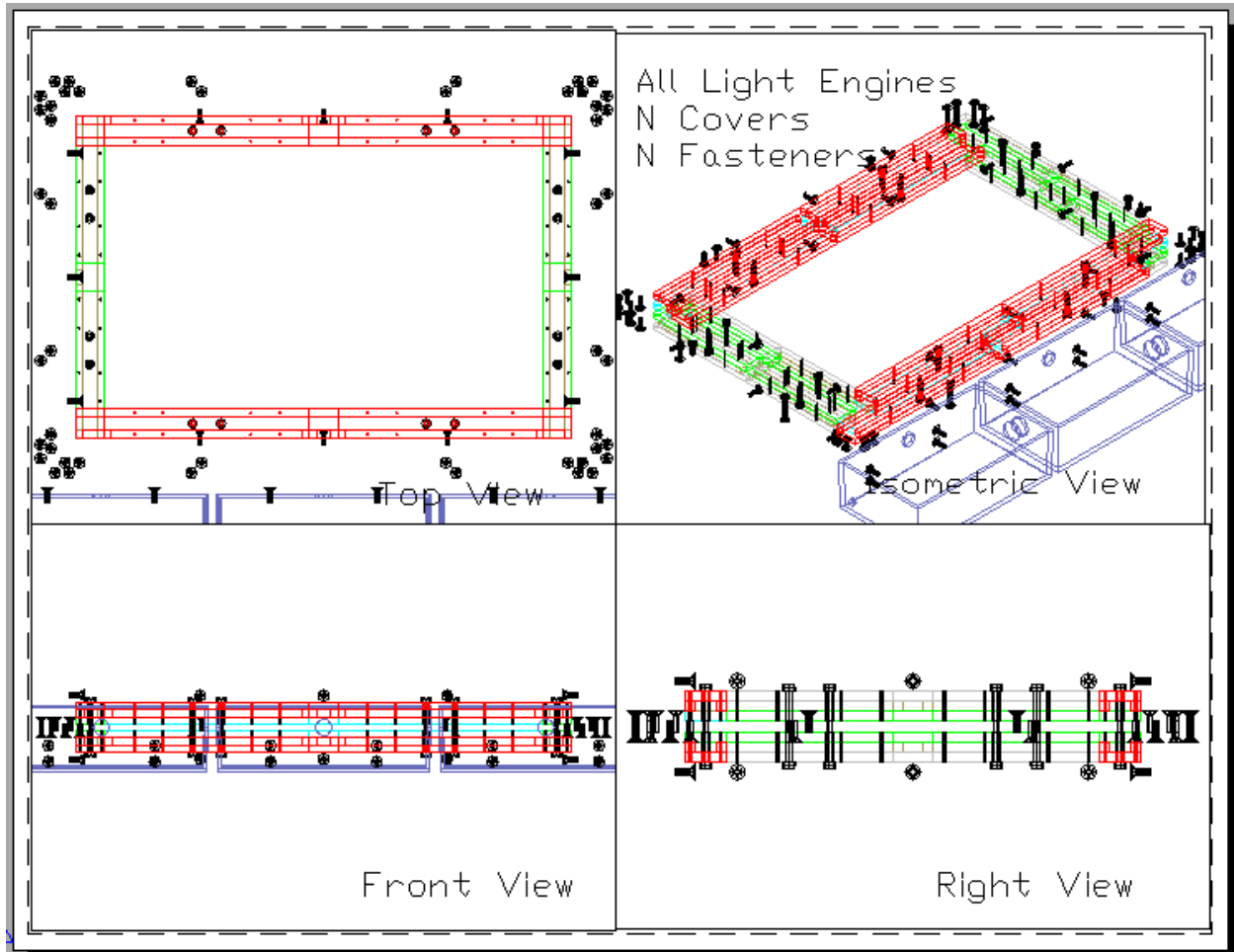
# APPENDIX\_B



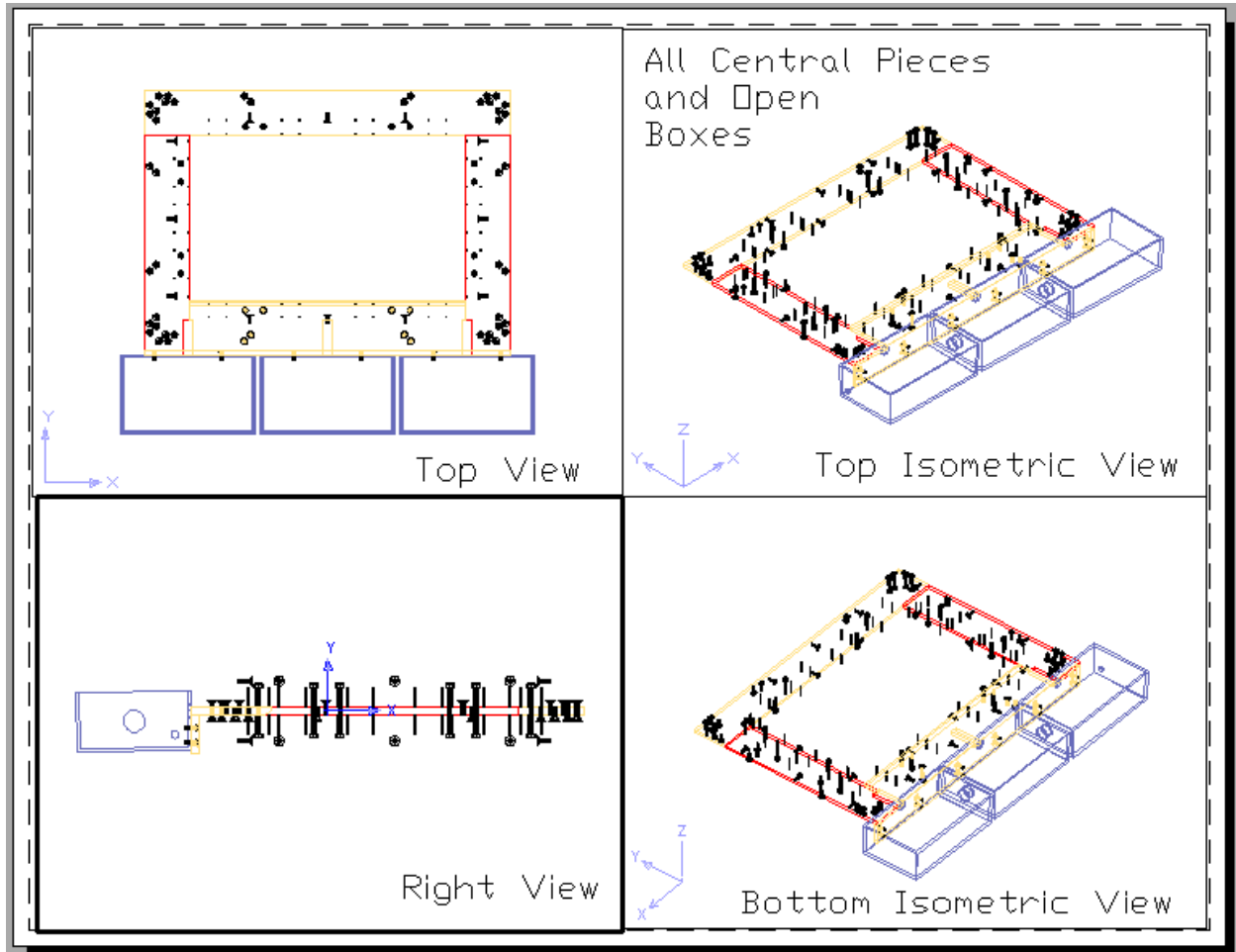
# APPENDIX\_B



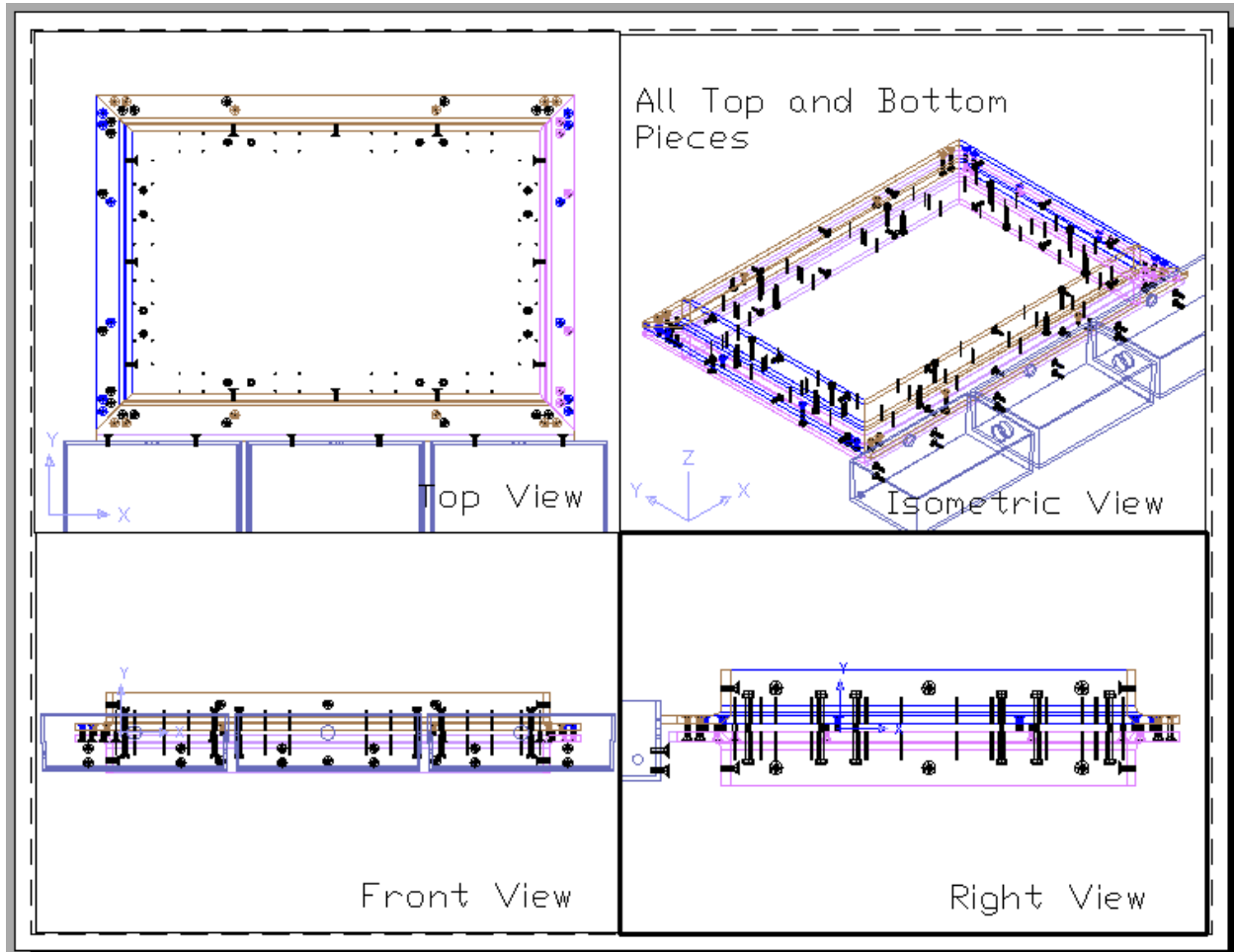
# APPENDIX\_B



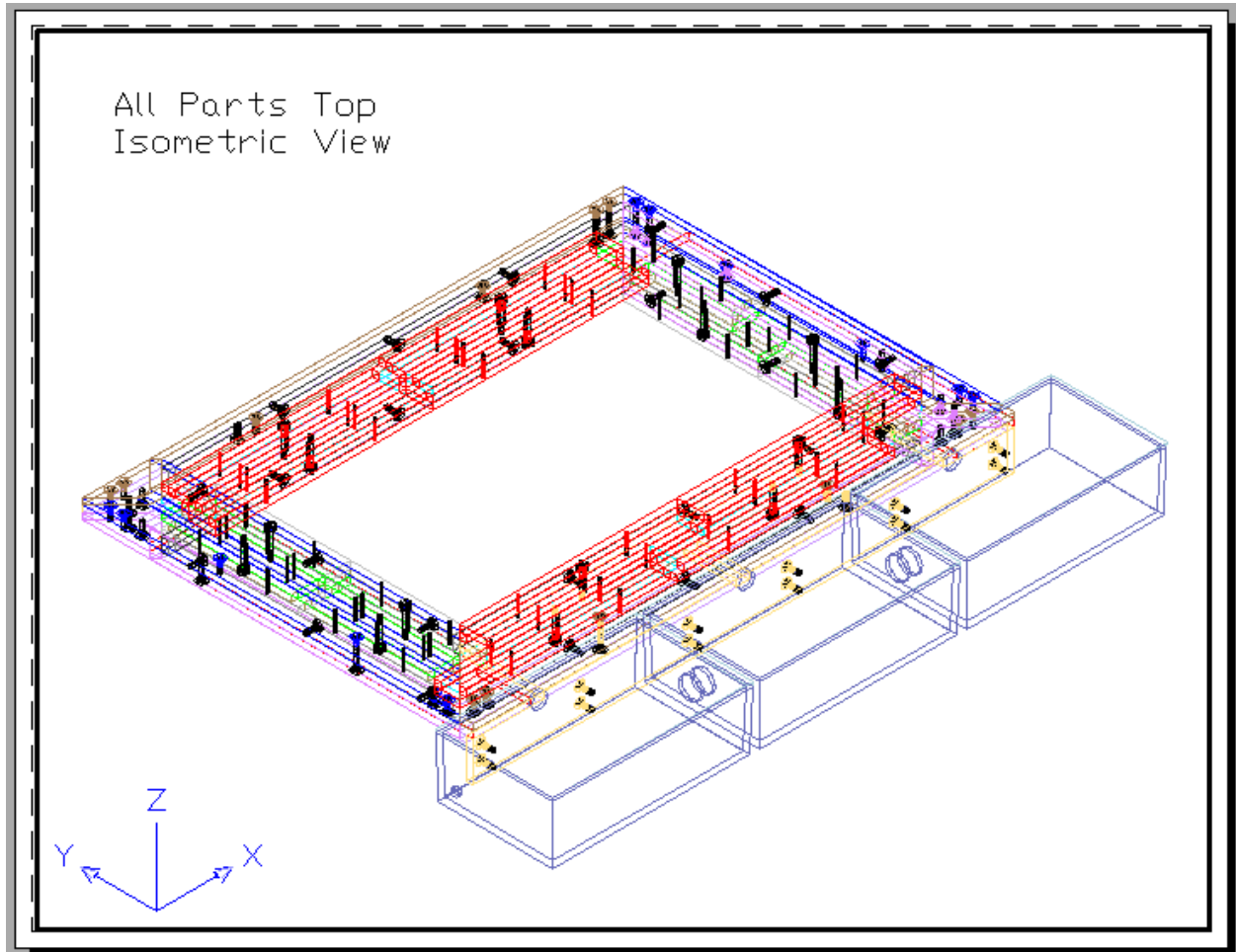
# APPENDIX\_B



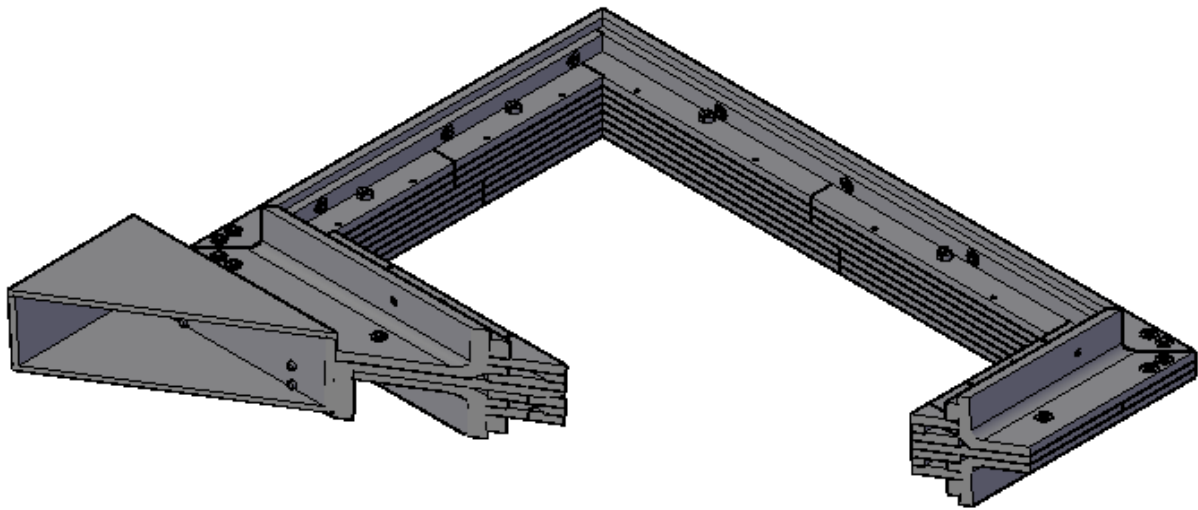
# APPENDIX\_B



# APPENDIX\_B



Cross Sectional View



# APPENDIX C

## TECHNICAL DATASHEETS FOR LUXEON REBEL LIGHT EMITTING DIODES



## LUXEON® Rebel Direct Color Portfolio

### Introduction

The LUXEON® Rebel Direct Color portfolio LEDs in this datasheet are ideal for a wide variety of lighting, signaling, signage and entertainment applications. These flux differentiated parts, like all other LUXEON Rebel LEDs, provide the industry's best lumen maintenance, superior reliability and quality light. Using the information in this document you can begin designing applications to your unique specifications.

### LUXEON Rebel Direct Color LEDs

- Deliver more usable light and higher flux density
- Optimize applications to reduce size and cost
- Tightly pack the LEDs for mixing
- Engineer more robust applications
- Utilize standard FR4 PCB technology
- Simplify manufacturing through the use of surface mount technology.

**PHILIPS**  
**LUMILEDS**

## Table of Contents

Product Nomenclature.....	3
Average Lumen Maintenance Characteristics .....	3
Environmental Compliance.....	3
Visual Appearance of LUXEON Rebel.....	3
Flux Characteristics.....	4
Flux Performance, Binning, and Supportability .....	5
Optical Characteristics.....	6
Electrical Characteristics.....	7
Absolute Maximum Ratings .....	8
JEDEC Moisture Sensitivity.....	8
Reflow Soldering Characteristics.....	9
Mechanical Dimensions .....	10
Pad Configuration.....	11
Solder Pad Design.....	11
Wavelength Characteristics.....	12
Typical Light Output Characteristics over Temperature.....	13
Typical Forward Current Characteristics .....	14
Typical Relative Luminous Flux .....	15
Current Derating Curves.....	16
Typical Radiation Patterns.....	19
Emitter Pocket Tape Packaging.....	21
Emitter Reel Packaging .....	22
Product Binning and Labeling.....	23
Luminous Flux Bins.....	24
Forward Voltage Bins.....	26
Color Bins.....	27

## Product Nomenclature

LUXEON Rebel is tested and binned at 350 mA.

The part number designation is explained as follows:

L X M L - A B C D - E F G H

Where:

- A — designates radiation pattern (value P for Lambertian)
- B — designates color (see LUXEON Rebel Binning and Labeling section)
- C — designates color variant (0 for direct colored variants)
- D — designates test current (value I for 350 mA)
- E — reserved for future product offerings
- FGH — minimum luminous flux (lm) or radiometric power (mW) performance

Therefore products tested and binned at 350 mA follow the part numbering scheme:

L X M L - P x 0 I - x x x x

## Average Lumen Maintenance Characteristics

Lifetime for solid-state lighting devices (LEDs) is typically defined in terms of lumen maintenance—the percentage of initial light output remaining after a specified period of time.

Philips Lumileds projects that green, cyan, blue and royal-blue LUXEON Rebel products will deliver, on average, 70% lumen maintenance (B50, L70) at 50,000 hours of operation at a forward current of 700 mA. This projection is based on constant current operation with junction temperature maintained at or below 135°C.

Philips Lumileds projects that red, red-orange and amber LUXEON Rebel products will deliver, on average, 70% lumen maintenance (B50, L70) at 50,000 hours of operation at a forward current of 350 mA. This projection is based on constant current operation with junction temperature maintained at or below 110°C.

This performance is based on independent test data, Philips Lumileds historical data from tests run on similar material systems, and internal LUXEON reliability testing. Observation of design limits included in this data sheet is required in order to achieve this projected lumen maintenance.

## Environmental Compliance

Philips Lumileds is committed to providing environmentally friendly products to the solid-state lighting market. LUXEON Rebel is compliant to the European Union directives on the restriction of hazardous substances in electronic equipment, namely the RoHS directive. Philips Lumileds will not intentionally add the following restricted materials to the LUXEON Rebel: lead, mercury, cadmium, hexavalent chromium, polybrominated biphenyls (PBB) or polybrominated diphenyl ethers (PBDE).

## Visual Appearance of LUXEON Rebel

All lighted LUXEON Rebel product will provide comparable lambertian beam performance, suitable for use with commercially available optical systems. Without power, LED die within different reels may appear visually different. Please contact your Philips Lumileds or Future Electronics representative for further information.

## Flux Characteristics

### Flux Characteristics for LUXEON Rebel, Thermal Pad Temperature=25°C

Table I.

Performance at Test Current				Typical Performance at Indicated Current	
Color	Part Number	Minimum Luminous Flux (lm) or Radiometric Power (mW) $\Phi_v^{[1]}$	Test Current (mA)	Typical Luminous Flux (lm) or Radiometric Power (mW) $\Phi_v^{[2]}$	Drive Current (mA)
Green	LXML-PM01-0040	40	350	80	700
	LXML-PM01-0050	50	350	95	700
	LXML-PM01-0070	70	350	130	700
	LXML-PM01-0080	80	350	145	700
	LXML-PM01-0090	90	350	160	700
	LXML-PM01-0100	100	350	180	700
Cyan	LXML-PE01-0030	30	350	65	700
	LXML-PE01-0040	40	350	80	700
	LXML-PE01-0060	60	350	110	700
	LXML-PE01-0070	70	350	130	700
Blue	LXML-PB01-0008	8.2	350	19	700
	LXML-PB01-0010	10.7	350	22	700
	LXML-PB01-0013	13.9	350	27	700
	LXML-PB01-0018	18.1	350	38	700
	LXML-PB01-0023	23.5	350	48	700
	LXML-PB01-0030	30.0	350	58	700
Royal-Blue	LXML-PR01-0175	175 mW	350	325 mW	700
	LXML-PR01-0225	225 mW	350	400 mW	700
	LXML-PR01-0275	275 mW	350	525 mW	700
	LXML-PR01-0350	350mW	350	625 mW	700
	LXML-PR01-0425	425mW	350	740 mW	700
Red	LXML-PD01-0030	30	350	65	700
	LXML-PD01-0040	40	350	85	700
Red-Orange	LXML-PH01-0040	40	350	85	700
	LXML-PH01-0050	50	350	100	700
Amber	LXML-PL01-0023	23.5	350	50	700
	LXML-PL01-0030	30.0	350	65	700

See table notes on next page.

## Flux Characteristics, Continued

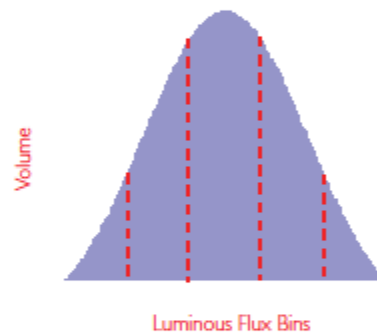
### Flux Characteristics for LUXEON Rebel, Continued

Notes for Table 1:

1. Minimum luminous flux or radiometric power performance guaranteed within published operating conditions. Philips Lumileds maintains a tolerance of  $\pm 6.5\%$  on flux and power measurements.
2. Typical luminous flux or radiometric power performance when device is operated within published operating conditions.

### Flux Performance, Binning, and Supportability

LEDs are produced with semiconductor technology that is subject to process variation, yielding a range of flux performance that is approximately Gaussian in nature. In order to provide customers with fine granularity within the overall flux distribution, Philips Lumileds separates LEDs into fixed, easy to design with, minimum luminous flux bins. To verify supportability of parts chosen for your application design, please consult your Philips Lumileds/Future Lighting Solutions sales representative.



## Optical Characteristics

### Lambertian LUXEON Rebel at Test Current <sup>[1]</sup> Thermal Pad Temperature = 25°C

Table 2.

Color	Dominant Wavelength <sup>[2]</sup> $\lambda_D$ , Peak Wavelength <sup>[2]</sup> $\lambda_p$ , or Color Temperature <sup>[3]</sup> CCT			Typical Spectral Half-width <sup>[5]</sup> (nm) $\Delta\lambda_{1/2}$	Typical Temperature Coefficient of Dominant Wavelength (nm/°C) $\Delta\lambda_D / \Delta T_j$	Typical Included Angle <sup>[6]</sup> (degrees) $\theta_{90\%V}$	Typical Viewing Angle <sup>[7]</sup> (degrees) 2 $\theta_{1/2}$
	Min.	Typ.	Max.				
	Green	520 nm	530 nm				
Cyan	490 nm	505 nm	520 nm	30	0.04	160	120
Blue	460 nm	470 nm	490 nm	33	0.05	160	120
Royal-Blue <sup>[8]</sup>	440 nm	447.5 nm	460 nm	24	0.04	160	120
Red	620.5 nm	627 nm	645 nm	20	0.05	160	120
Red-Orange	613.5 nm	617 nm	620.5 nm	20	0.08	160	120
Amber	584.5 nm	590 nm	597 nm	20	0.10	160	120

Notes for Table 2:

1. Test current is 350 mA for all LXML-Pxx1-0xxx products.
2. Dominant wavelength is derived from the CIE 1931 Chromaticity diagram and represents the perceived color. Philips Lumileds maintains a tolerance of  $\pm 0.5$  nm for dominant wavelength measurements.
3. Royal-Blue product is binned by radiometric power and peak wavelength rather than photometric lumens. Philips Lumileds maintains a tolerance of  $\pm 2$ nm for peak wavelength measurements.
4. CCT  $\pm 5\%$  tester tolerance.
5. Spectral width at  $1/2$  of the peak intensity.
6. Total angle at which 90% of total luminous flux is captured.
7. Viewing angle is the off axis angle from lamp centerline where the luminous intensity is  $1/2$  of the peak value.
8. All green, cyan, blue and royal-blue products are built with Indium Gallium Nitride (InGaN).
9. All red, red-orange, and amber are built with Aluminum Indium Gallium Phosphide (AlInGaP).
10. Blue and royal-blue power light sources represented here are IEC825 class 2 for eye safety.

## Electrical Characteristics

### Electrical Characteristics at 350 mA for LUXEON Rebel, Part Numbers LXML-PxxI-0xxx, Thermal Pad Temperature = 25°C

**Table 3.**

Color	Forward Voltage $V_f$ <sup>[1]</sup> (V)			Typical Temperature Coefficient of Forward Voltage <sup>[2]</sup> (mV/°C) $\Delta V_f / \Delta T_j$	Typical Thermal Resistance Junction to Thermal Pad (°C/W) $R\theta_{j-c}$
	Min.	Typ.	Max.		
Green	2.55	3.15	3.99	-2.0 to -4.0	10
Cyan	2.55	3.15	3.99	-2.0 to -4.0	10
Blue	2.55	3.15	3.99	-2.0 to -4.0	10
Royal-Blue	2.55	3.15	3.99	-2.0 to -4.0	10
Red	2.31	2.9	3.51	-2.0 to -4.0	12
Red-Orange	2.31	2.9	3.51	-2.0 to -4.0	12
Amber	2.31	2.9	3.51	-2.0 to -4.0	12

Notes for Table 3:

1. Philips Lumileds maintains a tolerance of  $\pm 0.06V$  on forward voltage measurements.
2. Measured between 25°C =  $T_j = 110^\circ C$  at  $I_f = 350$  mA.
- \* Dynamic resistance is the inverse of the slope in linear forward voltage model for LEDs. See figures 7 and 8.

### Typical Electrical Characteristics at 700 mA for LUXEON Rebel, Part Numbers LXML-PxxI-0xxx, Thermal Pad Temperature = 25°C

**Table 4.**

Color	Typical Forward Voltage $V_f$ (V)
Green	3.40
Cyan	3.40
Blue	3.40
Royal-Blue	3.40
Red	3.60
Red-Orange	3.60
Amber	3.60

Notes for Table 4:

1. Philips Lumileds maintains a tolerance of  $\pm 0.06V$  on forward voltage measurements.
2. Dynamic resistance is the inverse of the slope in linear forward voltage model for LEDs. See figures 7 and 8.
3. Measured between 25°C =  $T_j = 110^\circ C$  at  $I_f = 700$  mA.

# APPENDIX\_C

## Absolute Maximum Ratings

**Table 5.**

Parameter	Green / Cyan / Blue / Royal-Blue	Red / Red-Orange / Amber
DC Forward Current (mA)	1000	700
Peak Pulsed Forward Current (mA)	1000	700
Average Forward Current (mA)	1000	700
ESD Sensitivity	< 8000V Human Body Model (HBM) Class 3A JESD22-A114-B < 400V Machine Model (MM) Class 3A JESD22-A115-B	< 8000V Human Body Model (HBM) Class 3A JESD22-A114-B < 400V Machine Model (MM) Class 3A JESD22-A115-B
LED Junction Temperature <sup>(1)</sup>	150°C	135°C
Operating Case Temperature at 350 mA	-40°C - 135°C	-40°C - 120°C
Storage Temperature	-40°C - 135°C	-40°C - 135°C
Soldering Temperature	JEDEC 020c 260°C	JEDEC 020c 260°C
Allowable Reflow Cycles	3	3
Autoclave Conditions	121°C at 2 ATM 100% Relative Humidity for 96 Hours Maximum	
Reverse Voltage (Vr)	See Note 2	See Note 2

**Notes for Table 5:**

1. Proper current derating must be observed to maintain junction temperature below the maximum.
2. LUXEON Rebel LEDs are not designed to be driven in reverse bias.

## JEDEC Moisture Sensitivity

**Table 6.**

Level	Floor Life		Soak Requirements	
	Time	Conditions	Standard	
			Time (hours)	Conditions
I	unlimited	≤ 30°C / 85% RH	168 + 5 / -0	85°C / 85% RH

## Reflow Soldering Characteristics

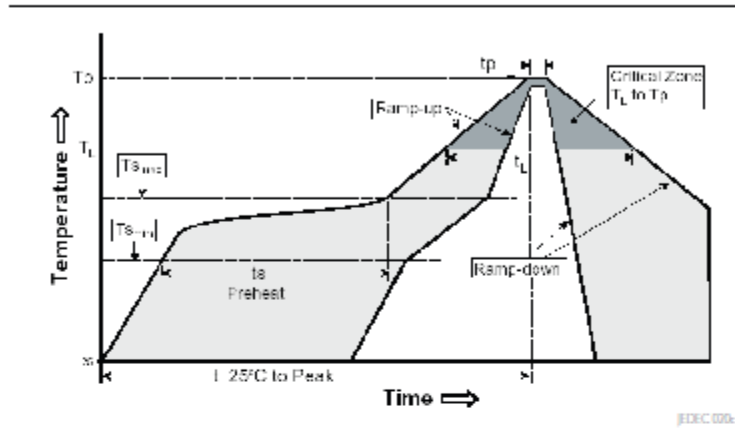


Table 7.

Profile Feature	Lead Free Assembly
Average Ramp-Up Rate ( $T_{s_{max}}$ to $T_p$ )	3°C / second max
Preheat Temperature Min ( $T_{s_{min}}$ )	150°C
Preheat Temperature Max ( $T_{s_{max}}$ )	200°C
Preheat Time ( $t_{s_{min}}$ to $t_{s_{max}}$ )	60 - 180 seconds
Time Maintained Above Temperature $T_1$ ( $t_1$ )	217°C
Time Maintained Above Time ( $t_1$ )	60 - 150 seconds
Peak / Classification Temperature ( $T_p$ )	260°C
Time Within 5°C of Actual Peak Temperature ( $t_p$ )	20 - 40 seconds
Ramp-Down Rate	6°C / second max
Time 25°C to Peak Temperature	8 minutes max

Note for Table 7:

- All temperatures refer to the application Printed Circuit Board (PCB), measured on the surface adjacent to the package body.

## Mechanical Dimensions

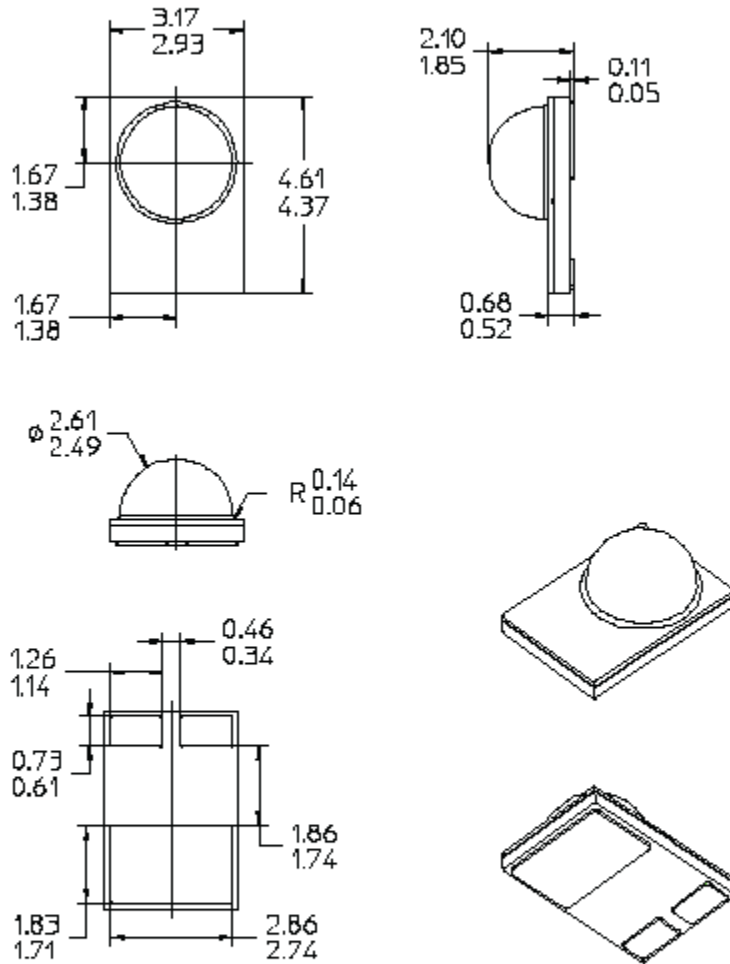


Figure 1. Package outline drawing.

Notes for Figure 1:

1. Do not handle the device by the lens—care must be taken to avoid damage to the lens or the interior of the device that can be damaged by excessive force to the lens.
2. Drawings not to scale.
3. All dimensions are in millimeters.
4. The thermal pad is electrically isolated from the anode and cathode contact pads.

## Pad Configuration

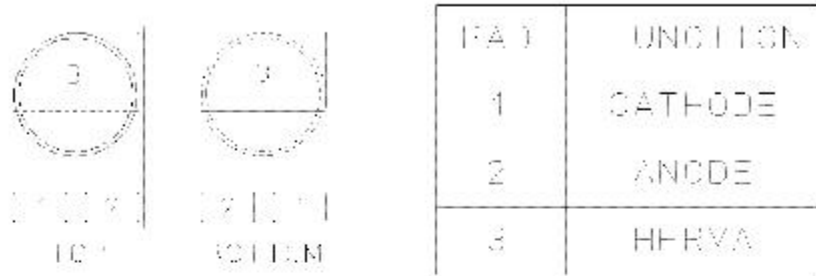


Figure 2. Pad configuration.

Note for Figure 2:

1. The thermal pad is electrically isolated from the anode and cathode contact pads.

## Solder Pad Design

Note for Figure 3:

The photograph below shows the recommended LUXEON Rebel layout on printed circuit board (PCB). This design easily achieves a thermal resistance of 7K/W.

Application Brief AB32 provides extensive details for this layout. In addition, the .dwg files are available upon request.

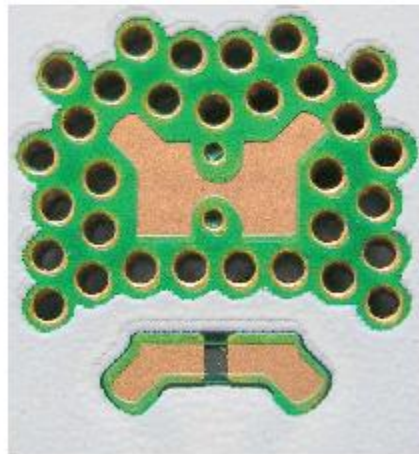


Figure 3. Solder pad layout.

## Wavelength Characteristics

Green, Cyan, Blue, Royal-Blue, Red, Red-Orange and Amber  
at Test Current Thermal Pad Temperature = 25°C

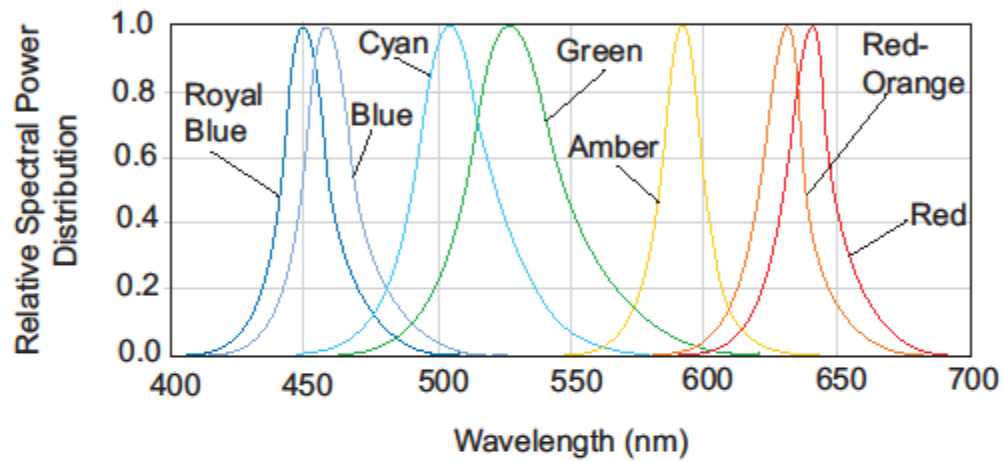


Figure 4. Relative intensity vs. wavelength.

## Typical Light Output Characteristics over Temperature

### Cyan, Blue and Royal-Blue at Test Current

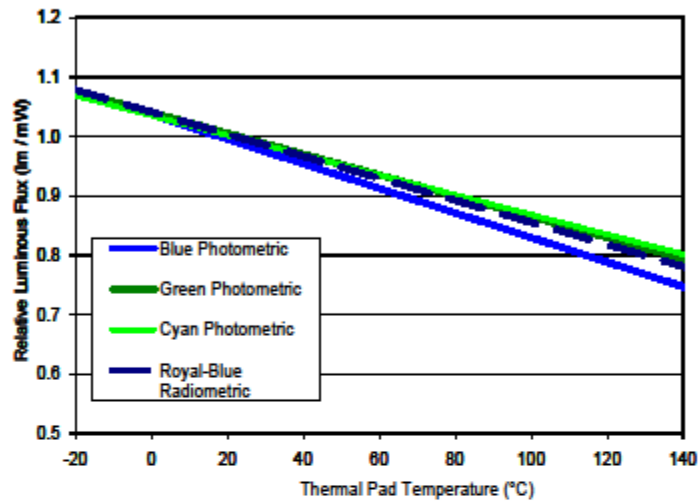


Figure 5. Relative light output vs. thermal pad temperature for green, cyan, blue and royal-blue.

### Red, Red-Orange and Amber at Test Current

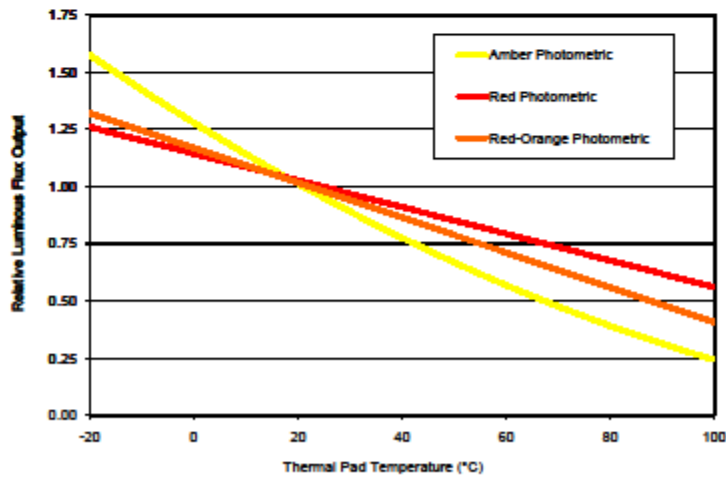


Figure 6. Relative light output vs. thermal pad temperature for red, red-orange and amber.

## Typical Forward Current Characteristics

### Green, Cyan, Blue and Royal-Blue Thermal Pad Temperature = 25°C

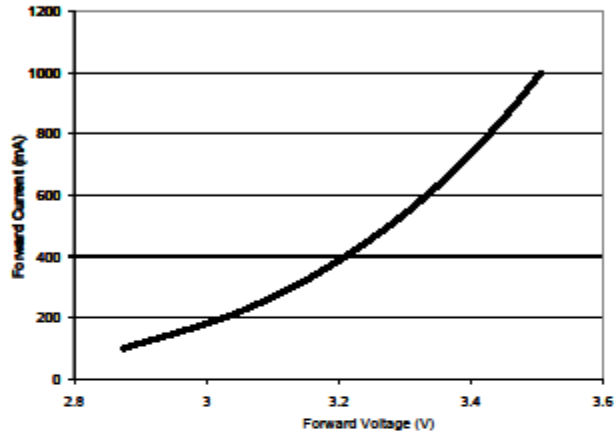


Figure 7. Forward current vs. forward voltage for green, cyan, blue and royal-blue.

### Red, Red-Orange and Amber Thermal Pad Temperature = 25°C

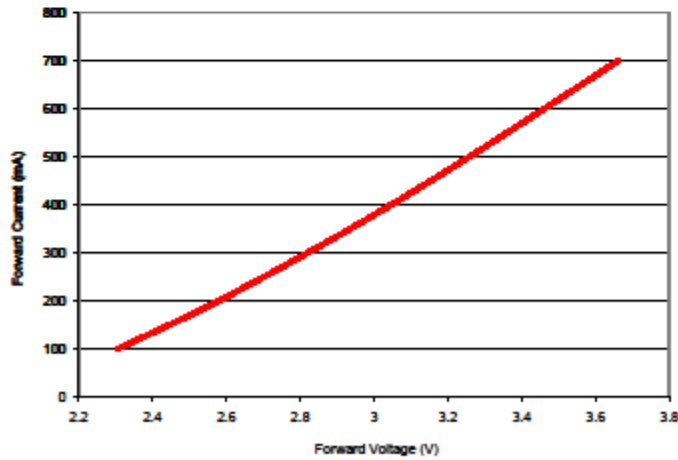


Figure 8. Forward current vs. forward voltage for red, red-orange, and amber.

## Typical Relative Luminous Flux

### Typical Relative Luminous Flux vs. Forward Current for Green, Cyan, Blue and Royal-Blue Thermal Pad Temperature = 25°C

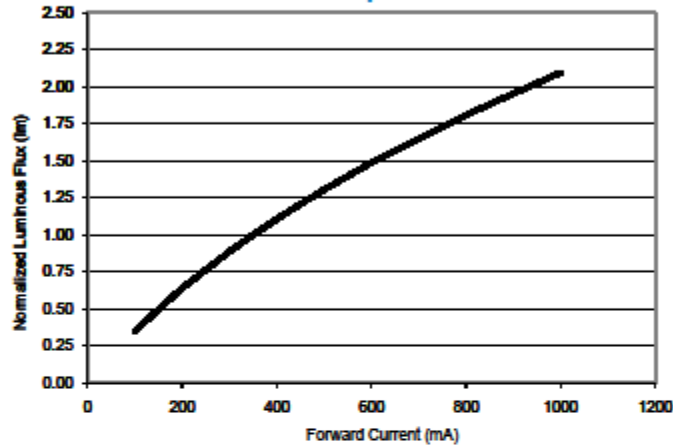


Figure 9. Relative luminous flux or radiometric power vs. forward current for green, cyan, blue and royal-blue at Thermal Pad = 25°C maintained, test current 350 mA.

### Typical Relative Luminous Flux vs. Forward Current for Red, Red-Orange, Amber Thermal Pad Temperature = 25°C

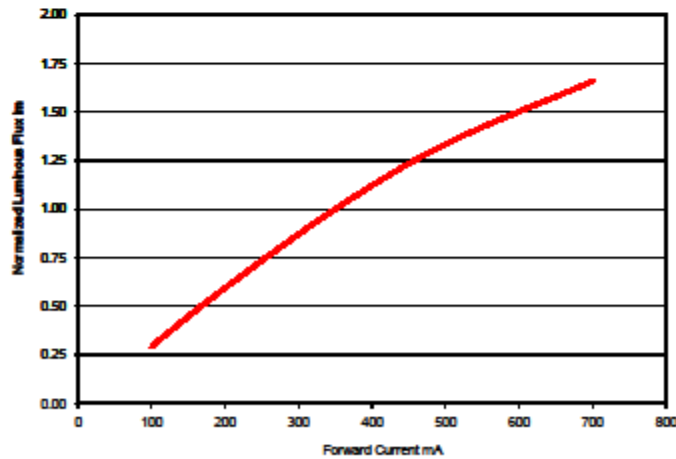


Figure 10. Relative luminous flux vs. forward current for red, red-orange and amber at Thermal Pad = 25°C maintained, test current 350 mA.

## Current Derating Curves

### Current Derating Curve for 350 mA Drive Current Green, Cyan, Blue and Royal-Blue

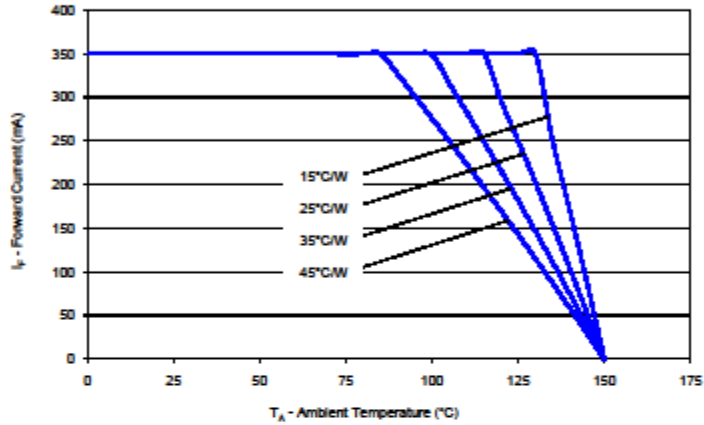


Figure 11. Maximum forward current vs. ambient temperature, based on  $T_{MAX} = 150^{\circ}C$ .

### Current Derating Curve for 350 mA Drive Current Red, Red-Orange, Amber

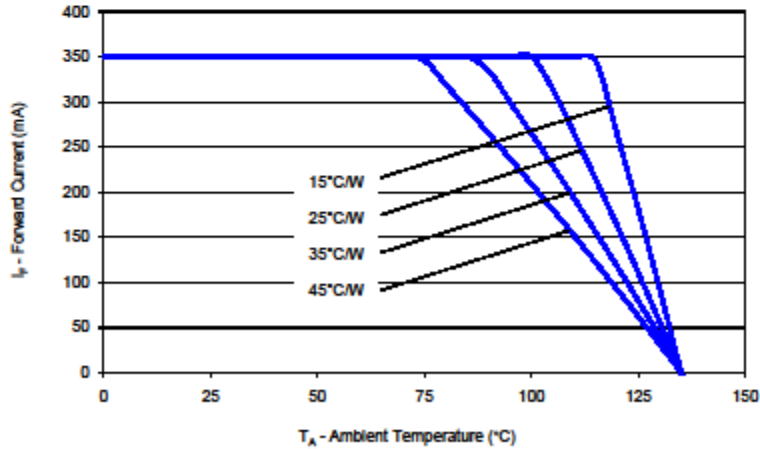


Figure 12. Maximum forward current vs. ambient temperature, based on  $T_{MAX} = 135^{\circ}C$ .

## Current Derating Curves, Continued

### Current Derating Curve for 700 mA Drive Current Green, Cyan, Blue and Royal-Blue

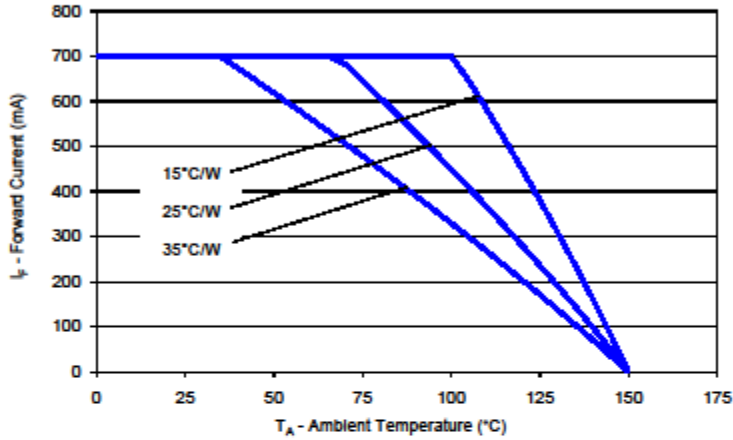


Figure 13. Maximum forward current vs. ambient temperature, based on  $T_{MAX} = 150^{\circ}C$ .

### Current Derating Curve for 700 mA Drive Current Red, Red-Orange, Amber

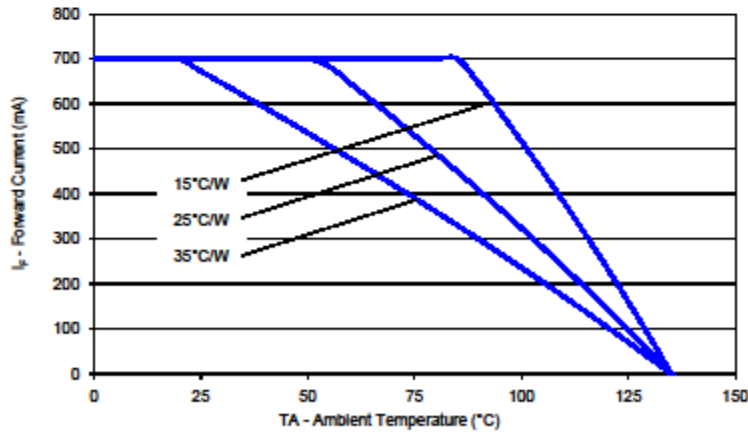


Figure 14. Maximum forward current vs. ambient temperature, based on  $T_{MAX} = 135^{\circ}C$ .

## Current Derating Curves, Continued

### Current Derating Curve for 1000 mA Drive Current Green, Cyan, Blue and Royal-Blue

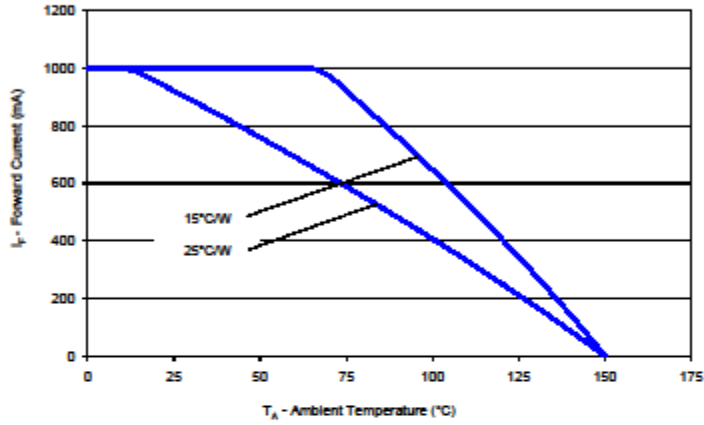


Figure 15. Maximum forward current vs. ambient temperature, based on  $T_{JMAX} = 135^\circ\text{C}$ .

## Typical Radiation Patterns

### Typical Representative Spatial Radiation Pattern for Green, Cyan, Blue and Royal-Blue Lambertian

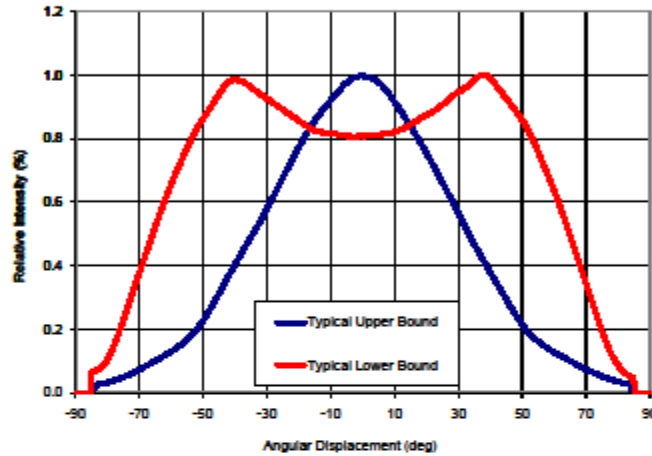


Figure 16. Typical representative spatial radiation pattern for green, cyan, blue, and royal-blue lambertian.

### Typical Polar Radiation Pattern for Green, Cyan, Blue and Royal-Blue Lambertian

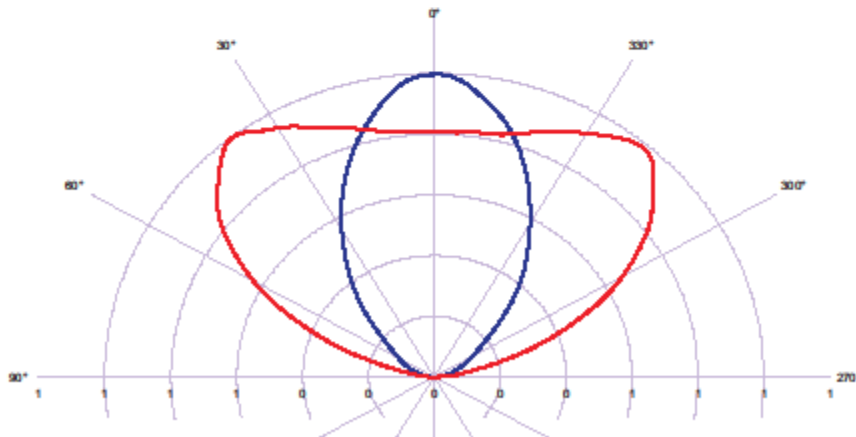


Figure 17. Typical polar radiation pattern for green, cyan, blue, and royal-blue lambertian.

## Typical Radiation Patterns, Continued

### Typical Representative Spatial Radiation Pattern for Red, Red-Orange and Amber Lambertian

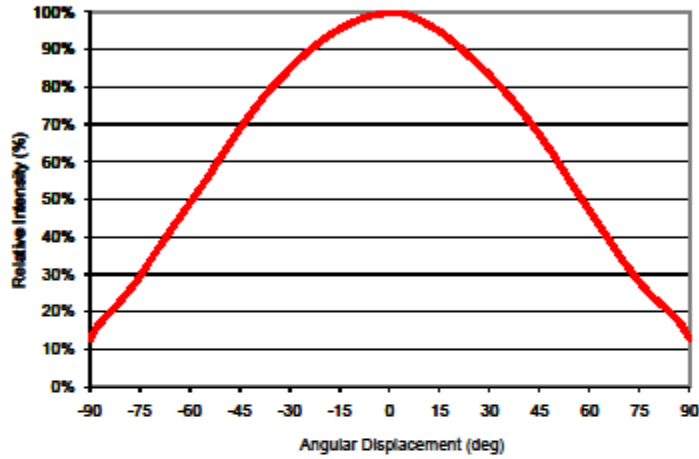


Figure 18. Typical representative spatial radiation pattern for red, red-orange and amber lambertian.

### Typical Polar Radiation Pattern for Red, Red-Orange and Amber Lambertian

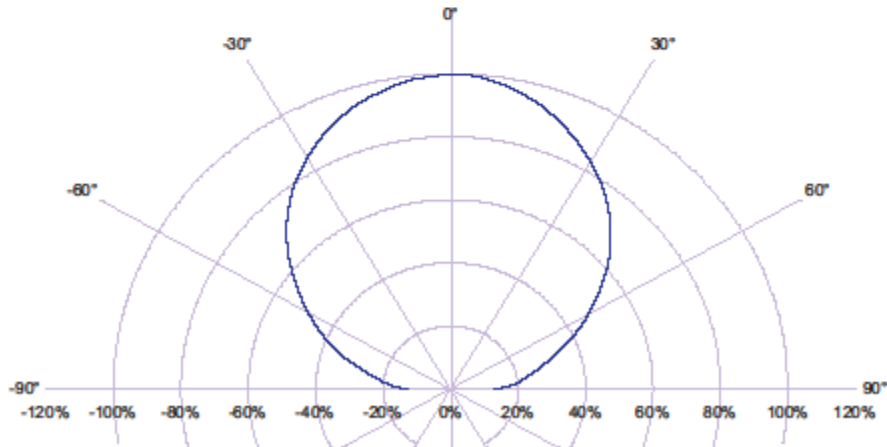


Figure 19. Typical polar radiation pattern for red, red-orange and amber lambertian.

## Emitter Pocket Tape Packaging

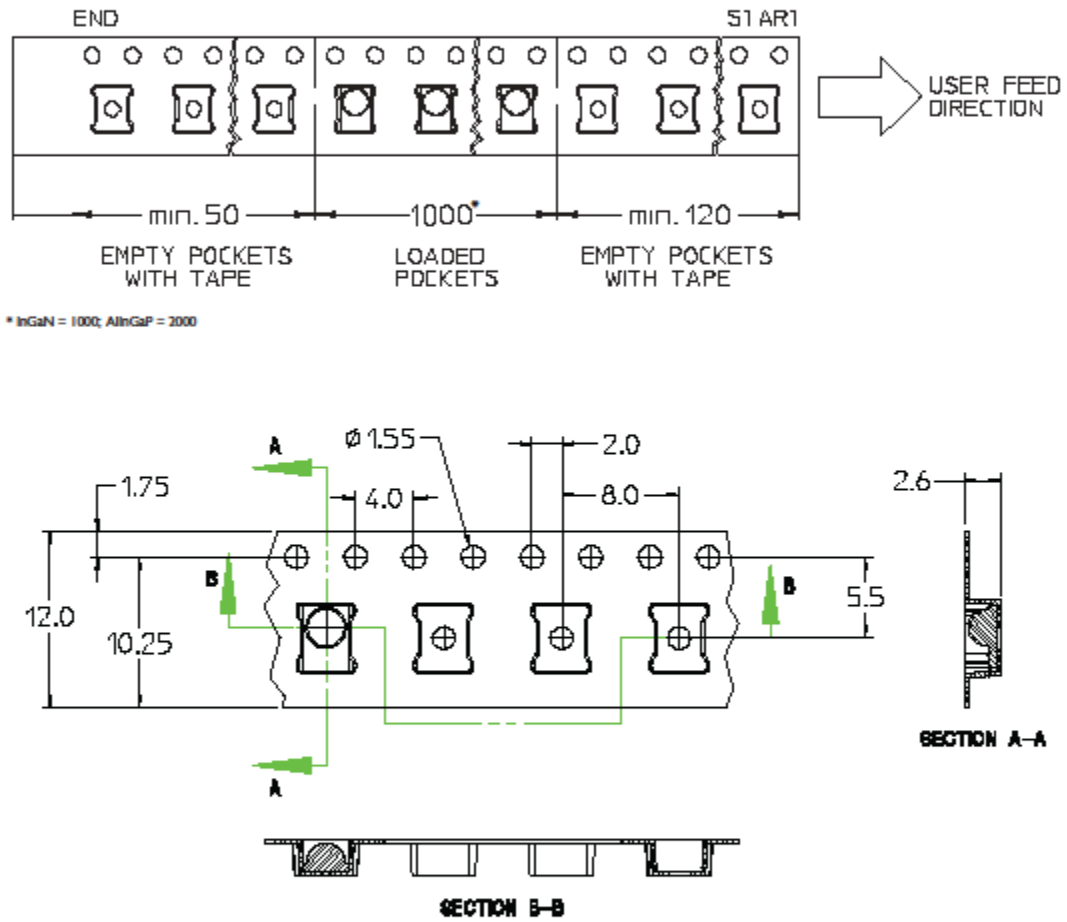


Figure 20. Emitter pocket tape packaging.

## Emitter Reel Packaging

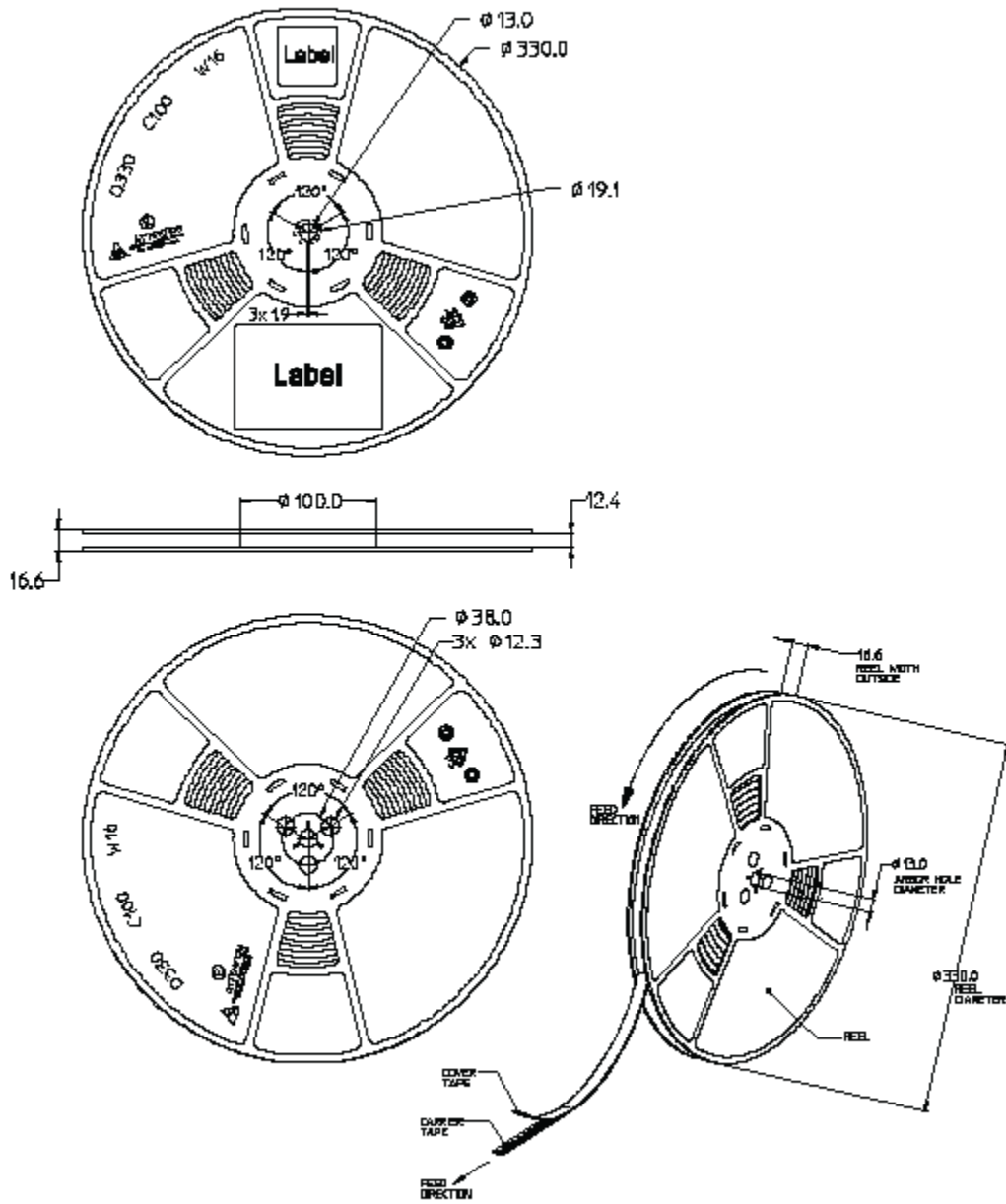


Figure 21. Emitter reel packaging.

## Product Binning and Labeling

### **Purpose of Product Binning**

In the manufacturing of semiconductor products, there is a variation of performance around the average values given in the technical data sheets. For this reason, Philips Lumileds bins the LED components for luminous flux, color and forward voltage ( $V_f$ ).

### **Decoding Product Bin Labeling**

LUXEON Rebel Emitters are labeled using a three or four digit alphanumeric code (CAT code) depicting the bin values for emitters packaged on a single reel. All emitters packaged within a reel are of the same 3-variable bin combination. Using these codes, it is possible to determine optimum mixing and matching of products for consistency in a given application. Reels of PC Amber Emitters are labeled with a three digit alphanumeric CATcode following the format below.

### **Format of Labeling for Emitters**

Reels of Green, Cyan, Blue, Royal-Blue, Red, Red-Orange and Amber Emitters are labeled with a three digit alphanumeric CAT code following the format below.

ABC

A = Flux bin (J, K, L, M etc.)

B = Color bin (2, 4, 6 etc.)

C =  $V_f$  bin (D, E, F, G etc.)

## Luminous Flux Bins

Table 8 lists the standard photometric luminous flux bins for LUXEON Rebel emitters (tested and binned at 350 mA).

Although several bins are outlined, product availability in a particular bin varies by production run and by product performance. Not all bins are available in all colors.

Table 8.  
Flux Bins All Colors (except Royal-Blue)

Bin Code	Minimum Photometric Flux (lm)	Maximum Photometric Flux (lm)
A	8.2	10.7
B	10.7	13.9
C	13.9	18.1
D	18.1	23.5
E	23.5	30
F	30	40
G	40	50
H	50	60
J	60	70
K	70	80
L	80	90
M	90	100
N	100	120
P	120	140
Q	140	160
R	160	180
S	180	200
T	200	220
U	220	240
V	240	260
W	260	280
X	280	300

## Luminous Flux Bins, Continued

**Table 9.**  
Flux Bins Royal-Blue Only (tested and binned at 350 mA)

Bin Code	Minimum Radiometric Flux (mW)	Maximum Radiometric Flux (mW)
A	175	225
B	225	275
C	275	350
D	350	425
E	425	500
F	500	600
G	600	700
H	700	800
J	800	900
K	900	1000

## Forward Voltage Bins

Table 10 lists minimum and maximum  $V_f$  bin values per emitter. Although several bins are outlined, product availability in a particular bin varies by production run and by product performance.

**Table 10.**

$V_f$ Bins		
Bin Code	Minimum Forward Voltage (V)	Maximum Forward Voltage (V)
A	2.31	2.55
B	2.55	2.79
C	2.79	3.03
D	3.03	3.27
E	3.27	3.51
F	3.51	3.75
G	3.75	3.99

## Color Bins

Green, Cyan and Blue LUXEON Rebel Emitters are tested and binned for dominant wavelength.

### Dominant Wavelength Bin Structure for Green Emitters

Table 11.

Bin Code	Minimum Dominant Wavelength (nm)	Maximum Dominant Wavelength (nm)
1	520	525
2	525	530
3	530	535
4	535	540
5	540	545
6	545	550

### Dominant Wavelength Bin Structure for Cyan Emitters

Table 12.

Bin Code	Minimum Dominant Wavelength (nm)	Maximum Dominant Wavelength (nm)
1	490	495
2	495	500
3	500	505
4	505	510
5	510	515
6	515	520

### Dominant Wavelength Bin Structure for Blue Emitters

Table 13.

Bin Code	Minimum Dominant Wavelength (nm)	Maximum Dominant Wavelength (nm)
1	460	465
2	465	470
3	470	475
4	475	480
5	480	485
6	485	490

Royal-Blue LUXEON Rebel Emitters are tested and binned for peak wavelength.

### Dominant Wavelength Bin Structure for Royal-Blue Emitters

Table 14.

Bin Code	Minimum Peak Wavelength (nm)	Maximum Peak Wavelength (nm)
3	440	445
4	445	450
5	450	455
6	455	460

## Color Bins, Continued

Red, Red-Orange and Amber LUXEON Rebel Emitters are tested and binned for dominant wavelength.

### Dominant Wavelength Bin Structure for Red Emitters

Table 15.

Bin Code	Minimum Dominant Wavelength (nm)	Maximum Dominant Wavelength (nm)
4	620.5	631.0
5	631.0	645.0

### Dominant Wavelength Bin Structure for Red-Orange Emitters

Table 16.

Bin Code	Minimum Dominant Wavelength (nm)	Maximum Dominant Wavelength (nm)
2	613.5	620.5

### Dominant Wavelength Bin Structure for Amber Emitters

Table 17.

Bin Code	Minimum Dominant Wavelength (nm)	Maximum Dominant Wavelength (nm)
1	584.5	587.0
2	587.0	589.5
4	589.5	592.0
6	592.0	594.5
7	594.5	597.0

## Company Information

Philips Lumileds is the world's leading provider of power LEDs for everyday lighting applications. The company's records for light output, efficacy and thermal management are direct results of the ongoing commitment to advancing solid-state lighting technology and enabling lighting solutions that are more environmentally friendly, help reduce CO<sub>2</sub> emissions and reduce the need for power plant expansion. Philips Lumileds LUXEON® LEDs are enabling never before possible applications in outdoor lighting, shop lighting and home lighting.

Philips Lumileds is a fully integrated supplier, producing core LED material in all three base colors, (Red, Green, Blue) and white. Philips Lumileds has R&D centers in San Jose, California and in the Netherlands, and production capabilities in San Jose, Singapore and Penang Malaysia. Founded in 1999, Philips Lumileds is the high flux LED technology leader and is dedicated to bridging the gap between solid-state technology and the lighting world. More information about the company's LUXEON LED products and solid-state lighting technologies can be found at [www.philipslumileds.com](http://www.philipslumileds.com).

[www.philipslumileds.com](http://www.philipslumileds.com)  
[www.futurelightingsolutions.com](http://www.futurelightingsolutions.com)

For technical assistance or the location of your nearest sales office contact any of the following:

North America:  
1 888 589 3662  
[americas@futurelightingsolutions.com](mailto:americas@futurelightingsolutions.com)

Europe:  
00 800 443 88 873  
[europe@futurelightingsolutions.com](mailto:europe@futurelightingsolutions.com)

Asia Pacific:  
800 5864 5337  
[asia@futurelightingsolutions.com](mailto:asia@futurelightingsolutions.com)

Japan:  
800 5864 5337  
[japan@futurelightingsolutions.com](mailto:japan@futurelightingsolutions.com)

©2009 Philips Lumileds Lighting Company. All rights reserved.  
Product specifications are subject to change without notice.  
LUXEON is a registered trademark of the Philips Lumileds Lighting Company in the United States and other countries.

**PHILIPS**  
**LUMILEDS**

# APPENDIX D

TECHNICAL

DATASHEETS FOR

THERMALLY

CONDUCTIVE ADHESIVE

TAPE

## Bond-Ply® 100

Thermally Conductive, Fiberglass Reinforced Pressure Sensitive Adhesive Tape

### Features and Benefits

- Thermal impedance: 0.52°C-in<sup>2</sup>/W (@50 psi)
- High bond strength to a variety of surfaces
- Double-sided, pressure sensitive adhesive tape
- High performance, thermally conductive acrylic adhesive
- Can be used instead of heat-cure adhesive, screw mounting or clip mounting



### Typical Applications Include:

- Mount heat sink onto BGA graphic processor or drive processor
- Mount heat spreader onto power converter PCB or onto motor control PCB

### Configurations Available:

- Sheet form, roll form and die-cut parts

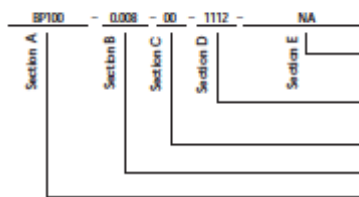
**Shelf Life:** The double-sided, pressure sensitive adhesive used in Bond-Ply products requires the use of dual liners to protect the surfaces from contaminants. Bergquist recommends a 6-month shelf life at a maximum continuous storage temperature of 35°C or 3-month shelf life at a maximum continuous storage temperature of 45°C, for maintenance of controlled adhesion to the liner. The shelf life of the Bond-Ply material, without consideration of liner adhesion (which is often not critical for manual assembly processing), is recommended at 12 months from date of manufacture at a maximum continuous storage temperature of 60°C.

### TYPICAL PROPERTIES OF BOND-PLY 100

PROPERTY	IMPERIAL VALUE	METRIC VALUE	TEST METHOD		
Color	White	White	Visual		
Reinforcement Carrier	Fiberglass	Fiberglass	—		
Thickness (inch) / (mm)	0.005, 0.008, 0.011	0.127, 0.203, 0.279	ASTM D374		
Temp. Resistance, 30 sec. (°F) / (°C)	392	200	—		
Elongation (%45° to Warp & Fit)	70	70	ASTM D412		
Tensile Strength (psi) / (MPa)	900	6	ASTM D412		
CTE (ppm)	325	325	ASTM D3386		
Glass Transition (°F) / (°C)	-22	-30	ASTM 1356		
Continuous Use Temp (°F) / (°C)	-22 to 248	-30 to 120	—		
<b>ADHESION</b>					
Lap Shear @ RT (psi) / (MPa)	100	0.7	ASTM D1002		
Lap Shear after 5 hr @ 100°C	200	1.4	ASTM D1002		
Lap Shear after 2 min @ 200°C	200	1.4	ASTM D1002		
Static Dead Weight Shear (°F) / (°C)	302	150	PSTC#7		
<b>ELECTRICAL</b>		<b>VALUE</b>	<b>TEST METHOD</b>		
Dielectric Breakdown Voltage - 0.005" (Vac)		3000	ASTM D149		
Dielectric Breakdown Voltage - 0.008" (Vac)		6000	ASTM D149		
Dielectric Breakdown Voltage - 0.011" (Vac)		8500	ASTM D149		
Flame Rating		V-0	UL94		
<b>THERMAL</b>					
Thermal Conductivity (W/m-K)		0.8	ASTM D5470		
<b>THERMAL PERFORMANCE vs PRESSURE</b>					
Initial Assembly Pressure (psi for 5 seconds)	10	25	50	100	200
TO-220 Thermal Performance (°C/W) 0.005"	5.17	4.87	4.49	4.18	4.10
TO-220 Thermal Performance (°C/W) 0.008"	5.40	5.35	5.28	5.22	5.20
TO-220 Thermal Performance (°C/W) 0.011"	6.39	6.51	6.51	6.50	6.40
Thermal Impedance (°C-in <sup>2</sup> /W) 0.005" (1)	0.56	0.84	0.52	0.50	0.50
Thermal Impedance (°C-in <sup>2</sup> /W) 0.008" (1)	0.82	0.80	0.78	0.77	0.75
Thermal Impedance (°C-in <sup>2</sup> /W) 0.011" (1)	1.03	1.02	1.01	1.00	0.99

1) The ASTM D5470 test fixture was used. The recorded value includes interfacial thermal resistance. These values are provided for reference only. Actual application performance is directly related to the surface roughness, fitness and pressure applied.

### Building a Part Number



Note: To build a part number, visit our website at [www.bergquistcompany.com](http://www.bergquistcompany.com).

Bond-Ply®: U.S. Patent 5,090,484 and others.

### Standard Options

- **NA** = Selected standard option. If not selecting a standard option, insert company name, drawing number, and revision level.
- 1112 = 11" x 12" sheets, 11250 = 11" x 250' rolls or 00 = custom configuration
- 00 = No adhesive
- Standard thicknesses available: 0.005", 0.008", 0.011"
- BP100 = Bond-Ply 100 Material



[www.bergquistcompany.com](http://www.bergquistcompany.com)

The Bergquist Company -  
North American Headquarters  
18830 West 78th Street  
Chanhassen, MN 55317  
Phone: 800.347.4572  
Fax: 952.835.0430

The Bergquist Company -  
European Headquarters  
Brammering St. 3755 BT Eindhoven  
Netherlands  
Phone: 31-35-5380664  
Fax: 31-35-5380795

The Bergquist Company - Asia  
Room 15, 8/F, Wan Wan Industrial Centre  
No. 33-40, Au Po Wan Street  
Tseung Kwan O, N.T. Hong Kong  
Ph: 852.26905996  
Fax: 852.26907344

All statements, technical information and recommendations herein are based on tests we believe to be reliable, and THE FOLLOWING IS MADE IN LIEU OF ALL WARRANTIES, EXPRESSED OR IMPLIED, INCLUDING THE IMPLIED WARRANTIES OF MERCHANTABILITY AND FITNESS FOR PURPOSE. Seller's and manufacturer's only obligation shall be to replace such quantity of the product proved to be defective. Before using user shall determine the suitability of the product for its intended use, and the user assumes all risks and liability whatsoever in connection therewith. NEITHER SELLER NOR MANUFACTURER SHALL BE LIABLE EITHER IN TORT OR IN CONTRACT FOR ANY LOSS OR DAMAGE, DIRECT, INCIDENTAL, OR CONSEQUENTIAL, INCLUDING LOSS OF PROFITS OR REVENUE ARISING OUT OF THE USE OR THE INABILITY TO USE A PRODUCT. No statement, purchase order or recommendations by seller or purchaser not contained herein shall have any force or effect unless in an agreement signed by the officers of the seller and manufacturer. PDS\_BP\_100\_12/08

# REFERENCES

## REFERENCES

---

- [1] Werner K. Noell, Virgil S. Walker, Bok Soon Kang, Steven Berman, 1966. *Retinal damage by light in rats*. Invest. Ophthalmol. 5, 450-473.
- [2] Daniel T. Organisciak, Dana K. Vaughan, 2010. *Retinal light damage: Mechanisms and protection*. Progress in Retinal and Eye Research. 29. 113-134.
- [3] The Nervous System: B. The Special Senses: 50 The Eye: II. Receptor and Neural Function of the Retina. pp. 148-553. (I cannot source this better as it was a photocopy from a book from a medical friend years ago)
- [4] [http://en.wikipedia.org/wiki/Visual\\_phototransduction](http://en.wikipedia.org/wiki/Visual_phototransduction)
- [5] [http://en.wikipedia.org/wiki/Photoreceptor\\_cell](http://en.wikipedia.org/wiki/Photoreceptor_cell)
- [6] Koen Clays, Sven Van Elshocht, André Persoons, September 15, 2000. *Bacteriorhodopsin: a natural (nonlinear) photonic bandgap material*. Vol. 25, No. 18 / OPTICS LETTERS. pp1391-1393.
- [7] Koen Clays, Sven Van Elshocht, Mingjun Chi\*, Erwin Lepoudre, Andre' Persoons. October 2001 *Bacteriorhodopsin: a natural, efficient (nonlinear) photonic crystal*. J. Opt. Soc. Am. B/Vol. 18, No. 10. pp1474-1482.
- [8] <http://en.wikipedia.org/wiki/Retina>
- [9] <http://en.wikipedia.org/wiki/Fovea>
- [10] [http://en.wikipedia.org/wiki/Retinal\\_ganglion\\_cell](http://en.wikipedia.org/wiki/Retinal_ganglion_cell)
- [11] [http://en.wikipedia.org/wiki/Outer\\_segment\\_disc\\_shedding](http://en.wikipedia.org/wiki/Outer_segment_disc_shedding)
- [12] Courtesy of a Power Point Presentation given by the Department of Physiology and the Neurosensory Laboratory, State University of New York at Buffalo, School of Medicine, Buffalo, N. Y.
- [13] <http://en.wikipedia.org/wiki/Lux>
- [14] [http://en.wikipedia.org/wiki/Integrating\\_sphere](http://en.wikipedia.org/wiki/Integrating_sphere)